

A Human-Robot Cooperative Vineyard Selective Sprayer

**Thesis submitted in partial fulfillment
of the requirements for the degree of
“DOCTOR OF PHILOSOPHY”**

by

Ron Berenstein

**Submitted to the Senate of Ben-Gurion University
of the Negev**

20.6.2016

Beer-Sheva

A Human-Robot Cooperative Vineyard Selective Sprayer

**Thesis submitted in partial fulfillment
of the requirements for the degree of
“DOCTOR OF PHILOSOPHY”**

by

Ron Berenstein

**Submitted to the Senate of Ben-Gurion University
of the Negev**

Approved by the advisor __Prof. Yael Edan  _____

Approved by the Dean of the Kreitman School of Advanced Graduate Studies

20.6.2016

Beer-Sheva

This work was carried out under the supervision of Prof. Yael Edan

In the Department of Industrial Engineering and Management

Faculty of Engineering Science

A handwritten signature in black ink, appearing to read "Yael Edan". The signature is written in a cursive, flowing style.

Research-Student's Affidavit when Submitting the Doctoral Thesis for Judgment

I Ron Berenstein, whose signature appears below, hereby declare that
(Please mark the appropriate statements):

X I have written this Thesis by myself, except for the help and guidance offered by my Thesis Advisors.

X The scientific materials included in this Thesis are products of my own research, culled from the period during which I was a research student.

X This Thesis incorporates research materials produced in cooperation with others, excluding the technical help commonly received during experimental work. Therefore, I am attaching another affidavit stating the contributions made by myself and the other participants in this research, which has been approved by them and submitted with their approval.

Date: 20.6.2016 Student's name: Ron Berenstein

Signature:



ABSTRACT

Background and Objectives

This thesis focuses on developing a novel framework and tools for the collaboration of a remote human operator and a robotic platform in performing the task of pesticide spraying in vineyards.

The use of pesticides is an integral part of worldwide agriculture. Between 30% and 35% of crop losses can be prevented when harmful insects and diseases are eliminated by the use of pesticides.

Although pesticides are necessary in modern agriculture, they are poisonous and dangerous for humans and for the environment. Current methods for pesticide application include a human operator travelling along the crop rows and selectively spraying the targets manually using a backpack sprayer and mechanized non-selective spraying in which a human drives a tractor with a sprayer connected to a trailer behind the tractor that sprays the crops continuously. Despite the use of pesticide protection equipment (personal head mask and central filtration system for the manual and mechanized spraying methods, respectively) the human is still exposed to hazardous pesticides that can cause negative health issues.

Robotic technology may provide a means of reducing agriculture's current dependence on herbicides, improving its sustainability and reducing its environmental impact. A target-specific robotic sprayer can reduce the quantity of pesticides applied in modern agriculture and potentially remove or minimize the human presence during the spraying pesticide process.

The spraying task of a spraying robot can be divided into three sub-tasks: navigation along the crop row, target detection, and the spraying of the target. The focus of this thesis was on the tasks of target detection and spraying.

This work aimed to develop a human-robot collaborative agriculture robotic sprayer. The specific research objectives are to develop a wheeled robotic platform suitable for the spraying of vineyards, machine vision algorithms for foliage and grape detection, a framework in which a human and robot collaborate in performing the spraying task, and to develop a smart spraying device for pesticide application. Collaboration between a human and a robot for the task of detection can create a simplified, flexible, and robust system that will use the advantages of both human and robot and can react and cope with dynamic and complex conditions. Another specific added value of such human-robot collaboration is to remove the human operator from the hazardous environment, and reduce the environment pollution by reducing the quantity of pesticide being used along with accurate targeting.

Methods

A fully operative robotic sprayer equipped with an adjustable spraying device and the ability to communicate with a remote user was designed and built. Human-robot collaboration methods were developed as well as methods for target marking by a remote human operator.

An agricultural robotic system was built to serve as a research tool to enable field experiments and reflect the real-world conditions that a future agricultural robot would have to cope with. The chassis of the robot is assembled from two identical platforms that are interconnected using a universal joint. The design payload of each platform is 300 kg. Each platform contains two wheels (one on each side) with a directly connected electric motor and optical encoders for control. The robot is equipped with all the hardware and software needed for operation, which included an industrial computer, screen, car batteries, power generator, and sensors (digital cameras, distance sensors). A kinematic model was developed for accurate navigation along a determined path (the path can be set manually using a xBox controller or as an output of a navigation algorithm).

Grape and foliage detection algorithms were developed and evaluated. The algorithms were developed under a new concept that considered pesticide reduction as the main optimization parameter. Three algorithms were developed for the grape clusters detection and a single algorithm was developed for the foliage detection. Algorithms were evaluated using a database of images acquired in commercial vineyards. The foliage detection algorithm was mainly based on the unique foliage green color. The grape clusters detection algorithms were based on: difference in edge distribution between the grape clusters and the foliage, decision tree algorithm using multiple grape and foliage properties, and pixel comparison between edge representations of the captured image with a predesigned edge mask that represents grapes. Both algorithms were developed to maximize hit rates and minimize pesticide application.

Human-robot collaboration methods were developed to evaluate the influence of such collaboration on the performance rate of the hit, false alarm (FA), and overall spraying task. The developed methods included three target-marking methods (circle with constant diameter, ellipse with varying diameter, and free hand) and four human-robot collaboration levels (fully human manual, robot suggests – human decides, robot decides – human supervises, and fully autonomous robot operation). Each of the target-marking methods and the collaboration levels were tested with groups of participants while using images captured in a commercial vineyard as the experimental database. A user interface was developed to implement the suggested target-marking methods and

the human-robot collaboration. The user interface was used both for conducting experiments in the lab and for conducting field experiments using the robotic sprayer.

In order to precisely apply the pesticide toward the target, a target specific spraying device was designed and built. Due to the amorphous shape and varying size of the grape clusters, a spraying nozzle with varying size is needed for accurate target spraying while maximizing the spray coverage and minimizing false alarm spraying. The core functionality of the device is to change the spray diameter according to the detected target. A commercial spraying nozzle (AYHSS 16) assembled from two parts, the nozzle base and the nozzle cap, changes the spray diameter by rotating the nozzle cup. The nozzle base was fixed to the device while the nozzle cup was connected to a stepper motor. The device also includes a color camera (for capturing targets), distance sensor, and two fan lasers (one positioned horizontally and the other vertically, to create a cross (+) on the target); all were mounted on a pan/tilt unit. In order to validate the spraying device operation, several experiments were conducted to evaluate the flow rate relative to the nozzle cup rotational position, the spray diameter relative to the nozzle cap rotational position, and the ability of the device to detect and spray targets with different sizes.

Experiments

Several experiments were conducted to evaluate the foliage and grape detection algorithms, human marking methods, human-robot collaboration methods, the adjustable spraying device, and the integrated system. The main goal was to evaluate the different elements suggested in the framework under as close as possible real world conditions. For that, a set of images, captured in two commercial vineyards, was used as the main database for the experiments. These images were analyzed by three experts with a goal to precisely mark the grape clusters in each image.

An integrative site-specific experiment was conducted to demonstrate and evaluate the three main components of the collaboration framework working in sync: human marking methods, levels of human-robot collaboration, and the specific spraying device. For better control of the experiment, artificial targets were used and robot navigation along the vineyard row was simulated by following red tape fixed to the ground. During the experiment, the robot traveled a total distance of 1044 [m] ($16 \text{ users} \times 3 \text{ repetitions per user} \times 18 \text{ [m]}$ for each repetition + $10 \text{ repetitions} \times 18 \text{ [m]}$ for each repetition), captured 1108 frames and sprayed 3378 targets. The experiment shows that despite the high complexity of such a robotic system and framework, collaboration of a human

in the spraying process is feasible. The collaboration between the remote robot and the human showed that the hit and the false alarm rate was improved (hit rate increased by 13.4% and false alarm rate decreased by 19.5%) compared to a fully autonomous operation (collaboration level 4).

Results

Grape clusters and foliage detection algorithms

Analysis of the grape clusters detection algorithms showed that the hit rate can reach ~91% while reducing the use of pesticides by ~30%. The minimum and maximum algorithm processing times were 0.65 and 1.43 [s/frame] respectively. These results refer solely to detection algorithms that are applied using a computer system without any human help. For better detection results the human was included in the framework.

Human-robot collaboration

The learning process of using the target-marking interface was evaluated with a goal to bring the user expertise to minimum of 90% hit rate. The learning experiment revealed that marking 30 images (that took 7.5min) will bring the user the level of expertise needed. The learning process was repeated for every new user using the marking interface.

Marking methods experiment results show that the hit rates are maximized when the users have more time to mark the targets, as expected. While using the collaboration level in which the user has full control over the marking process (defined in this thesis as collaboration level 1), the highest hit rate of 94.3% (with false alarm rate of 15.1%) was obtained when practicing the constant circle diameter marking method with 15 s image switching time (defined as the time the image was presented to the user); the lowest false alarm rate of 10.1% was obtained when practicing the free hand marking method with 15 s image switching time. Since the ellipse marking method did not excel in any category (hit or false alarm rate) it was not evaluated with the three collaboration levels.

Experimental results of the human-robot collaboration levels indicate that the highest hit rate is achieved with the collaboration level in which the robot marks the targets and the human supervises (can add, remove, and correct computer marking, defined as collaboration level 3), constant circle diameter and 15 [sec] image switching time: 92.66%; these results are statistically significant. The lowest FA was achieved with the collaboration level in which the computer suggests and the human decides (defined as collaboration level 2), free hand marking, and 15 [sec]

image switching time: 2.71%. Results from the ease of use questionnaire did not show any statistically significant difference between the different collaboration methods.

Specific target spraying

A flow rate experiment was conducted using constant pressure of 20 [bar]. The experiment revealed a linear curve representing the relation between the flow rate and the nozzle aperture ($flow\ rate = 6 \cdot 10^{-6} \cdot nozzle\ aperture + 0.0519 \left[\frac{L}{sec} \right]$).

A visual inspection of the sprayed target using the adjustable spraying device revealed that all the targets were fully covered by the spray. The results show constant increasing of the sprayed diameter when presented with a smaller target; however, the ratio between the sprayed diameter and the target size decreases as the target size increases. This ratio can be addressed as the false detection ratio.

Integrative site specific sprayer experiment

The overall performance of the free hand marking method was better than the circle marking method. Hit rate was improved for all cases when using the free hand marking method (except for “spray evaluation” in collaboration level 2, the collaboration level in which the computer suggests and the human decides). However, along with the improvement of the Hit rate, the FA measures increased, implying more wasted spraying material. In both marking methods (constant circle diameter and free hand) the Hit and FA rates increase with the collaboration level. The best Hit rate results were achieved when using the free hand marking method with collaboration level 3 (93.6%).

Summary

A human-robotic collaborative sprayer was designed, built, and tested. The robot showed the ability to perform the necessary tasks required for such a robot sprayer in vineyards. The overall work demonstrates the operation of a robotic sprayer performing the spraying task with a remote human assisting in the target detection in different modes of collaboration.

The main contribution of the work was the introduction and full implementation of a framework for human-robot collaboration for the task of vineyard spraying. During the work we examined different collaboration levels between the robot and the human and several target marking methods for the target detection task. Another contribution of this work is the development of a unique site-specific spraying device able to implement the enhanced detection accuracy to the actual pesticide

spraying process. The results obtained can be used to develop a human-robot operational system by using the best values obtained for the selected criterion (e.g., for highest hit rate use constant circle diameter, image switching time of 15 [sec], and fully manual collaboration level; for lowest false alarm rate use free hand, image switching time of 15 [sec], and collaboration level 2).

Our hope is that all or part of this work will be commercialized. This will contribute to less environmental pollution and eliminate the risk of human poisoning due to pesticides.

Key words: Agricultural engineering, agricultural machinery, human-robot interaction, image processing, levels of automation, machine learning, machine vision, object detection, pesticides, precision agriculture, robotic sprayer, spraying, teleoperators

This dissertation is in part based on the following publications which are all included in the attached DVD and are sorted numerically:

Published journal papers

1. Berenstein Ron, Edan Yael, Ben Shahar Ohad, Shapiro Amir. Grape clusters and foliage detection algorithms for autonomous selective vineyard sprayer (paper 1).
Berenstein, R.; Shahar, O.B.; Shapiro, A.; Edan, Y. Grape clusters and foliage detection algorithms for autonomous selective vineyard sprayer. *Intelligent Service Robotics* 2010, 3, 233–243.
2. Berenstein Ron, Hočevar Marko, Godeša Tone, Edan Yael, Ben Shahar Ohad. Distance-Dependent Multimodal Image Registration for Agriculture Tasks (paper 2).
Berenstein, R.; Hočevar, M.; Godeša, T.; Edan, Y.; Ben-Shahar, O. Distance-dependent multimodal image registration for agriculture tasks. *Sensors* 2015, 15, 20845-20862.

Journal papers under review/in preparation

3. Berenstein Ron, Edan Yael. Automatic adjustable spraying device for site-specific agricultural application (paper 3).
Berenstein, R.; Hočevar, M.; Godeša, T.; Edan, Y. Automatic adjustable spraying device for site-specific agricultural application. Submitted to *IEEE Transactions on Automation Science and Engineering*.
4. Berenstein Ron, Edan Yael. Human-robot collaboration for target detection in agricultural robotic sprayers (paper 4)
Berenstein, R.; Edan, Y. Human-robot collaboration for target detection in agricultural robotic sprayers. Submitted to *IEEE Transactions on Human-Machine Systems*.
5. Berenstein Ron, Edan Yael. Human robot collaborative target sprayer.
Berenstein, R.; Edan, Y. Human robot collaborative target sprayer. Submitted to *Journal of Field Robotics*.

Conference papers

6. Berenstein Ron, Edan Yael, Ben Shahar Ohad, Shapiro Amir. Image processing algorithms for a selective vineyard robotic sprayer (paper 5).
Berenstein, R.; Shahar, O.B.; Shapiro, A.; Edan, Y. Image processing algorithms for a selective vineyard robotic sprayer. *Joint International Agricultural Conference (JIAC), Wageningen, Holland, 2009*.
7. Berenstein Ron, Edan Yael. Robotic precision spraying methods (paper 6).
Berenstein, R.; Edan, Y. Robotic precision spraying methods. In the *American Society of Agricultural and Biological Engineers (ASABE) Annual Intl. Meeting, Dallas, Texas, 2012*.
8. Berenstein Ron, Edan Yael. Evaluation of Marking Techniques for a Human-Robot Selective Vineyard Sprayer (paper 7).
Berenstein, R.; Edan, Y. In *Evaluation of marking techniques for a human-robot selective vineyard sprayer, Intl. Conf. of Agricultural Engineering (CIGR-AgEng), Valencia, Spain, 2012*.
9. Berenstein Ron, Edan Yael, Ben Halevi Idan. A remote interface for a human-robot cooperative vineyard sprayer (paper 8).
Berenstein, R.; Edan, Y.; Ben Halevi, I. In *A remote interface for a human-robot cooperative vineyard sprayer, Intl. Society of Precision Agriculture (ICPA), Indianapolis, Indiana, 2012; Indianapolis, Indiana*.
10. Berenstein Ron, Edan Yael. Human-Robot Cooperative Precision Spraying - Collaboration Levels and Optimization Function (paper 9).
Berenstein, R.; Edan, Y. In *Human-robot cooperative precision spraying: Collaboration levels and optimization function, Symposiums on Robot Control (SYROCO), Dubrovnik, Croatia, 2012; Dubrovnik, Croatia*.

11. Berenstein Ron, Hočevár Marko, Godeša Tone, Edan Yael, Ben Shahar Ohad. Image registration for agriculture tasks (paper 10).

Berenstein, R.; Hočevár, M.; Godeša, T.; Edan, Y.; Ben Shahar, O.; Image registration for agriculture tasks, Intl. Conf. of Agricultural Engineering (AgEng), Zurich, Switzerland, 2014.

12. רון ברנשטיין, יעל אידן, מירב דיכטר, טל כהן. מציאת שיטה לסימון מטרות בממשק אדם-רובוט (paper 11).

רון ברנשטיין, יעל אידן, מירב דיכטר, טל כהן. מציאת שיטה לסימון מטרות בממשק אדם-רובוט. הכינוס ה-18 להנדסת תעשייה וניהול. תל אביב, ישראל, 2012.

Conference abstracts

13. Berenstein Ron, Ben Shahar Ohad, Shapiro Amir, Avital Bechar, Edan Yael. Image processing algorithms for a selective vineyard robotic sprayer (paper 12).

Berenstein, R.; Ben Shahar, O.; Shapiro, A.; Avital, B.; Edan, Y.; Image processing algorithms for a selective vineyard robotic sprayer. ICR 2008, Herzliya, Israel, 2008.

14. Ron Berenstein, Yael Edan, Udi Anconina, Dudi Amsallem. Machine vision algorithm for navigation along vineyard row (paper 13).

Berenstein, R.; Edan, Y.; Anconina, U.; Amsallem, D.; Machine vision algorithm for navigation along vineyard row. ICR 2010, Herzliya, Israel, 2010.

15. Ron Berenstein, Yael Edan. Marking and Spraying Techniques for a Human-Robot Vineyard Sprayer (paper 14).

Ron Berenstein, Yael Edan. Marking and Spraying Techniques for a Human-Robot Vineyard Sprayer. ICR 2013, Tel Aviv, Israel, 2013.

16. Ron Berenstein, Yael Edan. Human-robot selective vineyard sprayer (paper 15).

Berenstein, R.; Edan, Y.; Human-robot selective vineyard sprayer. The 26th Even-Ari Memorial Conference, Sede Boqer, Israel, 2015.

Seminars

17. Berenstein Ron, Edan Yael, Ben Shahar Ohad, Shapiro Amir. Image processing algorithms for a selective vineyard robotic sprayer

Berenstein, R.; Shahar, O.B.; Shapiro, A.; Edan, Y.; Image processing algorithms for a selective vineyard robotic sprayer. The seminar was held on 26.1.2009, at Ben-Gurion University of the Negev in the Department of Industrial Engineering and Management, Beer-Sheva, Israel, 2009.

18. Berenstein Ron, Edan Yael. A site-specific vineyard sprayer.

Berenstein, R.; Shahar, O.B.; Shapiro, A.; Edan, Y.; A site-specific vineyard sprayer. The seminar was held on 20.7.2012, at Purdue University in the Department of Agricultural and Biological Engineering, West Lafayette, Indiana, United States, 2012.

19. Berenstein Ron, Edan Yael. Image processing algorithms for a selective vineyard robotic sprayer.

Berenstein, R.; Edan, Y.; Image processing algorithms for a selective vineyard robotic sprayer. The seminar was held on 21.4.2010, at Volcani Research Center (ARO) in the Institute of Agricultural Engineering, Beit Dagan, Israel, 2010.

Table of Contents

ABSTRACT.....	V
Abbreviations	XIX
Acknowledgements	XX
1. Introduction.....	1
1.1. Description of the problem.....	1
1.2. Research objectives	4
1.3. Research significance	5
1.4. Research contribution and innovations	5
2. Scientific background	9
2.1. Pesticides in agriculture	9
2.2. Agricultural robots	9
2.3. Spraying robots in agriculture	12
2.4. Human-robot collaboration	12
2.5. Human interaction factors	17
3. Methods.....	20
3.1. Overview	20
3.2. Robotic sprayer system	20
3.3. Detection algorithms	21
3.4. Human-robot collaboration	21
3.5. Adjustable spraying device	21
3.6. Image registration techniques.....	22
4. Robotic sprayer	23
4.1. Overview	23
4.2. Robotic platform	23
4.3. Kinematic model for the robotic platform.....	26
5. Grapes and foliage Detection	30
5.1. Overview	30
5.2. Detection algorithms	30
5.2.1. Foliage detection algorithm	30
5.2.2. First grape detection algorithm	32
5.2.3. Second grape detection algorithm.....	32

5.2.4.	Third grape detection algorithm.....	36
5.3.	Experimental methods.....	37
5.4.	Detection algorithm results	38
6.	Human-robot collaboration	41
6.1.	Overview	41
6.2.	Human robot collaboration methods	42
6.2.1.	Collaboration level 1 – fully manual human target marking	42
6.2.2.	Collaboration level 2 – robot suggests, human approves	42
6.2.3.	Collaboration level 3 – robot marks, human supervises	43
6.2.4.	Collaboration level 4 – fully autonomous robot marking	44
6.3.	Human marking methods	44
6.4.	User interface	45
6.5.	Evaluation methodology	46
6.5.1.	Database.....	46
6.5.2.	Performance measures and data analysis	48
6.6.	Preliminary experiment – evaluating interface learning time	49
6.6.1.	Experimental setup.....	49
6.6.2.	Experimental design.....	49
6.6.3.	Results.....	50
6.7.	Evaluating human marking methods experiment.....	51
6.7.1.	Experimental setup.....	51
6.7.2.	Experimental design.....	51
6.7.3.	Results.....	51
6.8.	Evaluating collaboration level and marking method experiment.....	53
6.8.1.	Experimental setup.....	53
6.8.2.	Experimental design.....	54
6.8.3.	Results.....	54
7.	Site Specific target spraying device	57
7.1.	Overview	57
7.2.	Spraying deposition methods	57
7.2.1.	First spraying deposition method – fixed nozzle spacing	57
7.2.2.	Second spraying deposition method – optimal spray coverage	58
7.2.3.	Third spraying deposition method – one target-one shoot.....	59
7.2.4.	Spraying methods evaluation.....	59

7.2.5.	Spraying deposition methods – results	60
7.3.	The adjustable spraying device	64
7.4.	Preliminary experiments	66
7.4.1.	Flow rate evaluation.....	66
7.4.2.	Spray diameter evaluation.....	67
7.5.	Evaluating the ASD performance	70
7.5.1.	Experimental setup.....	71
7.5.2.	Experimental design.....	75
7.5.3.	Experimental results.....	75
8.	Integrative site-specific sprayer experiment.....	77
8.1.	Overview	77
8.2.	Experimental setup.....	77
8.2.1.	Robot side	77
8.2.2.	Human operations	81
8.2.3.	Spray evaluation.....	82
8.3.	Experimental design.....	83
8.4.	Experimental results.....	84
9.	Summary, conclusions, and future work	87
9.1.	Summary and conclusions.....	87
9.2.	Future work	90
9.2.1.	Robotic platform	90
9.2.2.	Navigation algorithm and path tracking	90
9.2.3.	Grape detection	90
9.2.4.	Spraying device.....	91
9.2.5.	Image registration	91
9.2.6.	Human-robot collaboration.....	91

Appendices

Appendix A.	Kinematic model of the robotic platform.	104
Appendix B.	Workload questionnaire.....	106
Appendix C.	Integrative site-specific sprayer experiment – detailed results.....	108
Appendix D.	Table of contents of thesis DVD	109

List of Figures

Figure 1 – Pesticide spraying methods. (a) Backpack sprayer. (b) Tractor sprayer.	2
Figure 2 – Robotic sprayer main components.	20
Figure 3 – Robotic platform during field experiments.	23
Figure 4 – Robotic sprayer overview.	25
Figure 5 – Robot position definitions.	27
Figure 6 – Definitions of the rotation and translation matrixes.	27
Figure 7 – Wheel speed for turning radius.	29
Figure 8 – FDA. (a) Captured image. (b) Final foliage image. (c) Algorithm block diagram.	31
Figure 9 – Different edge detection methods.	32
Figure 10 – GDA1.	33
Figure 11 – GDA2.	35
Figure 12 – Four edge masks.	36
Figure 13 – GDA3. (a) Captured image. (b) Edged image. (c) Index image. (d) Final image.	37
Figure 14 – Experimental towing cart.	38
Figure 15 – Evaluation results of the relation between saving potential and grape clusters in the image.	39
Figure 16 – Human-robot working diagram.	41
Figure 17 – Collaboration level 1. (a) User marked. (b) Binary image for analysis.	42
Figure 18 – Collaboration level 2.	43
Figure 19 – Collaboration level 3. (a) Robot marked image. (b) Binary image to be sprayed.	44
Figure 20 – Marking methods & results.	45
Figure 21 – User interface. (a) Setting window. (b) Marking window.	47
Figure 22 – Performance measures illustration	48
Figure 23 – Learning experiment results.	50
Figure 24 – Results of marking methods comparison	53
Figure 25 – Results of collaboration level	55
Figure 26 – Fixed nozzle spraying method.	58
Figure 27 – Pan\tilt head with spraying nozzle attached.	59
Figure 28 – Varying spray diameter.	59
Figure 29 – (a) Grape clusters. (b) Ground truth of grape clusters.	60

Figure 30 – Pesticide waste (False Alarm + overlapping).....	61
Figure 31 – Number of sprays.	62
Figure 32 – Economic function results.	63
Figure 33 – Economic function results ($WV = 6 \cdot 10^{-6} [\$]$).....	64
Figure 34 – Spraying device. (a) Isometric view – CAD. (b) Front view. (c) Side view.	66
Figure 35 – Flow rate evaluation results.....	67
Figure 36 – Experiment configuration.....	68
Figure 37 – Sprayed target.....	68
Figure 38 – Experimental results.....	69
Figure 39 – Robotic sprayer work procedure.	70
Figure 40 – Target detection procedure.....	73
Figure 41 – Experiment configuration.....	74
Figure 42 – Image captured immediately after spraying.....	75
Figure 43 – Experimental results.....	76
Figure 44 – Robotic sprayer work procedure.....	78
Figure 45 – Robot following red strip and targets spread along plastic net.....	79
Figure 46 – Target patterns.....	80
Figure 47 – Target groups. (a) Robot can detect. (b) Robot cannot detect.....	80
Figure 48 – Adding FA.....	80
Figure 49 – Human marking targets	82
Figure 50 – Evaluation documentation.....	83
Figure 51 – Target spraying evaluation scale 5 (outstanding) → 1 (poor).....	83
Figure 52 – Experimental results for the circles marking method.....	85
Figure 53 – Experimental results for the free hand marking method.....	86

List of Tables

Table 1 – Examples of robotic applications in agriculture.	11
Table 2 – Examples of work on robotic sprayers.	13
Table 3 – Examples of work in human-robot collaboration.	15
Table 4 – Examples of previous work on human factors.....	18
Table 5 – Robotic platform specifications.	26
Table 6 - Examples of work in grape detection.	30
Table 7 – Decision tree parameters.....	35
Table 8 – Robot speed in relation to processing time.	39
Table 9 – GDA3 performance of the four masks.....	40
Table 10 – Final GDA's performance.	40
Table 11 – Experimental design - learning time.	50
Table 12 – Experimental design - manual collaboration, three marking methods.	51
Table 13 – Number of clicks difference	52
Table 14 – Results of ease of use questionnaire.	52
Table 15 – Marking method results summary. paired t-test, df=49, t-critical=2.0095.	53
Table 16 – Experimental design.	54
Table 17 – Robot automatic image analysis grape detection performance.	56
Table 18 – Human-robot collaboration level results summary.....	56
Table 19 – Equilibrium points.	64
Table 20 – Experimental results summary.....	69
Table 21 – Number of sprays.....	85

Abbreviations

ACP	–	Artificial Control Point
ASD	–	Adjustable Spraying Device
CP	–	Control Point
DDTM	–	Distance Dependent Transformation Matrix
DOF	–	Degree Of Freedom
FDA	–	Foliage Detection Algorithm
GDA	–	Grape Detection Algorithm
OTOS	–	One Target-One Shoot
POV	–	Point Of View
PTU	–	Pan Tilt Unit
RTM	–	Rotation and Translation Matrix
SA	–	Situation Awareness
TM	–	Transformation Matrix
TTC	–	Time To Complete
UAV	–	Unmanned Aerial Vehicle

Acknowledgements

This work is dedicated to my father **Haim Berenstein** who passed away unexpectedly during my Ph.D studies. My father, a mechanical engineer, equipped me with the basic instincts of an engineer which led me into the world of engineering development.

First, I would like to acknowledge **Prof. Yael Edan** for her long guidance and enormous support throughout the different stages of my M.Sc and Ph.D work. Also, I thank Prof. Edan for teaching me the essential principals of becoming a researcher.

I would like to acknowledge the following for their assistance with the creation of the robotic sprayer: **Nissim Abu-Hazera** and **Yossi Zahavi** for their enormous support during all stages of this work, **Prof. Amir Shapiro** for his assistance with the design and kinematics of the robotic platform, **Prof. Ohad Ben-Shahar** for his assistance with machine vision algorithms and image registration algorithms, **Itay Levental** and **Elad Levi** for their assistance with the mechanical design of the robotic platform, **Udi Anconina** and **Dudi Amsalem** for their contribution with the vineyard navigation algorithm, **Merav Dichter** and **Tal Cohen** for assisting with the human collaboration experiments, **Sapir Rozenthal** for assisting with the human collaboration levels experiments.

Finally, I would like to acknowledge my family, my mother **Ilana Berenstein** and my two sisters **Anat** and **Yasmin**, for their unconditional support and smart advices.

1. INTRODUCTION

1.1. Description of the problem

Pesticides are an integral part of agriculture worldwide. Between 30% and 35% of crop losses can be prevented when harmful insects and diseases are eliminated by applying pesticides (Cho and Ki 1999). Application of nutrients, fungicides, and pesticides is one of the most important processes in agricultural production and can have a significant impact on yield, quality, and ultimately profitability (Singh, Burks and Lee 2005).

Although pesticides are necessary in modern agriculture, they are poisonous and dangerous for humans (Rogan and Chen 2005; Dasgupta, Meisner, Wheeler, Xuyen and Thi Lam 2007) and for the environment (Pimentel and Lehman 1993; Reus, Leendertse, Bockstaller, Fomsgaard, Gutsche, Lewis, Nilsson, Pussemier, Trevisan and Van der Werf 2002), and therefore one of the goals in agriculture research is to reduce the use of pesticides while maintaining the crop quantity and quality.

Two common methods are currently used to apply pesticides in the field. Each method has its pros and cons:

Manual – humans manually spray targets using back-pack sprayers

Using this method, a human operator walks along the rows and selectively sprays targets using a backpack sprayer (Figure 1a). This method is often used when high spraying accuracy is needed (e.g., spraying tomatoes in a greenhouse) and the human, due to his excellent perceptual skill, can achieve this accuracy. This method has several disadvantages, high time to complete (TTC), large number of working hands required to complete the task, and high human fatigue. Due to the high operative costs of this spraying method and lack of human labor and availability it is less used in modern western agriculture practice.

Mechanical – human drives a sprayer tractor

Using this method, a human drives a tractor with a sprayer connected to a trailer behind the tractor (Figure 1b). The human can control the opening/closing of the spray from the tractor cabin and usually opens the spray at the beginning of the row and closes it at the end of the row. This method is often used in open field crops, and in orchards and greenhouses when the entire crop (foliage and fruit) must be sprayed. This method is also used in the absence of human workers. This spraying method is very cost effective since it requires a single operator to cover large areas. The main

disadvantage of this method is the high waste of pesticide when needing to spray isolated targets and even while spraying the foliage (since the foliage top and bottom borders are not straight). Aerial spraying (both by plane and helicopter) is another method commonly used for pesticide application, but since this method is applied from above the crop and at great distance from it (~35 m compared to 1 m used in ground spraying), the accuracy of this spraying method is very limited and therefore not considered for accurate grape clusters spraying.



Figure 1 – Pesticide spraying methods. (a) Backpack sprayer. (b) Tractor sprayer.

Despite the use of pesticide protection equipment (personal head mask for the manual spraying method and central air filtration system for the mechanized spraying method) the human is still exposed to hazardous pesticides that can cause negative health issues (Swan, Kruse, Liu, Barr, Drobnis, Redmon, Wang, Brazil, Overstreet and Group 2003) when applying pesticides using the traditional methods.

Robotic technology may provide a means of reducing agriculture's current dependence on herbicides, improving its sustainability and reducing its environmental impact (Slaughter, Giles and Downey 2008). A target-specific robotic sprayer can reduce the quantity of pesticides applied in modern agriculture and potentially remove or minimize the human presence during the spraying pesticide process (Lee, Slaughter and Giles 1999). Studies show that pesticide use can be reduced up to 60% when the spraying material is targeted toward the designated object (Elkabetz, Edan, Grinstein and Pasternak 1998; Goudy, Bennett, Brown and Tardif 2001; Gil, Escol, Rosell, Planas and Val 2007). The spraying task of a spraying robot can be divided into three sub-tasks:

1. Navigating – driving along the crop row (including end of the row turn),
2. Target detection – detect the target needing to be sprayed. The detection process includes accurate resolution of the target coordinates and surrounding perimeter, and

3. Spraying – spraying the target area.

In this work we focus on the tasks of target detection and spraying. The case study for this work was specific grape clusters spraying. Gibberellic acid (GA_3) has been routinely used for seedless grape production in modern table grape growth to increase berry and bunch weight, and cause thinning of clusters (Lu, Lamikanra and Leong 1995). Growers can minimize undesirable effects by applying GA_3 directly to the clusters (Fidelibus and Vasquez 2012). However, to date this direct application is impractical due to lack of technology (Fidelibus and Vasquez 2012).

Extensive work has been conducted throughout the past decade on object detection in the complex agricultural environments (Kapach, Barnea, Mairon, Edan and Ben-Shahar 2012), but detection rates in real world conditions remain limited to a 90% hit rate and are often much less (Jimenez, Ceres and Pons 2000; Kapach, Barnea, Mairon, Edan and Ben-Shahar 2012). The limited performance is usually caused by the complicated agricultural conditions (Jimenez, Ceres and Pons 2000; Kapach, Barnea, Mairon, Edan and Ben-Shahar 2012) that are due to the high variability of the agricultural objects (i.e., color, texture, orientation), their amorphous size and shape, and the unstructured and dynamic environmental conditions (e.g., changing illumination directions, shading, and targets occlusion). Recent work by Correa, Valero, Barreiro, Diago and Tardáguila (2012) showed a 95% hit rate for detecting red grape clusters, but with an artificial white screen as background (to avoid confounding effects from the background vegetation); it is reasonable to assume that the hit rate performance of these algorithms will decrease under real world conditions and for green grapes. According to Blackmore, Have and Fountas (2001), in order for the robot to be economically feasible it must be able to detect and spray more than 95% of the targets successfully. In this thesis we developed *machine vision algorithms that are able to detect green grapes and foliage with ~95% detection rates* (Berenstein and Edan 2012).

Unlike robotic sprayers, humans can easily fit themselves into such changing environments due to their high perception skills. By taking advantage of the human perception skills and incorporating this with the robot's accuracy and consistency, a combined human-robotic system can be simplified and result in improved performance (Fong and Thorpe 2001).

Vast research has been conducted in the area of HRI (Human-Robot Interaction) focusing on interaction modalities (Goodrich and Schultz 2007; Jaimes and Sebe 2007; Sim and Loo 2015) and models for collaboration (Bechar and Edan 2003; Chen, Barnes and Harper-Sciarini 2011; Cherubini, Passama, Fraisse and Crosnier 2015). In order to increase target detection rates in agriculture conditions, in this thesis we *propose a framework that includes a human operator to help*

the robot with the target detection task. The suggested framework places the human at a remote location and uses the human's excellent perception skills to mark targets on images captured from a robot in the field.

Recent work performed in parallel to this thesis shows some design principles for developing a teleoperated user interface for an agricultural sprayer (Adamides, Katsanos, Christou, Xenos, Kostaras and Hadzilacos 2013; Adamides, Christou, Katsanos, Xenos and Hadzilacos 2015). As opposed to Adamides's work, which focuses on teleoperation only, in this thesis we focus on the question of *how the human and the remote robotic sprayer should collaborate to successfully complete the pesticide spraying task.* The assumption is that some tasks can be performed autonomously, and some tasks collaboratively.

This thesis focuses on several questions that arise from the suggested human-robot collaborative framework, such as *how the human should mark the targets* and *what is the best collaboration method between the human and the robot for the target detection task.*

No other research to date has focused on **human-robot collaboration in agricultural applications.** Increasing the pesticide accuracy can also be achieved by improving traditional spraying methods. Due to the amorphous shape and varying position of the targets in the agriculture domain, a novel spraying device must be able to direct the spraying nozzle toward the target to accurately spray the target (i.e., adjust the spraying diameter to the target). In this thesis such *a spraying device was developed and tested.*

1.2. Research objectives

This research aimed to develop a human-robot collaborative agriculture robotic sprayer. The main objectives were to introduce a collaborative human-robot system into agricultural robotics applications and maximize spray coverage efficiency.

The specific research objectives were to develop:

- a wheeled robotic platform for selective spraying in vineyards,
- machine vision algorithms for foliage detection and grape detection,
- a human-robot collaborative framework system for detecting and marking areas to be sprayed, and
- a smart spraying device for pesticide application.

1.3. Research significance

The development of a fully autonomous robotic system performing tasks in unstructured environments, such as military, medical, and agricultural, is problematic, due to the dynamic, unpredictable, and unknown nature of these unstructured environments and due to sensor limitations. Humans, on the other hand, have good perception skills and can easily fit themselves into such undefined and changing environments. Collaboration between a human and a robot for the task of detection can create a simplified, flexible, and robust system that will use the advantages of both human and robot and can react and cope with dynamic and complex conditions. *A framework for human-robot collaboration was developed and implemented for the specific task of targeted spraying including extensive field evaluation.* The insights from this work can be applied to many additional agricultural tasks and to robots performing other target detection tasks in unstructured environments.

Current practice of pesticide spraying is conducted similarly for different types of targets (e.g., round with constant size such as apples, and amorphous shape and size like grape clusters) since traditional spraying technology is not able to detect and isolate the targets, and moreover is not able to adjust the spray coverage according to the target at hand. In previous work dealing with agricultural robots (Bechar and Edan 2003), targets were defined and marked by a human operator as a singulated point usually located at the target's center of mass. In crops with relatively constant object shape and size such as citrus and apples the center of mass can provide a good indicator for target (center of mass coordinated with a relatively constant size can provide a full description of the target); however, when considering the detection and marking of targets with amorphous shape and varying size, the center of mass will not provide sufficient description of the target. Spraying only the target center of mass will cause either extensive area misses when using a small spraying diameter or extensive pesticide waste when using a large spraying diameter. *In this work we developed target marking methods specifically for amorphous shaped targets. We developed a site-specific spraying device able to implement the enhanced detection accuracy to the actual pesticide spraying process.* The best spraying method can be selected based on the task objective which can be selected by the farmer: the farmer can aim to maximize the hit rate or minimize false alarms.

1.4. Research contribution and innovations

This work was developed under *a new concept that considered pesticide reduction as the main optimization parameter while maximizing target spray accuracy*. Machine vision algorithms were developed for the task of detecting fruit and foliage in vineyards. *Foliage and grape clusters detection algorithm were developed* (Berenstein, Shahar, Shapiro and Edan 2010). The algorithms' development was based on images captured from a commercial vineyard in Israel. Since the algorithms are not solely based on color recognition, but also use the shape and texture properties of the grape cluster, the detection of all grapes varieties is possible (i.e., green and red type grapes). Three algorithms were developed, each with a different strategy for the grape clusters detection. The first algorithm was based on the difference in edge distribution between the grape clusters and the foliage. Using the different edge distribution between the grape clusters and the foliage, the grape clusters can be isolated. The second algorithm was based on a decision tree algorithm that used 72 different parameters. The third algorithm is based on pixel comparison between edge representations of the captured image with a predesigned edge mask that represents grapes. *The second algorithm showed the best detection rate (~91% hit rate), which according to state of the art literature (Gongal, Amatya, Karkee, Zhang and Lewis 2015) is considered a very high detection rate*. Blackmore, Have and Fountas (2001) argue that 95% is the lowest barrier for detection in order for the spraying process to be economically feasible.

Further improvement of the detection rate was achieved by applying collaboration between a human operator and a robotic sprayer. *A novel human-robot collaboration framework and methods for the target detection task were developed and evaluated in a series of experiments*. The suggested framework places the human in a remote location from the field and by using an imaging device (e.g., computer screen, tablet, PDA, smartphone) helps the robot to detect the targets. Four levels of collaboration were developed based on Sheridan (1992) suggested 10 levels of human-robot collaboration levels. Fully manual - the human operator marks the targets in the image without any help from the robot. Robot suggests, human approves - using this collaboration method the grape clusters in the captured image are automatically marked using Berenstein, Shahar, Shapiro and Edan (2010) detection algorithms. The marked areas are considered as recommendations for the human operator to mark the grape areas. Robot marks, human supervises - the human receives an image with grape clusters marked using Berenstein, Shahar, Shapiro and Edan (2010) detection algorithms. The human has the ability to manually reject robot marked areas and add areas to be sprayed. Fully autonomous robot marking - the robot is fully independent and there is no human intervention.

One of the questions that arise with the collaboration of a human operator into the target detection of grape clusters is: *what is the marking technique that the human should use when the task is to mark amorphous shapes with varying size as the grape clusters are?* In this work we answered this question by developing a user interface equipped with several target marking options. *Three target-marking methods were developed, implemented in a user interface, and tested.* The suggested marking methods were: (i) circle with constant diameter, (ii) ellipse with changeable diameters, and (iii) free hand (the human marks surround the target). Evaluating different combinations of the marking methods with the collaboration levels provides the optimal combination of marking method with collaboration level for different marking goals (i.e., if the goal is high hit rate then the optimal combination is a constant circle with collaboration level 3).

The collaborative aspect between the human and the robotic sprayer is applied only for the target detection task; the actual pesticide spray is conducted solely by the robotic sprayer. In order to reduce the quantity of pesticide being used, a smart accurate spraying device is needed to accurately spray the marked targets. Preliminary evaluation of three spraying options revealed that the optimal spraying method (for the grape cluster type targets) is to use a single nozzle with an adjustable spray diameter. Thus, *a smart spraying device able to control the spray diameter was designed, built, and tested.* In the heart of the device lies a stepper motor connected to a nozzle cup, and by rotating the nozzle cup the spray diameter is changed. The device was mounted to a pan-tilt unit with two DOF allowing it to rotate horizontally and vertically. A series of experiments were conducted to evaluate the nozzle flow-rate with different nozzle apertures, the nozzle spray diameter according to the nozzle cup rotational position, and the entire device including automatic target detection and spray. *A custom mobile robotic platform was designed and built specifically for the vineyard environment aiming to provide a research platform for pesticide spraying in vineyards.* The robot was constructed from two identical platforms interconnected with universal joint. Four wheels were connected to the robot, two for each platform. Each platform was equipped with an electric motor. The robotic platform was equipped with an electric box containing all the electrical components. The robot was also equipped with a commercial “off the shelf” 200L sprayer, power generator, and two car batteries. This robot platform can serve additional human-robot collaborative R&D.

Additional contribution of this research is related to development of a novel image registration algorithm. *An image registration algorithm and methods were developed to enable the fusion of different imaging sensors in the agricultural domain* (Berenstein, Hočevár, Godeša, Edan and Ben-Shahar 2015). The novel concept of the algorithm is to capture a scene containing custom design

control points, by the two sensors from varying distances between the sensors and the control points. A Transformation Matrix (TM) is then calculated for each distance. Once obtaining the TMs from varying distances, a regression is performed on each of the elements of the TM and a distance-dependent relation function is created for each element of the TM. The concept of the operation is to detect the distance between the sensors and the target (using distance sensor, e.g., SICK laser distance sensor DT35) and calculate TM according to the measured distance. Although the algorithm was designed and tested for two different sensors, the algorithm can be easily expanded for additional sensors of the same type and for different sensors. Since it was not included in the vineyard robotic experiments in this thesis, it is not included as a separate chapter here.

2. SCIENTIFIC BACKGROUND

2.1. Pesticides in agriculture

Pesticides are those substances that are used to control, destroy, repel, or attract pests to minimize their detrimental effects. Pests are those organisms, such as weeds, insects, bacteria, fungi, viruses, and animals, which adversely affect our way of life. Pests can reduce the quality and quantity of food produced by lowering production and destroying stored produce (Kent 1992). Without the use of pesticides, the production and quality of food would be severely jeopardized, with estimates that food supplies would immediately fall to 30 to 40% of their current levels due to the ravages of pests (Kent 1992; Cho and Ki 1999); thus, modern agriculture relies on the use of pesticides to increase crop yields and sustain food safety and security for the global population (Cooper and Dobson 2007). Pesticides are poisonous and wrong use of them is dangerous for humans (Betarbet, Sherer, MacKenzie, Garcia-Osuna, Panov and Greenamyre 2000; Eddleston, Karalliedde, Buckley, Fernando, Hutchinson, Isbister, Konradsen, Murray, Piola and Senanayake 2002; Rogan and Chen 2005; Dasgupta, Meisner, Wheeler, Xuyen and Thi Lam 2007; Dawson, Eddleston, Senarathna, Mohamed, Gawarammana, Bowe, Manuweera and Buckley 2010; Remoundou, Brennan, Hart and Frewer 2014) and for the environment (Tardiff 1992; Pimentel and Lehman 1993; Reus, Leendertse, Bockstaller, Fomsgaard, Gutsche, Lewis, Nilsson, Pussemier, Trevisan and Van der Werf 2002; Bozdogan, Yarpuz-Bozdogan and Tobi 2015; Lambropoulou, Hela, Koltsakidou and Konstantinou 2015). Recent work in the United States showed that banning pesticides and chemical fertilizers would cause loss of half of the fruits and vegetables, and loss of 40%–70% of grains and cotton. This loss would cause increase of food costs of more than 40% (MOH 2006).

Latest studies show that pesticide use can be reduced up to 60% by using selective sprayers (Elkabetz, Edan, Grinstein and Pasternak 1998; Goudy, Bennett, Brown and Tardif 2001; Gil, Escol, Rosell, Planas and Val 2007; Song, Sun, Li and Zhang 2015).

2.2. Agricultural robots

Agricultural robots have been developed for many operations, such as field cultivation, planting, spraying, pruning, and selective harvesting (Edan, Kondo and Shufeng 2009). Intensive research has focused on selective harvesting of citrus, apples, tomato, cucumbers, melons, strawberries, and grapes (Kondo 1991; Edan and Miles 1993; Monta, Kondo and Ting 1998; Bulanon, Kataoka, Ota and Hiroma 2001; Van Henten, Hemming, Van Tuijl, Kornet, Meuleman, Bontsema and Van Os

2002; Hannan and Burks 2004; Bac, Henten, Hemming and Edan 2014). Other aspects that were thoroughly studied are target detection and end effectors for fruits and vegetables (Table 1).

Agriculture robots must operate in unstructured, dynamically changing, and undefined environments that demand a high level of sophistication and complicate the development process (Bac, Henten, Hemming and Edan 2014). Agriculture robots have been demonstrated by several researchers, but despite the intensive research, commercial robots are still rare (Bac, Henten, Hemming and Edan 2014). Although commercial agriculture robots exist (Hannan and Burks (2004); Harvest Automation Co HV-10), the lack of economic justification is the main reason for the absence of robots in agriculture (Edan, Kondo and Shufeng 2009). This is mainly limited by low performance rates (low detection) and lack of robustness (Bac, Henten, Hemming and Edan 2014).

Another field of study in agricultural robots is the use of unmanned aerial vehicles (UAVs) mostly applied for precision agriculture imagery tasks. Zhang and Kovacs (2012) reviewed the field of small UAVs for precision agriculture and concluded that although in the past decade the number of UAVs for agriculture increased they still possess many significant shortcomings such as high initial cost, platform reliability, sensors capabilities, lack of standardized procedure, aviation regulations, and lack of interest from farmers.

There is limited work published on UAV's in agriculture in tasks other than imagery tasks. Xue, Lan, Sun, Chang and Hoffmann (2016) developed a UAV equipped with an automatic control spraying system. The UAV was equipped with ultra-low volume spraying. Results showed 0.2 m route accuracy. The spraying accuracy was not reported. Façal, Pessin, Filho, Carvalho, Furquim and Ueyama (2014) proposes a methodology based on Particle Swarm Optimization (PSO) for the fine-tuning of control rules during the spraying of pesticides in crop fields. This methodology can be employed with speed and efficiency and achieves good results by taking account of the weather conditions reported by a Wireless Sensor Network (WSN). In this scenario, the UAV becomes a mobile node of the WSN that is able to make personalized decisions for each crop field.

Although UAVs are a promising field of research for precision agriculture, we do not expect it to replace robots in the field for tasks like picking, pruning, and spraying, mainly due to the payload limitation of current UAV's.

Table 1 – Examples of robotic applications in agriculture.

Application	Sensor	Moving platform	References
Melon harvester	2 CCD BW cameras	Tractor carrying robotic platform	(Edan and Miles 1993)
Grape harvester	TV camera	Crawler	(Kondo 1991)
Navigating tractor along crop row	CCD camera	Tractor modified to robot	(Gerrish, Fehr, Van Ee and Welch 1997)
Mapping agricultural field	Ultrasonic	4-wheeled, angle and speed control for each wheel	(Toda, Kitani, Okamoto and Torii 1999)
Greenhouse tasks	CCD camera	Rail platform	(Belforte, Deboli, Gay, Piccarolo and Aimonino 2006)
Eggplants harvester	CCD camera	Crawler	(Hayashi, Ganno, Ishii and Tanaka 2002)
Plantation sprayer	2 CCD camera for stereo vision, laser scanner	Tractor modified to robot	(Stentz, Dima, Wellington, Herman and Stager 2002)
Weed management	2 CCD cameras one for overall picture and one for focus image	Tractor carrying robotic platform	(Blasco, Aleixos, Roger, Rabatel and Molto 2002)
Weed eradicate	2 CCD cameras, one for navigation and one for weed detection	4-wheeled, angle and speed control for each wheel	(Strand and Baerveldt 2002)
De-leafing cucumber plants	CCD camera	Move along heat pipes	(Van Henten, Van Tuijl, Hoogakker, Van Der Weerd, Hemming, Kornet and Bontsema 2006)
General field propose	Currently no sensors	4-wheeled, angle and speed control for each wheel	(Khot, Tang and Hayashi 2006)
Strawberry harvester	CCD camera	Using greenhouse infrastructure	(Cui, Nagata, Guo, Hiyoshi, Kinoshita and Mitarai 2007)
Arecanut tree climbing	Currently no sensors	X-bar with two identical clamping units	(Mittal, Varada, Dave, Khanna, Korpu and Tilak 2014)
Weed management	GPS, CCD camera	Autonomous tractor	(Pérez-Ruiz, Gonzalez-de-Santos, Ribeiro, Fernandez-Quintanilla, Peruzzi, Vieri, Tomic and Agüera 2015)
Monitoring field operations	GPS, IMU, CCD camera	Six geared motors with skid steering method	(Durmuş, Güneş, Kırıcı and Üstündağ 2015)
Wheat precision seeding	Not reported	4-wheeled, angle and speed control for each wheel	(Haibo, Shuliang, Zunmin and Chuijie 2015)

2.3. Spraying robots in agriculture

Spraying robots are commonly used in the field of automotive painting and vast research was applied in this field (Chen, Fuhlbrigge and Li 2008) with the main focus on path planning of the robotic arm and achieving uniform paint thickness layers (Arikan and Balkan 2000; Zaki and Eskander 2000; Conner, Greenfield, Atkar, Rizzi and Choset 2005; Diao, Zeng and Tam 2009; Wei and Dean 2009; From, Gunnar and Gravdahl 2011). The common denominator of these robots is that the shape, position, and orientation of the target to be sprayed/painted is known and the robot trajectory and nozzle operation are pre-planned accordingly. Unlike these industrial robots, spraying robots in agriculture must include two core technologies: sensing – for target detection and “robotics” for the spray execution (Song, Sun, Li and Zhang 2015). Since the technologies of the automotive industry and the agricultural domain are completely different, this literature review will focus solely on the agricultural domain.

Several spraying robots designed for the agricultural domain have been developed (Table 2) and, much like other agriculture robots, these developments have yet to become commercial products. The review below focuses mainly on weed control and plant protection applications (Table 2).

2.4. Human-robot collaboration

Humans have superior recognition capabilities and can easily adapt to changing environmental and object conditions (Rodriguez and Weisbin 2003). Their acute perception capabilities enable humans to deal with flexible, vague, changing, and wide scope of definitions (Chang, Song and Hsu 1998). This set of skills makes the Human Operator (HO) perfect for supervising a machine. In the strictest sense, supervisory control means that one or more HOs are intermittently programming and continually receiving information from a computer that itself closes an automation control loop through artificial effectors and sensors to the controlled process or task environment (Sheridan 1992).

There are several motivators for developing human-robot collaborative control. First, it combines the advantages of the robot with the advantages of the HO. Specifically; it achieves the accuracy, reliability, and high yield of the robot with the cognitive capability and adaptability of the human. Moreover, by collaboration, the workload of the HO is reduced and in the event of robot or human failure, either can reduce the damage. Second, it makes control possible even where there are time delays in communication between human and robot. Last, it saves lives and reduces costs by eliminating the need for the HO to be present in hazardous environments (Sheridan 1992).

Furthermore, it simplifies the robotic system since the complex tasks can be performed by the human. Research in the field of human supervisory control started in 1967 with the work of Ferrell and Sheridan (1967) and continues, with much effort, until this day (Table 3).

Table 2 – Examples of work on robotic sprayers.

Application	Sensor	Results	Reference
Greenhouses	Ultrasonic + camera	Navigate autonomously along the greenhouse	(Mandow, Gomez-de-Gabriel, Martinez, Munoz, Ollero and Garcia-Cerezo 1996)
Tomatoes	RGB camera	8% incorrect spray (4 of 51)	(Lee, Slaughter and Giles 1999)
Orchards	Color + Ultrasonic	NOT REPORTED	(Shin, Kim and Park 2002)
Weed in cotton	Color CCD	Sprayed 88.8% of weed while correcting, rejecting, and not spraying 78.7% of cotton	(Lamm, Slaughter and Giles 2002)
Weed sprayer	Color video	Reduce up to 91% with max speed of 14 [km/h]	(Steward, Tian and Tang 2002)
Rice	NIR	Reduce of pesticides (no quantitative results)	(Nishiwaki, Amaha and Otani 2004)
Weed control	USB camera	83% success rate with less than 3 seconds per target	(Jeon, Tian and Grift 2005)
Greenhouse navigation	Ultrasonic	Navigate autonomously along the greenhouse	(Singh, Burks and Lee 2005)
Greenhouses	CCD Camera	Present the ability to navigate in artificial greenhouse	(Younse and Burks 2005)
Grapes	Ultrasonic	NOT REPORTED	(Ogawa, Kondo, Monta and Shibusawa 2006)
Clean road shoulder	Color CCD	Reduce pesticide use by up to 97%	(Slaughter, Giles and Downey 2008)
Palms	Stereo camera	Scale down model proves the ability to track palm trees	(Shapiro, Korkidi, Demri, Ben-Shahar, Riemer and Edan 2009)
Blueberry	color camera	Variable rate sprayer was used for spot-application of fungicide in a wild blueberry field	(Esau, Zaman, Chang, Schumann, Percival and Farooque 2014)
Technology review of smart spray in agriculture			(Song, Sun, Li and Zhang 2015)
Grapevine	color camera	Selective spraying of grapevine using robot arm manipulator	(Oberti, Marchi, Tirelli, Calcante, Iriti, Tona, Hočevár, Baur, Pfaff, Schütz and Ulbrich 2016)
Blueberry	machine vision	Economic evaluation of selective sprayer	(Esau, Zaman, Groulx, Corscadden, Chang, Schumann and Havard 2016)

Scientific research in the field of human-robot collaboration in agricultural tasks has been very limited with hardly any work that included field experiments (Cheein, Herrera, Gimenez, Carelli, Torres-Torriti, Rosell-Polo, Escolà and Arnó 2015).

Bechar and Edan (2003) provide proof of the advantage of such collaborations in target recognition tasks. According to their research, collaboration of human and robot increases detection by 4% when compared to an HO alone and by 14% when compared to a fully autonomous system. In addition, when compared to the human alone, detection times of integrated systems are reduced by 20%. (Bechar, Meyer and Edan 2007) defined four basic levels of human-robot collaboration for target recognition tasks. In order to quantify performance and determine the best collaboration level for a given set of parameter values, an objective function that includes operational and time costs was developed. The findings indicate that the best system performance, the optimal values of performance measures, and the best collaboration level depend on the task, the environment, human and robot parameters, and the system characteristics.

This work has been expanded for dynamic real-time switching between collaborative levels and for evaluating the influence of humans' reaction times on performance of integrated human-robot target recognition (Tkach, Edan and Bechar 2009). The switching algorithm developments enable smooth real-time adaptation of the combined human-robot system to many possible changes of the environment, human operator, and robot performance. Tkach showed that increasing the switching execution frequency greatly improves the score achieved by the switching algorithm and increases system performance (Tkach 2009). Analysis of the model developed to evaluate the effect of reaction time on the human-robot collaboration level reveals an extreme threshold selection in two cases: when human sensitivity decreases and when the cost of time increases (Yashpe 2009; Yashpe, Bechar and Edan 2009). The above research was conducted on field data; however, studies were limited to human-robot collaboration in laboratory studies and simulations.

Adamides, Christou, Katsanos, Xenos and Hadzilacos (2015) presented usability guidelines for agricultural teleoperated robot based on a focused literature review, teleoperation interface design guidelines, user centered methods, and limited field experiments. Murakami, Ito, Will, Steffen, Inoue, Kita and Miyaura (2008) developed a teleoperated system for a crawler robotic vehicle that aimed to navigate the robot along a pre-defined path. Two degree cooperation between the robot and the remote operator was set, including direct and supervisory control. The study shows that the direct control was difficult for the operator due to high delay time between the operator command

and the robotic response. The supervisory mode showed ability to travel straight with a maximum lateral error of 0.3 m.

Table 3 – Examples of work in human-robot collaboration.

Application	Results	Reference
New methodology to incorporate sensor and model-based computer assistance into human-controlled teleoperator systems	Application of the strategy shows improved machine performance	(Everett and Dubey 1998)
Improving the performance of HOs in tasks that involve motion planning and control of complex objects in environments with obstacles	Proposed configuration space control mode performed significantly better than the traditional work	(Ivanisevic and Lumelsky 1998)
Propose that automation can be applied to four broad classes of functions: 1) information acquisition; 2) information analysis; 3) decision and action selection; and 4) action implementation. Within each of these types, automation can be applied across a continuum of levels from low to high, i.e., from fully manual to fully automatic.	The model can be used as a starting point for considering what types and levels of automation should be implemented in a particular system. The model also provides a framework within which important issues relevant to automation design may be profitably explored.	(Parasuraman, Sheridan and Wickens 2000)
Developed a teleoperated system for electrical live-line maintenance	With the operator on the ground, a great improvement in human safety has been introduced	(Aracil, Ferre, Hernando, Pinto and Sebastian 2002)
Outlines a theory of human-robot interaction and proposes the interactions and information needed by both humans and robots for the different levels of interaction, including an evaluation methodology based on situational awareness.	Propose that human-robot interactions are of five varieties, each needed different information and being used by different types of users.	(Scholtz 2003)
Outlines a preliminary perspective on teamwork and adjustable autonomy in groups involving a mix of humans and autonomous agents.	Implement a model of the work practice of human-robot teamwork, by focusing on the differences between people and autonomous agents.	(Sierhuis, Bradshaw, Acquisti, Van Hoof, Jeffers and Uszok 2003)
Automated detection and recognition system of road signs combined with the monitoring of the drivers' response	Automatic sign classification was significantly improved by online image enhancement of the sequences of approaching signs	(Fletcher, Loy, Barnes and Zelinsky 2005)

Application	Results	Reference
Human-Robot collaboration for space missions	The implementation of the method is shown to provide a correlated comparison that maximizes the actual performance of human-robotic systems operating in the real world.	(Howard 2006)
Nature of interactions between children and robots	Their findings may have therapeutic implications for autistic children	(Salter, Dautenhahn and Boekhorst 2006)
Describes an effort to identify common metrics for task-oriented human-robot interaction (HRI).	Assess system performance and operator performance. The author point the need to select appropriate test populations when applying the developed metrics.	(Steinfeld, Fong, Kaber, Lewis, Scholtz, Schultz and Goodrich 2006)
Present findings from a human user study showing that people use the reward signal not only to provide feedback about past actions, but also to provide future directed rewards to guide subsequent actions.	Demonstrates the importance of understanding the human teacher/robot learner system as a whole in order to design algorithms that support how people want to teach while simultaneously improving the robot's learning performance.	(Thomaz and Breazeal 2006)
We evaluate and quantify the effects of human, robot, and environmental factors on perceived trust in human-robot interaction (HRI).	The effects of human, robot, and environmental characteristics were examined with an especial evaluation of the robot dimensions of performance and attribute-based factors.	(Hancock, Billings, Schaefer, Chen, de Visser and Parasuraman 2011)
Mechanical weed control was achieved by a co-robot actuator that automatically positioned a pair of miniature hoes into the intra-row zone between crop plants.	57.5% reduction in hand labor requirements for intra-row weed control	(Pérez-Ruíz, Slaughter, Fathallah, Gliever and Miller 2014)
Summarize the state of the art in human-robot interaction in farmable fields	Introduce the guidelines for designing a human-robot interaction strategy for harvesting tasks	(Cheein, Herrera, Gimenez, Carelli, Torres-Torriti, Rosell-Polo, Escolà and Arnó 2015)

Application	Results	Reference
Analyzes the benefit of planning motion that explicitly enables the collaborator's inferences on the success of physical collaboration, as measured by both objective and subjective metrics.	Results suggest that legible motion, planned to clearly express the robot's intent, leads to more fluent collaborations than predictable motion, planned to match the collaborator's expectations. Functional motion was found to negatively affect coordination, increasing the time it takes to achieve the task, as well as the participant's perception of the collaboration.	(Dragan, Bauman, Forlizzi and Srinivasa 2015)
Intelligent low cost telecontrol system for agricultural vehicles in harmful environments	Describes how to design and implement a low cost telecontrol system for agricultural machinery	(Gazquez, Castellano and Manzano-Agugliaro 2016)
addresses the gap by proposing a novel methodology to generate multimodal lexicons which maximizes multiple performance metrics over a wide range of communication modalities	Experimental results show that predicted optimal lexicons significantly outperform predicted suboptimal lexicons in all metrics validating the predictability of the methodology.	(Jacob and Wachs 2016)

2.5. Human interaction factors

The field of human factors emerged as the confluence of engineering psychology, ergonomics, and accident analysis (Goodrich and Schultz 2007). Key concepts of interaction in human factors (Goodrich and Schultz 2007) include mental workload (Hart and Staveland 1988; Goodrich, Boer, Crandall, Ricks and Quigley 2004), situation awareness (Endsley 2016), mental models mental models (Johnson-Laird 1988; Vicente 1997), and trust in automation (Hoffman, Johnson, Bradshaw and Underbrink 2013).

Human factors are especially important when incorporating the human with his/her exceptional perception skills for target detection under a human-robot collaboration framework. Table 4 summarizes recent work related to human factors in human-robot collaborative studies.

Table 4 – Examples of previous work on human factors

Research	Reference
Situation-awareness global assessment technique (SAGAT), developed to assist maintaining pilot high SA by providing an objective measure of pilot's SA with any given aircraft design, is described.	(Endsley 1988)
SAGAT has been used to assess SA at a various levels of autonomy.	(Kaber, Onal and Endsley 2000; Scholtz, Antonishek and Young 2003)
This paper provides a set of definitions that form a framework for describing the types of awareness that humans have of robot activities and the knowledge that robots have of the commands given them by humans. The case study for this work was an urban search and rescue. Results revealed that primarily critical incidents were due to lack of human-robot awareness of location and surroundings.	(Drury, Scholtz and Yanco 2003)
Operate multiple robotic vehicles and participate in collaborative tasks with these systems. The paper examines SA needs in the context of a collaborative military task. Cognitive task analysis was conducted for the task, along with an examination of potential function allocations that may require operator multi-tasking and frequent task switching.	(Riley and Endsley 2005)
This paper discusses the design of automation support in C2 systems with multiple uninhabited vehicles that operators can best be supported by high-level automation of information acquisition and analysis functions. The results support the use of adaptive automation to enhance human-system performance in supervision of multiple uninhabited vehicles, balance operator workload, and enhance situation awareness.	(Parasuraman, Barnes, Cosenzo and Mulgund 2007)
NASA-TLX (Task Load index) was proposed as a reliable estimation of workload. The estimation is based on six combined workload-related factors.	(Hart and Staveland 1988)
The NASA-TLX has been widely used to measure human performance and workload in teleoperation scenarios.	(Draper and Blair 1996; Kaber, Onal and Endsley 2000; Scholtz, Antonishek and Young 2003)

Research	Reference
Evaluating the workload while using PDA for remotely drive robot. Two screens are available for the user, vision, provides the forward facing camera image, and sensory, provides the on-board ultrasonic and LIDAR sensors. Results show that working with both the vision and sensory screens increased the human workload. When the human was able to view the environment and the robot the workload decreased. The evaluation of the workload conducted using the NASA-TLX method.	(Adams and Kaymaz-Keskinpala 2004)
This work goal was to examine the use of scalable interfaces and to examine operator span of control when controlling one versus two autonomous unmanned ground vehicles. Soldiers instructed to perform missions that included monitoring, surveillance, target acquisition images, and responding to unplanned operator intervention requests from the robot. The results do not indicate major effect on the operator workload when decreasing the interface size.	(Hill and Bodt 2007)
This paper reviewed the empirical literature on operator information processing and action execution. The paper is organized by the operator perceptual and responding demands which are routinely manipulated in HRI studies. The paper also review the utility of different interventions for reducing the strain on the perceptual system (e.g., multimodal displays) and responses (e.g., automation).	(Prewett, Johnson, Saboe, Elliott and Coover 2010)

3. METHODS

3.1. Overview

A fully operative robotic sprayer equipped with an adjustable spraying device and the ability to communicate with a remote user was designed and built. Human-robot collaboration methods were developed as well as methods for target marking by a remote human operator.

In this chapter the different components (Figure 2) that comprised the fully operational robotic sprayer are described.

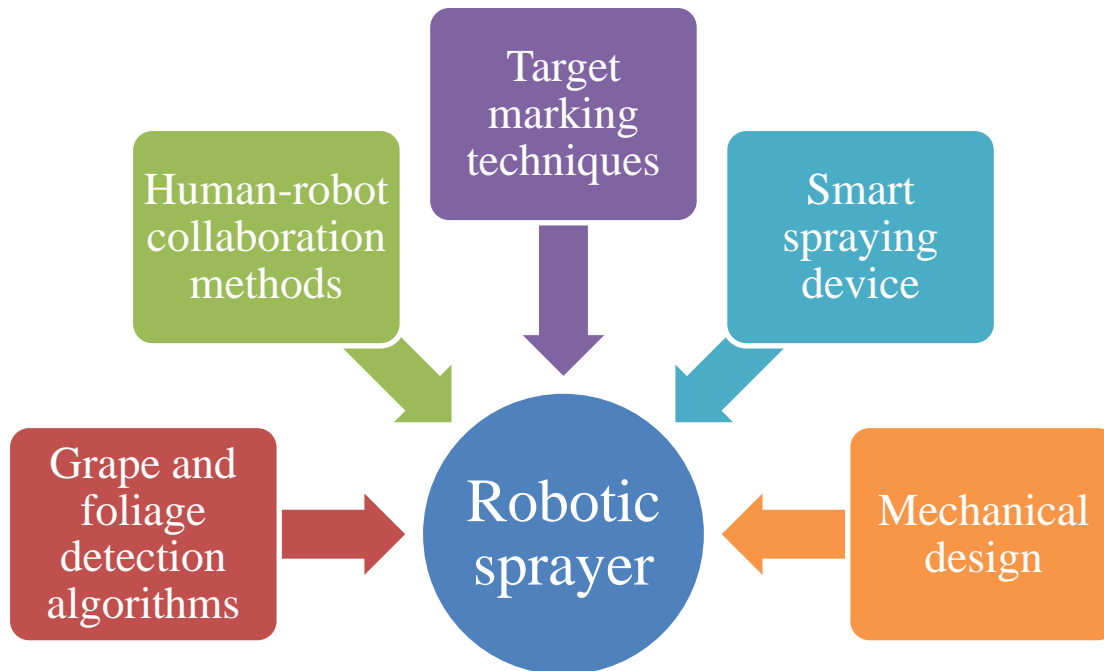


Figure 2 – Robotic sprayer main components.

3.2. Robotic sprayer system

An agricultural robotic system was built to serve as a research tool to enable field experiments and reflect the real-world conditions that a future agricultural robot would have to cope with. The robot is based on two identical platforms interconnected with a Cardan Joint. Each platform includes two electrically controlled wheels. The platform is equipped with an electrical control box containing PC computer, 7" touch screen, controllers, and all of the peripheral equipment needed for the robot operation and conduction of field experiments. The robotic platform is described in detail in Chapter 4.

3.3. Detection algorithms

Machine vision algorithms were developed for the two critical aspects of targeted vineyard spraying: foliage and grape clusters detection. The algorithms were used to enable the robot to autonomously spray the vineyard foliage and the grape clusters specifically while steering autonomously along the vineyard row.

The foliage detection algorithm is mainly based on color thresholding on the different color channels. Three algorithms were developed for the grape clusters detection task. The algorithms were based on: high density edge detection, decision tree, and shape correspondence between an artificial mask and the grape cluster edges (Berenstein, Shahar, Shapiro and Edan 2010). Detailed description of the foliage and grape clusters detection methods are presented in Chapter 5.

3.4. Human-robot collaboration

Human-robot collaboration methods were developed to evaluate the influence of such collaboration on the performance of the hit and false alarm rates. The developed methods included three target marking methods (circle with constant diameter, ellipse with varying diameter, and free hand) and three human-robot collaboration levels (fully manual, robot suggests – human decides, and robot decides – human supervises) corresponding to Sheridan (1992) 10 levels of human-robot collaboration. Each of the target marking methods and the human-robot collaboration levels were tested with groups of participants while using images captured in a commercial vineyard as the experimental database.

A custom design user interface was developed to implement the suggested target marking methods and the human-robot collaboration. The user interface was used both for conducting experiments in the lab and for conducting field experiments using the robotic sprayer. Detailed descriptions of the human-robot collaboration and experiments are presented in Chapter 6.

3.5. Adjustable spraying device

A target-specific spraying device was designed and built for the agricultural task of specific target spraying. The main problem with spraying agricultural targets in general and specifically grape clusters is that their amorphous shape and varying sizes requires adjusting the spraying nozzle for each target. The core functionality of the device is to change the spray diameter according to the detected target. A commercial spraying nozzle (AYHSS 16) assembled from two parts, the nozzle base and the nozzle cap, changes the spray diameter by rotating the nozzle cup. The nozzle base was

fixed to the device while the nozzle cup was connected to a stepper motor. The device also includes a color camera (for capturing targets), distance sensor, and two fan lasers (one positioned horizontally and the other vertically, to create a cross (+) on the target); all were mounted to a pan/tilt unit.

In order to validate the spraying device operation, several experiments were conducted to evaluate the flow rate relative to the nozzle cup rotational position, the spray diameter relative to the nozzle cap rotational position, and the ability of the device to detect and spray targets of different sizes. Detailed description of the adjustable spraying device and experiments are presented in Chapter 7.

3.6. Image registration techniques

A novel registration method suitable for unstructured environments with long intervals of sensing ranges was developed. The registration approach is based on the computation of a “dynamic” transformation matrix in which each element is a function of the distance from the object in the image. In the field this distance can be measured by a range sensor. We demonstrate the utility of our approach using an RGB and thermal camera, as well as a laser scanner. Within the interval, the method offers compact representation of multiple (or infinite, if one considers the continuous range) registration transformations. Thanks to the regression algorithm, the procedure permits registration at distances for which the sensors were not calibrated.

The registration approach (see thesis DVD @ \Papers\ Paper 2 - *Distance-Dependent Multimodal Image Registration for Agriculture Tasks*) was implemented on another robotic platform and hence is not detailed in a separate chapter in this thesis.

4. ROBOTIC SPRAYER

4.1. Overview

This chapter describes the robotic sprayer platform designed and built to serve as a research tool for investigating methods and devices designated for the agricultural domain in general and specifically for vineyards operations. Detecting and spraying the grape clusters was the main agricultural task this thesis focused on.

4.2. Robotic platform

The robotic platform was designed and built at Ben-Gurion University of the Negev (Figure 3).



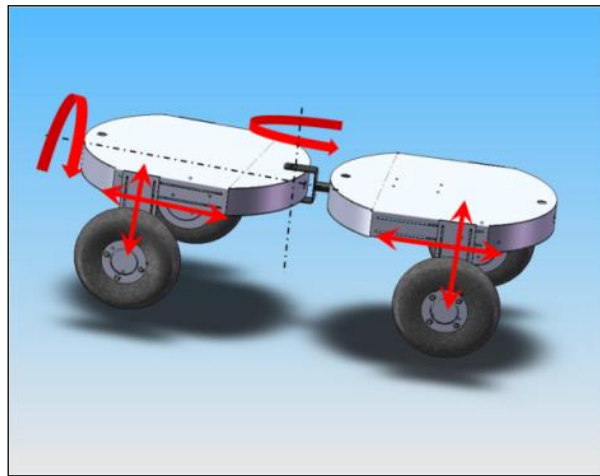
Figure 3 – Robotic platform during field experiments.

The robotic sprayer (Figure 4, Table 5) chassis is assembled from two identical platforms (Figure 4a) that are interconnected using a two DOF universal joint (Cardan Joint, Figure 4b). The first DOF (Figure 4b-A) is used to improve the turning radius, the second DOF (Figure 4b-B) allows the platform designers to neglect the need for complicated suspension system. Despite the fact that the robot is capable of turning with differential steering, allowing a relative angle between the platforms contributes to a smaller turning radius and minimizes side slip of the wheels, resulting in reduced wear of the vehicle and less damage to the field. The design payload of each platform is 300Kg. A modular approach is taken with four identical wheel modules. Each wheel module consists of: ATV wheel (0.5m diameter), wheel shoulder that connect the wheel to the platform, and a 24V-480W electric motor. The electric motor is fixed to the platform and connected to the wheel using chain wheels. An incremental encoder (US DIGITAL – E5) is attached to each electric motor and is used to control the robot. The robot is equipped with an electrical box that is mounted to the front platform and contains the following:

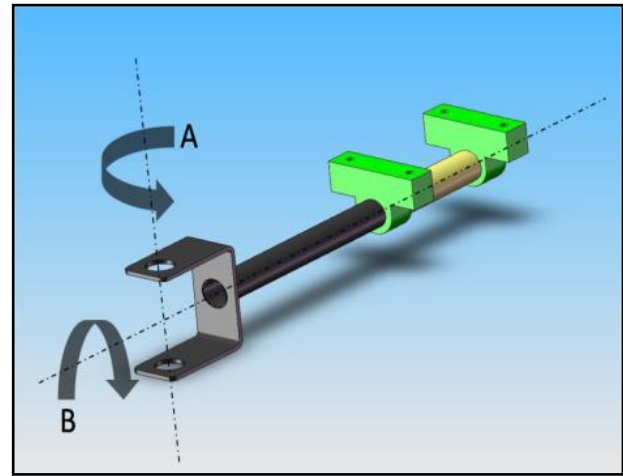
- Small size industrial PC computer with Intel i7 processor,
- 7” touch screen connected permanently to the computer allowing the operator to control and reprogram the robot in field conditions,
- Two electric motor controllers (Roboteq AX3500), each able to control 2 electric motors with current up to 60A each. The controllers are connected to the computer through RS232,
- Other peripheral hardware such as: Arduino boards, flat screen, small batteries; additional devices can be changed according to the experiment.

Other peripheral equipment on the robot includes (Figure 4d):

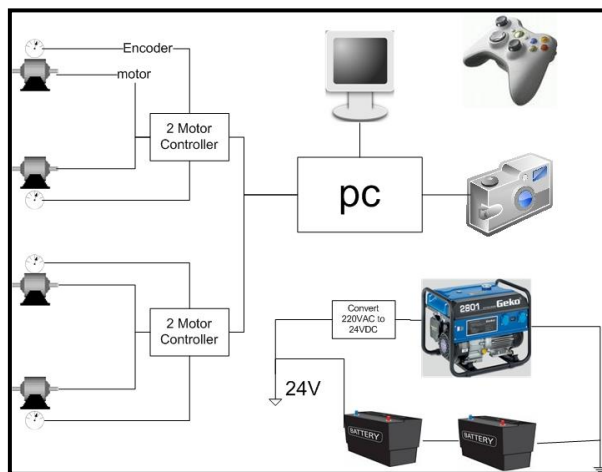
- Color camera (Microsoft LifeCam Studio) mounted to the front platform facing forward,
- Two car batteries 12V 110A/h. The batteries are connected together to get 24V,
- Power generator 2500W (Geko 2801) for continuous power supply during field work,
- Commercial sprayer (200L tank with patrol motor and pressure pump) is mounted to the rear platform,
- Gamepad controller (Microsoft Xbox 360 wireless controller). The controller is used to manually control the robot’s movement.



a



b



c



d

Figure 4 – Robotic sprayer overview. (a) Two identical platforms. (b) Joint that connects the two platforms. (c) Electric power scheme. (d) Robot overview.

Table 5 – Robotic platform specifications.

Mechanical	
Dimensions	120X220X160 [cm] (W-L-H)
Weight	200 [Kg]
Load capacity	500 [Kg] (250 for each platform)
Speed	3 [m/s]
Traction system	Wheels
Traction motors	400W motor (per wheel)
Batteries	2x110[Ah]
Autonomy	½ [h]
Temperature range	-10° ~ 50° [C]
Max. climbing angle	15°
Control	
Modular system	Can attach several platforms
	Possibility for robotic arms
	Connection to different sensors
connection	WIFI
	rs232
	usb
	Ethernet
controllers	Roboteq AX3500
	Arduino board
	phidgets
Sensors	color camera (Microsoft studio cam)
	Incremental encoder for each wheel
	Single beam laser distance sensor
Software	Custom build based on Visual Studio C#

(The robotic platform CAD files are included in the thesis DVD \Robotic platform CAD files\).

4.3. Kinematic model for the robotic platform

The robot desired trajectory is determined by a machine vision navigation algorithm aimed to follow a visual path. The path trajectory is converted into segments of curves or straight lines. Inputs for the kinematic model are the robot velocity and the curve radius. Outputs of the kinematic model are the velocity of each one of the four wheels. In case that the trajectory of the robot is a straight line, all four robot wheels will have the same velocity corresponding to the desired robot velocity. In case that the trajectory is a curve, each wheel will have different velocity, according to the kinematic model, and the robot's chassis will travel at the desired velocity.

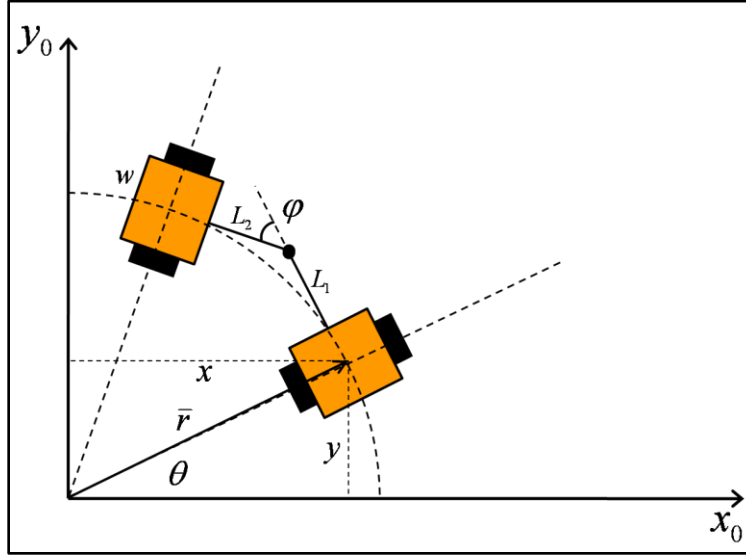


Figure 5 – Robot position definitions.

The robot is described as the two orange rectangles (Figure 5) where each rectangle represents one of the two robot platforms. The lower platform represents the rear part of the robot and the upper platform represents the front part of the robot. As shown in Figure 5, the robot is moving counterclockwise with a turning radius of \bar{r} . The state variables are $q = [x \ y \ \theta \ \varphi]$ where x and y represent the center position of the rear robot platform relative to the world coordinates system x_0, y_0 . θ represents the angle between the horizontal axis of the robot and the horizontal axis x_0 , and φ represents the angle between the robot platforms.

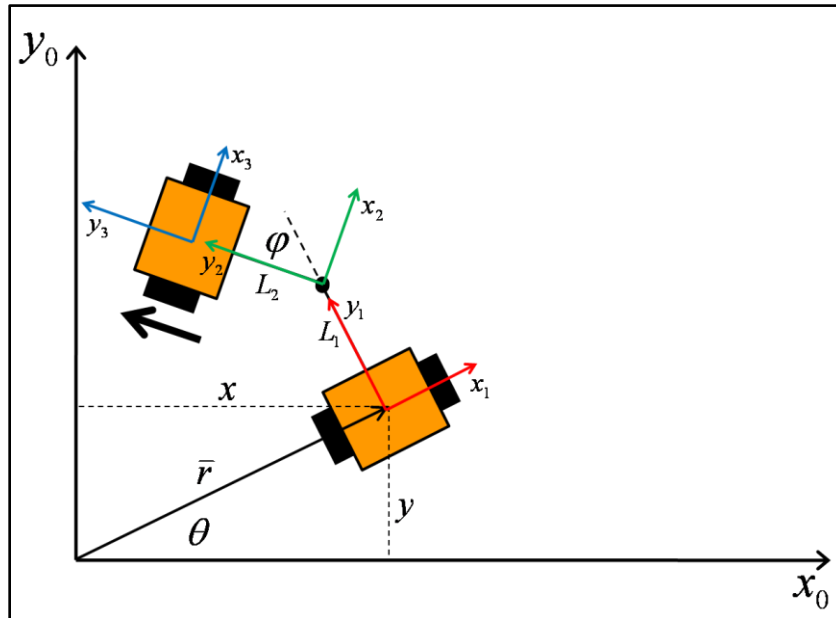


Figure 6 – Definitions of the rotation and translation matrixes.

In order to define the position of each one of the robot wheels relative to one main coordinate systems, RTM's were used. Three RTM's were constructed, the first A_{01} (red in Figure 6) is used to convert between coordinate system 1 to 0, the second A_{12} (green in Figure 6) is used to convert between coordinate system 2 to 1 and the third A_{23} (blue in Figure 6) is used to convert between coordinate system 3 to 2. The RTM between the third coordinate system and the world system 0, is the multiplication of all the RTMs to that point (i.e., $A_{03} = A_{01} \cdot A_{12} \cdot A_{23}$). Detailed description of the RTM's is shown in Appendix A.

In order to determine the wheel position relative to the world coordinate system 0, the vector of each wheel, relative to its one coordinate system was multiplied by the corresponding RTM. For example, to determine the position of the rear left wheel, the wheel vector in coordinate system 1 $\begin{bmatrix} -w/2 \\ 0 \end{bmatrix}$ was multiplied by RTM A_{01} :

$$\text{Back Left Wheel} = \begin{bmatrix} x_{BL} \\ y_{BL} \end{bmatrix} = A_{01} \cdot \begin{bmatrix} -w/2 \\ 0 \\ 1 \end{bmatrix} = \begin{bmatrix} -(1/2) w \cdot \cos[\theta] + x \\ -(1/2) w \cdot \sin[\theta] + y \end{bmatrix} \quad \text{Equation 1}$$

The position of each one of the robot wheels was calculated in a similar way, Appendix A.

The wheels velocity was calculated using the derivate by t the wheel position. The detailed results of the robot's wheels velocities are summarized in Appendix A. The wheels velocities are given as the shape of x-value and y-value. Due to the nonholonomic robot constraints, the velocity of the wheel can be only in the direction where the wheel is facing. In order to calculate the velocity toward the momentarily direction of the wheel, two vectors were constructed to project the x and y velocities to the momentarily wheel position. The two vectors are:

1. $Rot_1 = (-\cos[\theta] \quad \sin[\theta])$
2. $Rot_2 = (-\cos[\theta + \varphi] \quad \sin[\theta + \varphi])$

Where, Rot_1 is used to project the vectors of the rear robot platform and Rot_2 is used to project the front robot platform. The velocities results of each wheel are summarized in Appendix A.

Detailed analysis of the kinematic model for different turning curves produced the relation between the four wheels velocities and the turning curve (Figure 7). The colored lines represent each of the wheels speed and the black line shows the angle between the platforms (φ)

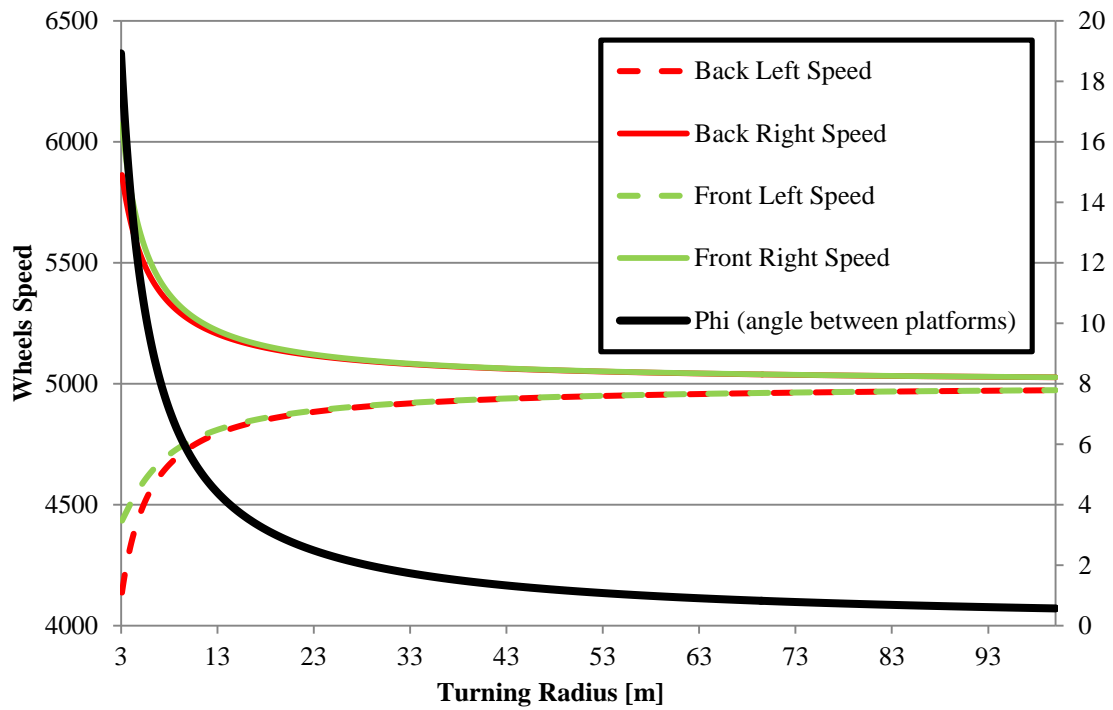


Figure 7 – Wheel speed for turning radius.

The robotic platform is controlled using the results in Figure 7 and Appendix A.

5. GRAPES AND FOLIAGE DETECTION

5.1. Overview

Three algorithms were developed for the grape clusters detection and a single algorithm was developed for the foliage detection. The algorithms were evaluated by comparing performance on images acquired in the field. This work was published in the Intelligent Service Robotics Journal (Berenstein, Shahar, Shapiro and Edan 2010). Several previous works related to the detection of grape berries and grape clusters are described in Table 6.

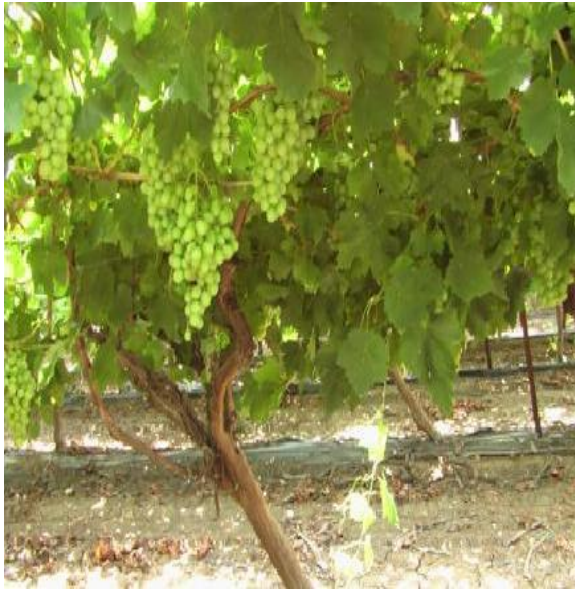
Table 6 - Examples of work in grape detection.

Application	Sensor	Reference
Grape bunch detection - SVM classifier	RGB images	(Liu and Whitty 2015)
Counting red grapes	high-resolution images	(Font, Pallejà, Tresanchez, Teixidó, Martinez, Moreno and Palacín 2014)
Yield prediction	color camera	(Nuske, Wilshusen, Achar, Yoder, Narasimhan and Singh 2014)
Grapevine yield and leaf area estimation	color camera	(Diago, Correa, Millán, Barreiro, Valero and Tardaguila 2012)
Automatic detection of bunches of grapes	color images	(Reis, Morais, Peres, Pereira, Contente, Soares, Valente, Baptista, Ferreira and Cruz 2012)

5.2. Detection algorithms

5.2.1. Foliage detection algorithm

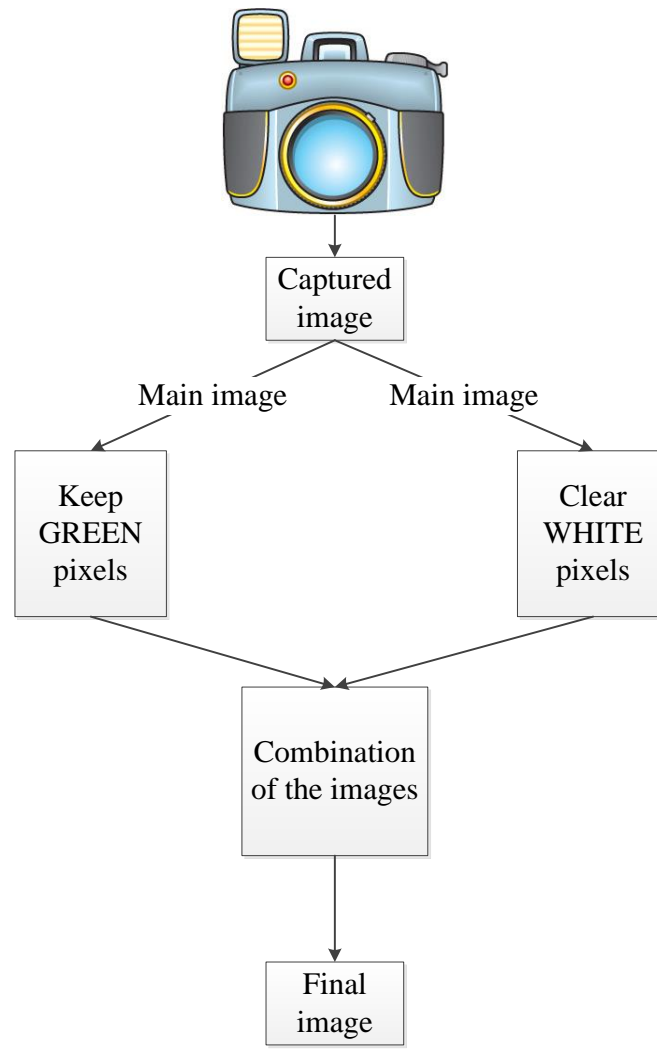
The Foliage Detection Algorithm (FDA) is based on the fact that the foliage color is green. Two filters operate on the captured image; one removes white pixels (sky, sun, etc. by applying a thresholds on each of the three RGB channels) and the other traces the green pixels (by applying a threshold on the green RGB channel only green pixels are kept). These filters are combined to produce the foliage image (Figure 8). Along this process the ground pixels are also removed. The FDA is not designed to separate the grapevine foliage close to the camera from the foliage of a grapevine in the next row. Such a separation is not necessary to identify the grapevine foliage and the grapes clusters (included in the thesis DVD \Foliage and Grapes Detection Algorithms\Foliage detection algorithm\).



a



b



c

Figure 8 – FDA. (a) Captured image. (b) Final foliage image. (c) Algorithm block diagram.

5.2.2. First grape detection algorithm

The first Grape Detection Algorithm (GDA1) is based on the difference in edge distribution between the grape clusters and the foliage. The algorithm was created by examining images from the vineyard and noticing that regions of grape clusters contain more edges than those in foliage regions. GDA1 includes three main stages (Figure 10): FDA, edge detection, and thresholding the high density edge from the low density edge areas. The edge detection algorithm was based on the Canny edge detection algorithm (Canny 1986). The Canny algorithm was empirically selected after experimenting with different edge detection algorithms on an assortment of 100 grape images. Examples of different edge detection methods are shown in Figure 9. These edge detection methods operated after converting the image to a gray-scale image. Results indicated that the Canny algorithm produced the most highly detailed edge images (Figure 9); hence, it was selected for this assignment. These results correspond to previous research (Shin, Goldgof and Bowyer 1998; Sharifi, Fathy and Mahmoudi 2002).

(The Matlab program code is included in the thesis DVD \Foliage and Grapes Detection Algorithms\Grapes clusters detection algorithms\Edge detection).

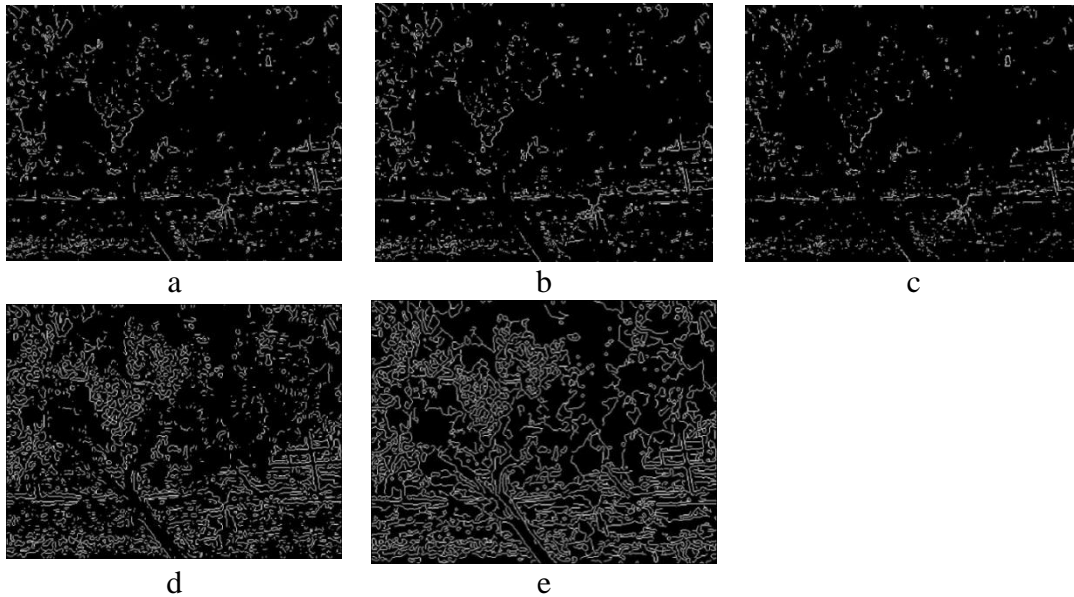


Figure 9 – Different edge detection methods.
(a) Sobel. (b) Prewitt. (c) Roberts (d) Laplacian of Gaussian (e) Canny.

5.2.3. Second grape detection algorithm

The second GDA (GDA2) is based on a decision tree algorithm. First, the color image is represented in both the common RGB representation and the perceptually motivated HSV (hue, saturation, and intensity) representation. Then, supervised patches taken from the grape areas and the foliage areas

are used to extract the following parameters from each of the R, G, B, H, S, and V channels: mean value, standard deviation, and the mean and standard deviation of the gradient magnitude. Using three patch sizes, 72 different parameters were extracted from each image according to Table 7 and a total of 1708 samples of these parameters were extracted from the entire image collection. Pearson's Correlation (Breiman, Friedman, Stone and Olshen 1984) was used to filter the parameters that have weak correlation to the classified data: high Pearson correlation represents high correlation between the parameter and the classification. All parameters with a Pearson correlation less than 0.5 were removed from further consideration. The most significant parameters that were selected using the correlation test were the mean gradient magnitude of the R, G, B, and V channels, all exhibiting Pearson correlation above 0.6. Interestingly enough, this result supports the approach taken in GDA1 which is based on edges density in the image.

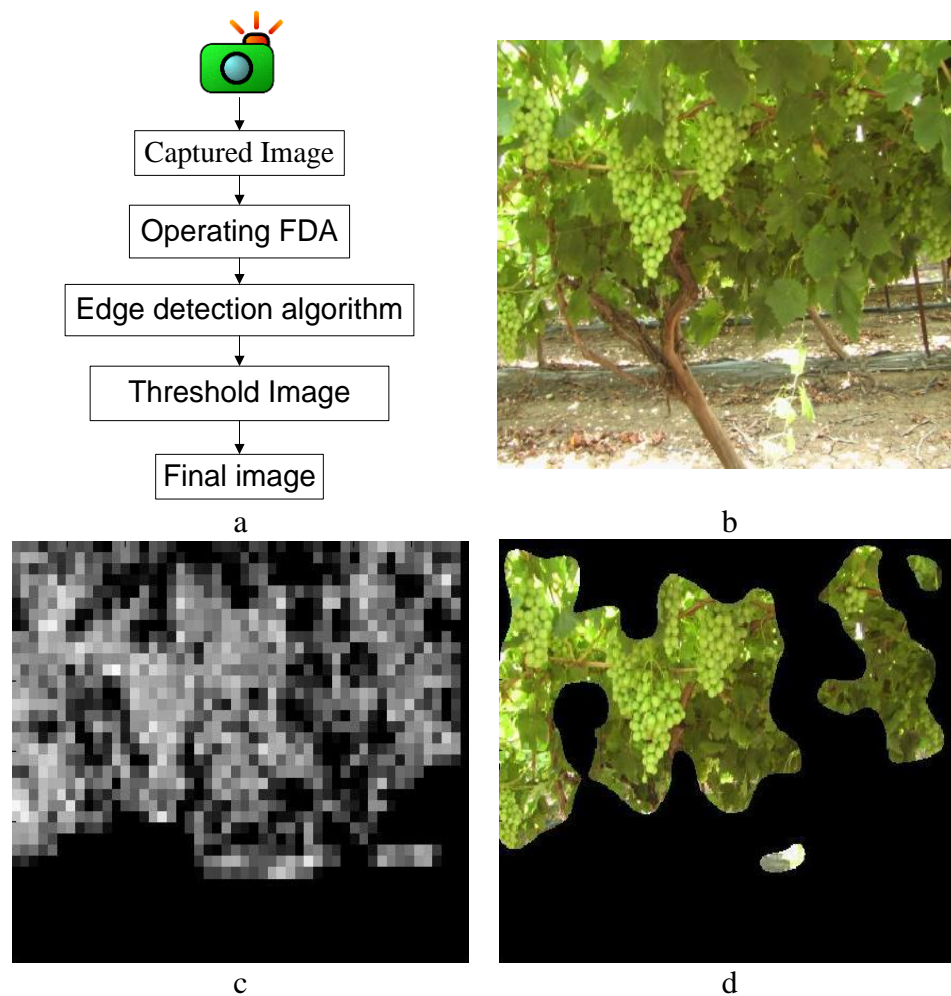


Figure 10 – GDA1.
(a) Algorithm block diagram. (b) Captured image. (c) Edges image. (d) Final grape image.

Training the decision tree was done using the C5.0 algorithm (Breiman, Friedman, Stone and Olshen 1984). The dataset was divided into two groups of 70% and 30% for training and testing, respectively, as commonly practiced. Once the decision tree was constructed, it was used for the classification: the same parameters that were extracted during the learning process were extracted from the given image around each pixel, and then each pixel was classified as grape or non-grape using the trained decision tree. Selected results of GDA2 are shown in Figure 11.

(Matlab program is included in the thesis DVD \Foliage and Grapes Detection Algorithms\Grapes clusters detection algorithms\Decision tree).

Table 7 – Decision tree parameters.

Mask diameter = 11							
Mean				Standard deviation			
Image		Gradient Image		Image		Gradient Image	
R,G,B	H,S,V	R,G,B	H,S,V	R,G,B	H,S,V	R,G,B	H,S,V
Mask diameter = 15							
Mean				Standard deviation			
Image		Gradient Image		Image		Gradient Image	
R,G,B	H,S,V	R,G,B	H,S,V	R,G,B	H,S,V	R,G,B	H,S,V
Mask diameter = 21							
Mean				Standard deviation			
Image		Gradient Image		Image		Gradient Image	
R,G,B	H,S,V	R,G,B	H,S,V	R,G,B	H,S,V	R,G,B	H,S,V

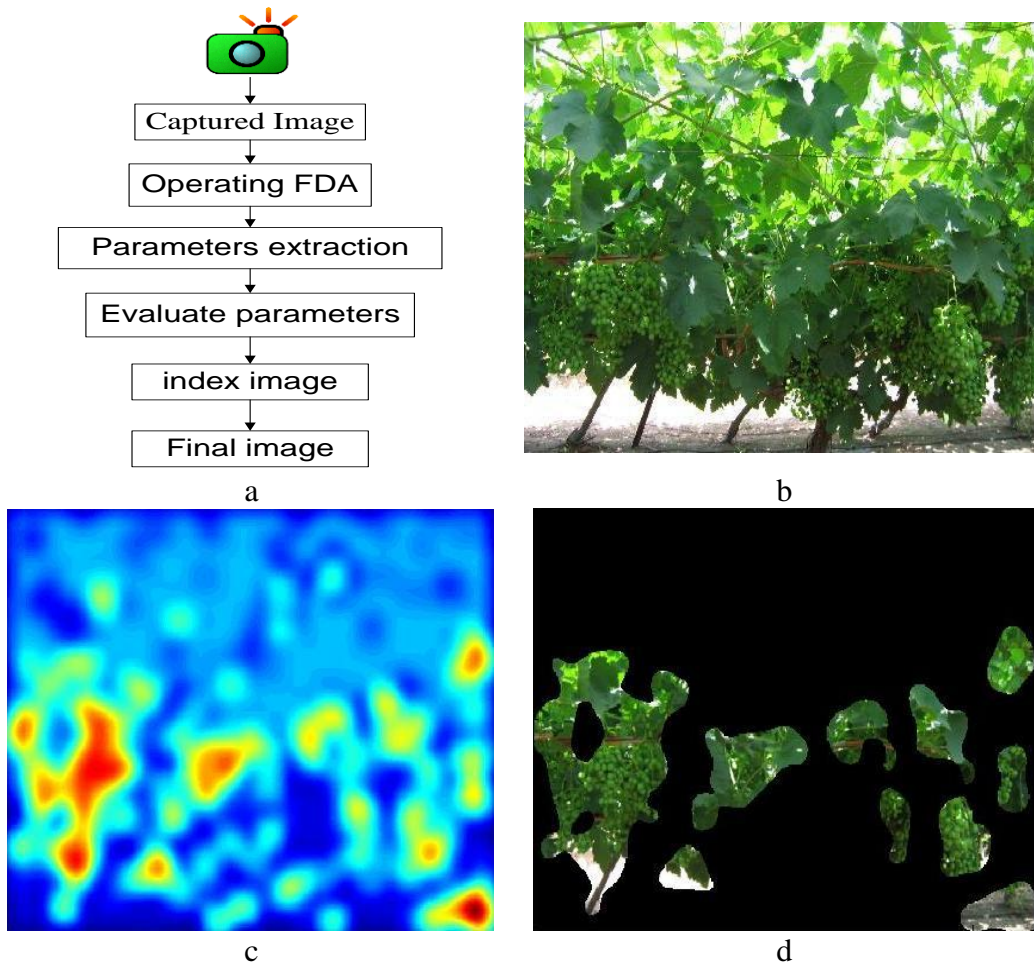


Figure 11 – GDA2.

(a) Algorithm block diagram. (b) Captured image. (c) Index image. (d) Final image.

5.2.4. Third grape detection algorithm

GDA3 is based on pixel comparison between edge representations of the captured image with a predesigned edge mask that represents grapes. A large number of overlapping pixels between the edged image and the edge mask indicates that the area in the image is similar to the area in the mask and therefore a high probability for a grape cluster. The algorithm uses a moving average and compares the mask over the edged image using two-dimensional convolutions. Four-edge masks were evaluated (Figure 12): (a) edge mask of single grape, (b) edge mask of grape cluster, (c) perfect circle with varied thickness and diameter of one grape with zero value at the center, and (d) perfect circle with varied thickness and diameter of one grape, with negative value at the center. Unlike the third mask, the fourth mask was designed to distinguish between circular edged patterns with and without response in its interior (which would be less preferable in terms of hits).

Given the proposed alternatives, the best mask for the algorithm was selected using the methodology described in the *Image Evaluation Methodology* section. Figure 13 presents descriptive results of GDA3.

(Matlab program is included in the thesis DVD \Foliage and Grapes Detection Algorithms\Grapes clusters detection algorithms\Moving mask).

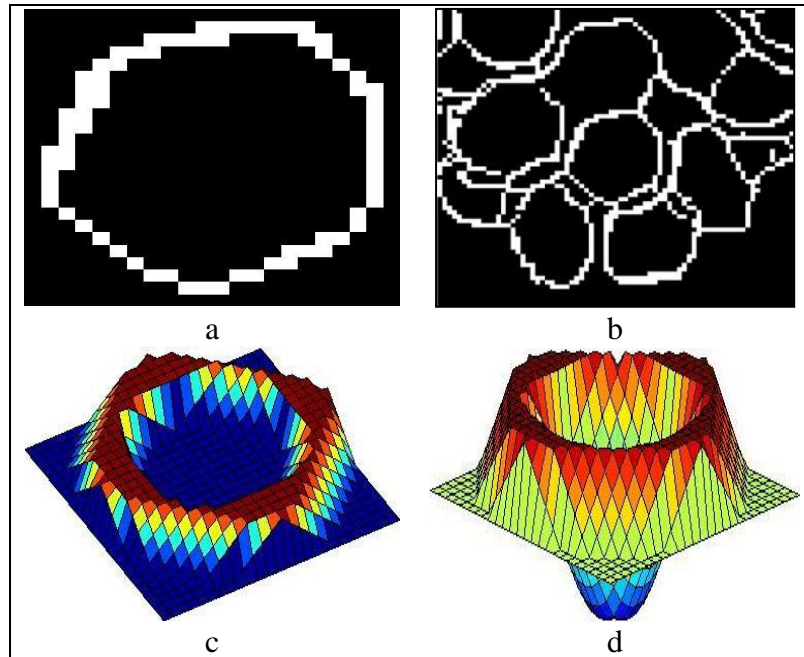


Figure 12 – Four edge masks.

(a) Single grape. (b) Grape cluster. (c) Center zero. (d) Negative center.

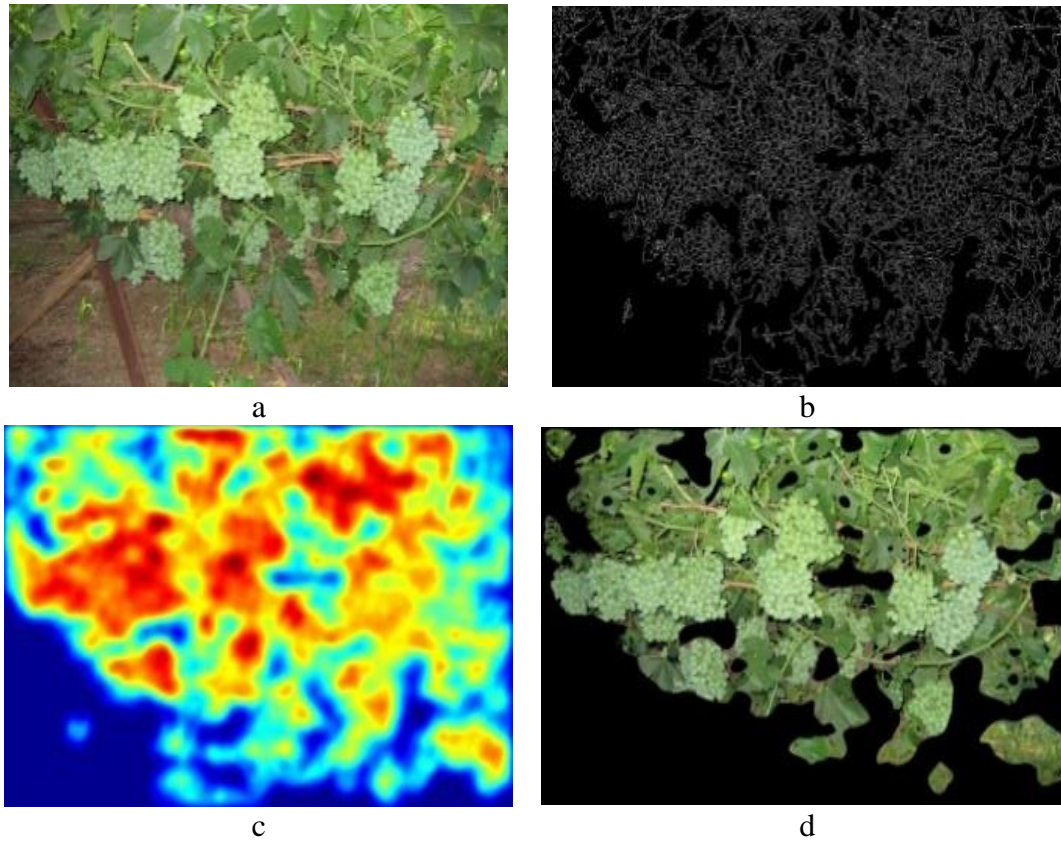


Figure 13 – GDA3. (a) Captured image. (b) Edged image. (c) Index image. (d) Final image.

5.3. Experimental methods

A color camera (IDS Inc., uEye USB video camera with a Wide VGA [752×480] resolution) was attached to a custom-built towing cart designed specifically for the image sampling test (Figure 14). This cart imitates the movement of a wheeled vehicle so as to ensure the images taken using the cart are as similar as possible to images taken from a moving wheeled robot (including the minor image blur occurred for exposure during motion). The camera was connected to a DELL® Core2 laptop computer. Images were acquired using Matlab® Image Acquisition Toolbox and saved for offline processing. The images were captured under natural illumination field conditions in mid-day during the summer time (rarely cloudy weather). The vineyard rows were positioned north-south. Field experiments were conducted during the growing season of 2008. The cart was manually dragged through the vineyard row and images were captured at a rate of 30 fps and stored on the computer. This process was repeated every two weeks from mid April to the end of July 2008. The dragging speed of the cart was set at 4 to 5 [km/h], to imitate the normal speed of manual spraying.



Figure 14 – Experimental towing cart.

To obtain a large variety of grape and foliage images, the experiments were performed in two different vineyards, one with green grapes (located in Arogot, Israel) and the other with red grapes (located in Lachish, Israel). We assume that a minor percentage of the grape clusters in the images were totally occluded by leaves, branches, and other grape clusters. 100 random images were extracted from 16 different movies that were sampled in the field. For comparison and algorithm test accuracy, the grape cluster areas were marked manually in each image (the photos are included in the thesis DVD \Foliage and Grapes Detection Algorithms\ and are available for public use under demand@

<https://drive.google.com/open?id=0B5nYMTLWCcUqTFRtTkR1SVdlakE>

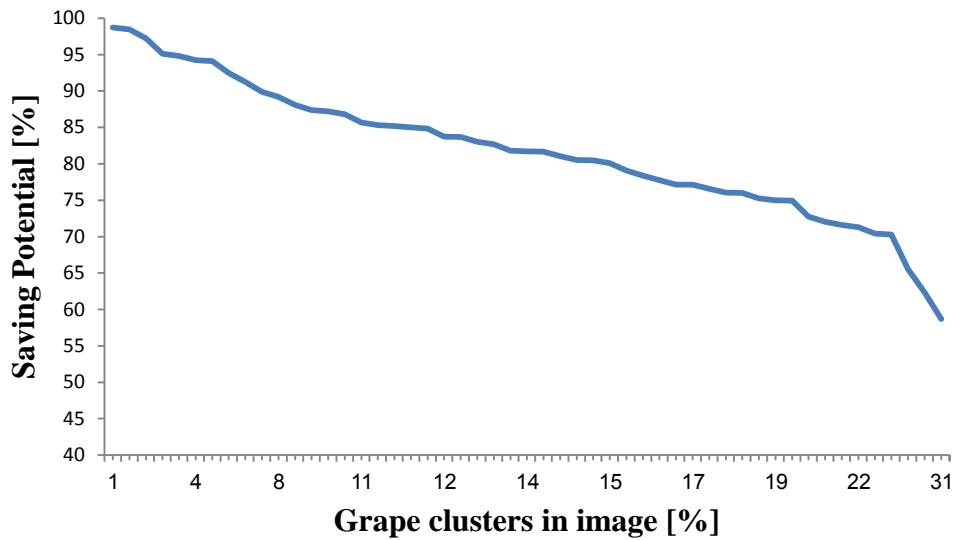
5.4. Detection algorithm results

The robot's spraying speed relative to the algorithm processing time is important for real-time implementation. The following condition must be met: $v \cdot t \leq x$, where v is the robot's speed, t is the machine vision processing time, and x is the real world field-of-view length. Laboratory measurements showed that the field of view length as perceived by the camera is 2 m, with 1.5 m distance from the camera to the grape clusters. The robot speed as related to the processing time can be calculated by using $v \leq x / t$ and substituting $x = 2m$. The maximal robot speed as a function of the processing time is shown in Table 8.

Table 8 – Robot speed in relation to processing time.

Algorithm	Processing time [S]	Maximal Robot speed [m/s] (km/h)
GDA1	0.65	3.07 (11.07)
GDA2	1.43	1.39 (5.03)
GDA3	1.15	1.73 (6.26)

The potential to save pesticides is the percent of maximal feasible saving possible in a given image (based on experts manually mark areas as grape clusters). The saving potential depends on the percent of grape clusters in the given image. Saving potential of 100 implies that there are no grapes in the image and there is no need to spray. The saving potential is inversely proportional to the percent of grape clusters in the image. The relation between the percent of grape clusters in real field images to the saving potential is shown in Figure 15. The saving potential increases with a smaller number of grape clusters in the image. Such conditions of few grape clusters could be a result of images taken early in the season or a gap between the grapevines.

**Figure 15 – Evaluation results of the relation between saving potential and grape clusters in the image.**

Three of the four masks suggested for GDA3 resulted in similar pesticide reduction (Table 9), indicating the validity of using an artificial perfect circle mask as an alternative to masks created from real-world edged image. Furthermore, later in this work (7) the size (diameter) of the artificial circle mask can be updated dynamically during the field spraying. These masks are sensitive to varying grape size and to use this algorithm throughout the growing season the masks size must be adjusted. A self-calibration process can be developed to adjust the mask size to the changing grapes size.

Table 9 – GDA3 performance of the four masks.

Mask	Detection rate [%]	Pesticide reduction [%]
grape cluster	90.45	24.08
center zero	89.95	23.90
single grape	90.10	22.20
negative center	90.53	12.73

The performance of the three GDA's is summarized in Table 10 indicating reduction between 25% and 30% of pesticides. The detection of grapes as grapes (TP) is more than 90%, which is considered very high with respect to other agriculture detection systems which reach average localization success of 85% detection rates and usually do not evaluate false negative rates (Bac, Henten, Hemming and Edan 2014). The overall detection results show high ability to detect grape clusters in the vineyard environment.

Table 10 – Final GDA's performance.

Algorithm	Reduction of pesticide agent [%]	Grape as Grape TP [%]	Foliage as Grape TN [%]	Grape as Foliage FP [%]	Processing time [S]
GDA1	30.59	90.4	9.59	73.48	0.65
GDA2	25.58	90.73	9.26	78.73	1.43
GDA3	26.79	90.7	9.67	79.18	1.15

6. HUMAN-ROBOT COLLABORATION

6.1. Overview

This chapter presents a new concept and methods for remote collaboration between a human operator and a robotic sprayer for the target detection task. The framework places the human at a remote location and uses the human's excellent perception skills to collaborate with the robot on the target detection task. The human and robot work in a sequential mode as described in the workflow diagram (Figure 16). The suggested concept positions the human at a remote location (e.g., home, office) equipped with a target marking device (e.g., stationary computer, laptop, tablet, PDA, or smart phone). Berenstein, Shahar, Shapiro and Edan (2010) grape cluster detection algorithm is operated on images acquired by the robotic system. Depending on the collaboration level (described in section 06.2), the human can mark additional targets and/or erase targets detected by the imaging algorithm. The marked targets are then sent back to the robot for actual spraying. Different marking methods are proposed and compared.

This work presents several collaboration levels and different human target marking methods and a methodology for their evaluation. Experiments were specially designed to compare the different options. Performance measures and a procedure for ground truth measurement were defined. Collaboration is expected to yield better target detection results since it benefits from the robot's consistency and accuracy (the image detection algorithm) combined with the human's perception and learning skills.

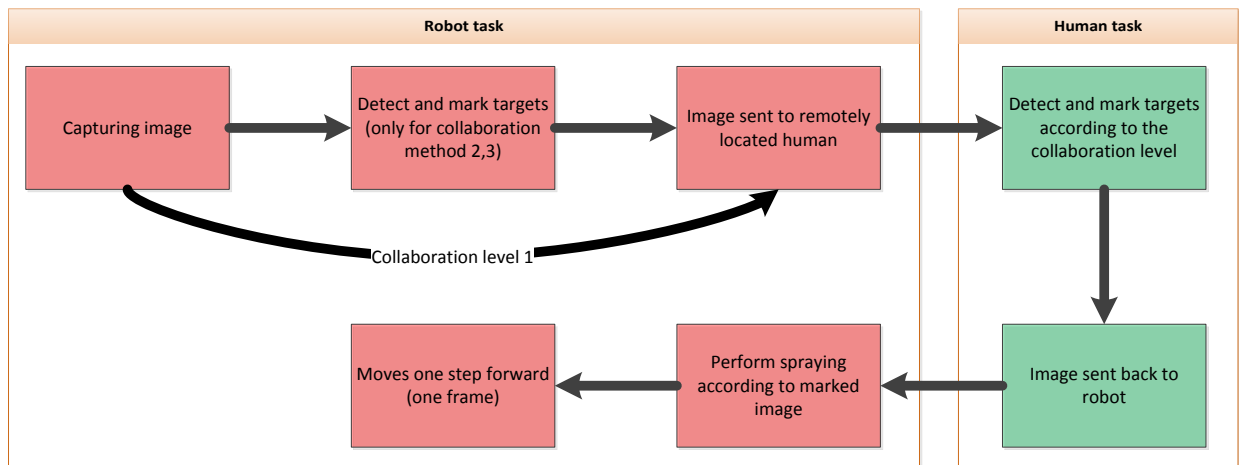


Figure 16 – Human-robot working diagram.

6.2. Human robot collaboration methods

Four levels of human–robot collaboration for detection and marking of the targets were developed based on Sheridan’s 10 levels of human-robot collaboration (Sheridan 1992) and based on previous work in agricultural target detection (Bechar and Edan 2003). The four collaboration levels presented below are based on Sheridan’s scale however the numbers are sequential and therefore not consistent with Sheridan’s levels of automation. In each collaboration level description (sections 6.2.1 to 6.2.4) the corresponding collaboration level according to Sheridan’s work is noted.

The human operator has to mark all the target area with maximum accuracy of the targets in the image in a fixed period of time. Maximum accuracy is defined as maximum target area along with minimum foliage within the marked area. All marked areas will later be considered as areas to be sprayed by the robot.

6.2.1. Collaboration level 1 – fully manual human target marking

The human operator is presented an image and must mark all areas to be sprayed. No automatic image analysis algorithm is executed. Figure 17a shows an image marked by a human (constant circle diameter marking method). This collaboration level corresponds to Sheridan’s level of collaboration 1 ("the computer offers no assistance, human must do it all").

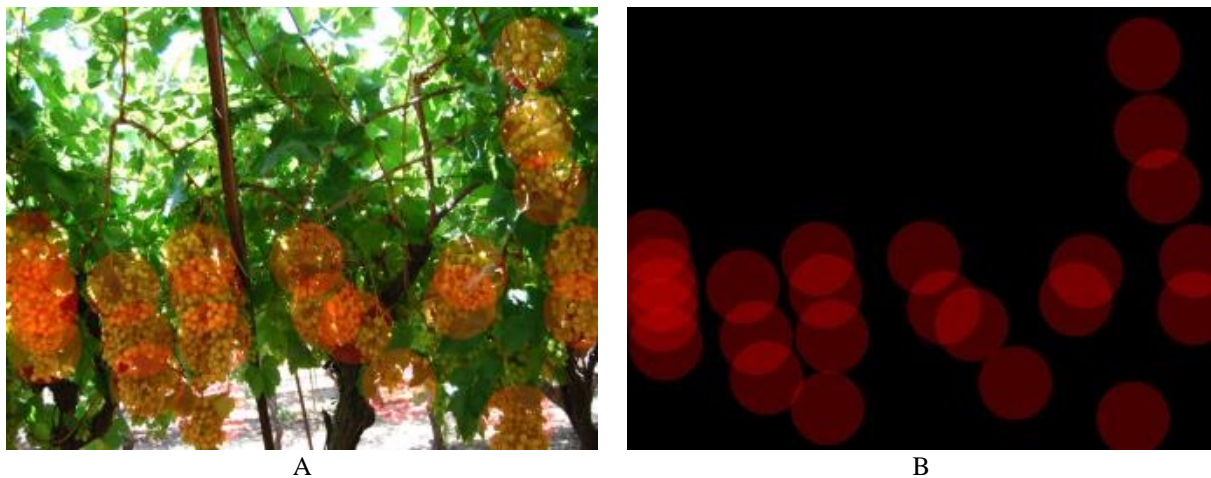


Figure 17 – Collaboration level 1. (a) User marked. (b) Binary image for analysis.

6.2.2. Collaboration level 2 – robot suggests, human approves

Captured image grape clusters are automatically marked using a machine vision algorithm for grape clusters detection (Berenstein, Shahar, Shapiro and Edan 2010). These marked areas are considered as recommendations for the human operator. The operator must mark each target he/she wants to spray. The operator can use the robot-recommended areas to achieve enhanced target hit rate. All

areas to be sprayed must be marked by the human. Figure 18 illustrates the collaboration procedure. The image captured in the field is processed by the robot using Berenstein, Shahar, Shapiro and Edan (2010) grape detection algorithms (Figure 18a blue colored areas), the processed image is transferred to the human operator for further analysis. Figure 18b shows the areas marked by the human operator (red areas). Figure 18c shows the binary image to be sprayed; only the red area will be sprayed. This collaboration level corresponds to Sheridan's level of collaboration 4 ("the computer offers a complete set of action alternatives, and suggests one").

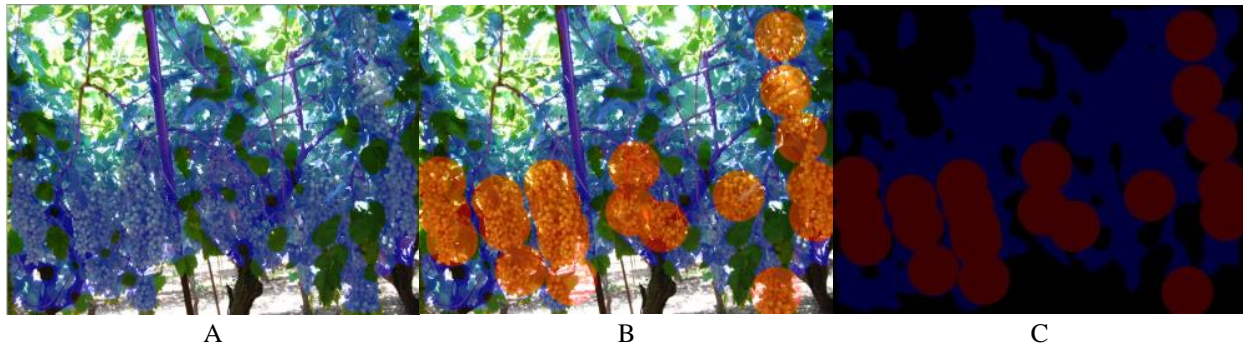


Figure 18 – Collaboration level 2.

(a) Robot suggested mark. (b) Human mark area. (c) Binary image to be sprayed.

6.2.3. *Collaboration level 3 – robot marks, human supervises*

The human receives an image with grape clusters marked by the robot using Berenstein, Shahar, Shapiro and Edan (2010) machine vision algorithms. The human has the ability to manually reject robot marked areas and add areas to be sprayed (Figure 19a,b). In case the human does not make any change in the robot-marked image (Figure 19a), the entire robot-marked area will be considered as targets and will be sprayed. As opposed to collaboration level 2, the human does not need to confirm the robot markings but can change existing markings. This collaboration level corresponds to Sheridan's level of collaboration 5 ("the computer offers a complete set of action alternatives, and executes that suggestion if the human approves").



Figure 19 – Collaboration level 3. (a) Robot marked image. (b) Binary image to be sprayed.

6.2.4. Collaboration level 4 – fully autonomous robot marking

This collaboration method corresponds to Sheridan’s 10th level of automation where the computer decides everything and acts autonomously with no human operations (Sheridan 1992). With this collaboration level the robot uses (Berenstein, Shahar, Shapiro and Edan 2010) machine vision algorithms to detect the grape clusters and sprays solely the detected areas. The human has no ability to intervene. This collaboration level corresponds to Sheridan’s level of collaboration 4 (“the computer decides everything and acts autonomously, ignoring the human”).

6.3. Human marking methods

Three marking methods were developed and evaluated: (i) **constant circle diameter** – the operator sets the center of a constant diameter circle and by clicking the left mouse button the circle is marked on the image (Figure 20a). Using this method, the operator cannot change the circle diameter. (ii) **ellipse with changeable size** – by holding the left mouse button the user sets the ellipse center point, and at the point of releasing the left mouse button the end point of the ellipse is set (Figure 20b). (iii) **free hand** – the operator holds the left mouse button and surrounds the target area. When releasing the mouse button the area bounded is marked as target (Figure 20c).

In each method the area bounded within the marked area is considered as “detected” and is colored in red. With each of the marking methods, the operator can use the right mouse button to erase a marked target. The erasing method is identical to the marking method (e.g., when using the constant circle diameter method, the operator can click the right mouse button and the target marked within that area will be erased).

When the target marking process is completed (due to marking all the targets or end of marking time for the image) a binary image is saved for post-analysis (Figure 20d-f).

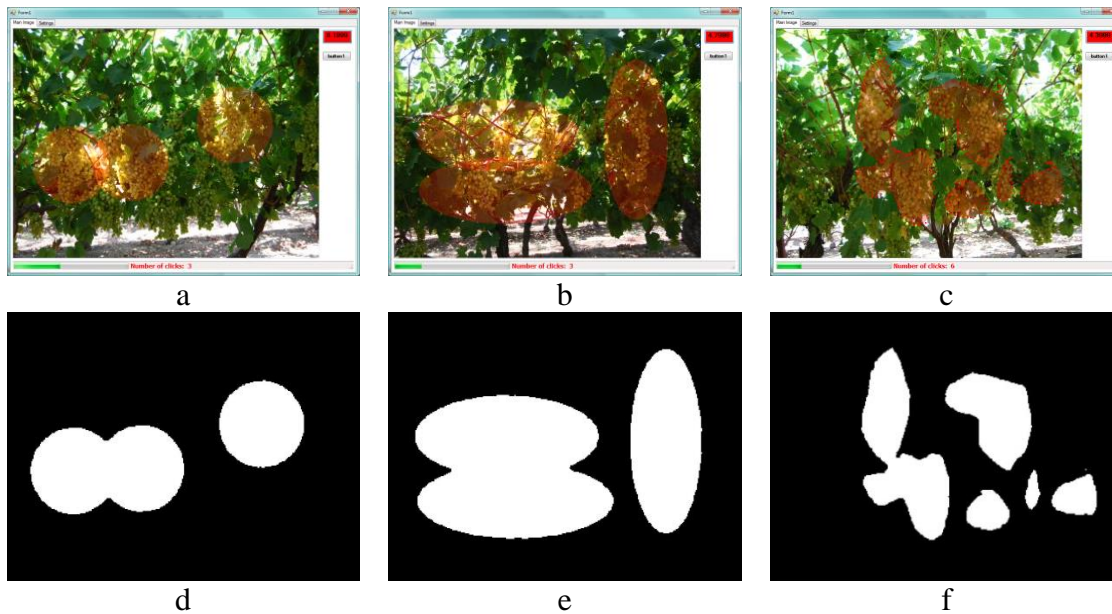


Figure 20 – Marking methods & results. (a) Constant circle diameter. (b) Ellipse. (c) Free hand. (d) Constant circle diameter result. (e) Ellipse result. and (f) Free hand result.

6.4. User interface

The main goal of the interface is to present the human with images captured from the commercial vineyard. Using the suggested marking method, the human marks targets within the image; the images are presented sequentially to the user switching at a fixed time. Presenting the user an image for a fixed time contributed in two ways: first, the user was not able to dawdle on images more than the allocated time, resulting in a costly non-effective process, second, the user did not have the option to mark the images fast, resulting in bad marking (e.g., the user can finish marking the targets and continue to the next image instead of using the remaining time to unmark FA areas).

The interface (Figure 21) consists of two main windows – the settings and the marking window. Using the settings window (Figure 21a), the user can select different properties of the marking task such as: marking method, circle diameter (relevant only for the constant circle diameter marking method), marking time (image switching time), image to mark (relevant only for experiments), and the address path to save the marked images (relevant only for experiments). The experiment properties are pre-selected by the user and cannot be changed during the experiment. The marking window (Figure 21b) is used for displaying images.

The human's task is to detect and mark targets within the image while using one of three marking methods. The marking window also contains two indicators, the time left to mark the current image (both numeric and visual), and a counter for the number of mouse clicks. Each marked target is marked in red.

The interface was implemented in the Microsoft Visual Studio environment with the C# language (detailed program codes included in the thesis DVD\Human-Robot Collaboration\).

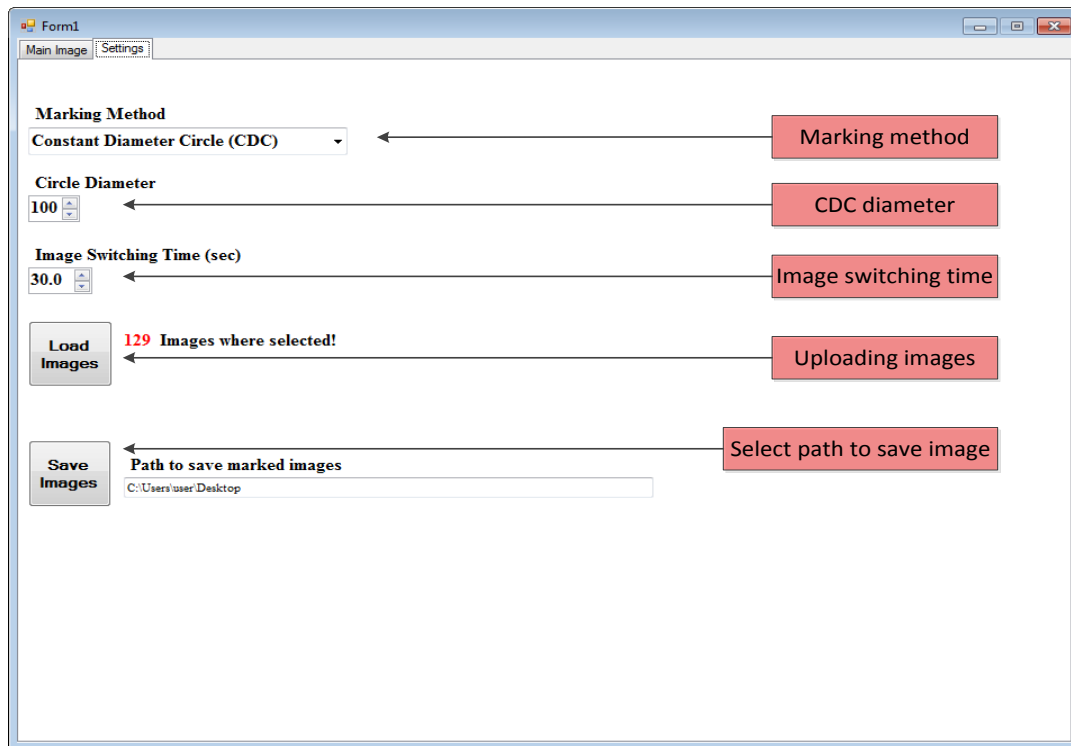
6.5. Evaluation methodology

Experiments were designed aiming to evaluate the influence of the human-robot collaboration level, human target marking method, and the switching time of the image captured in the field. This was achieved through a series of user experiments in which images captured in the field were presented to users on a computer screen in the lab. The work included four experiments to evaluate the: 1) human learning time to determine the time needed for the human to reach a hit rate expertise of 90%, 2) human marking methods, 3) human-robot collaboration levels, and 4) computer detection value on the hit rate. During the experiments two image switching times were evaluated. The image switching times, simulating different robot speeds, were 15 and 12 [sec] per image corresponding to 1 and 1.25 [m/s] travel speed along the row.

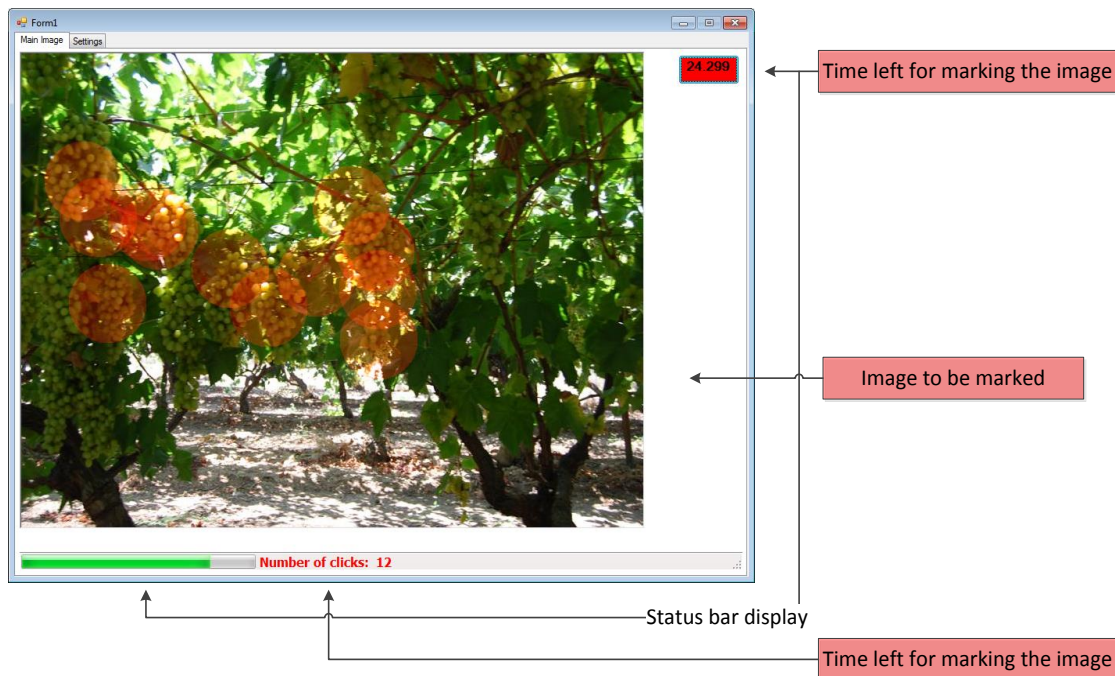
All of the following experiments were conducted in a computer lab at Ben-Gurion University of the Negev. Each participant occupied a single stand-alone computer equipped with a 19" screen. The performance measures for evaluation were hit rates (true positive, TP) and false alarms (FA).

6.5.1. Database

Creating a collection of ground truth images is necessary for target detection evaluation. Hit and False Alarm (FA) performance measures were used. Since the case study for this work is a robotic sprayer for vineyards, the images used originated from a commercial vineyard growing green grapes of the "superior" variety. An RGB camera (Microsoft NX-6000) with 600×800 resolution was manually driven, at mid-day, along a commercial vineyard in Lachish, Israel, during the summer season of 2011, one month before harvest time. The images were captured from 5 different growing rows.



a



b

Figure 21 – User interface. (a) Setting window. (b) Marking window.

The targets were defined as the grape clusters. A group of three experts was guided to mark the closing perimeter of each grape cluster in the image. The experts were guided to mark the targets with no time limit for either a single target or the complete image. The experts had the flexibility to zoom in and out of the image to achieve precise marking of the target. The final ground truth was marked using the judge rules criteria (if a given pixel was marked by two or more experts, it was considered a target).

A set of 129 images were marked using this technique and used as a ground truth for the following experiments (the images are available for public use @ <https://drive.google.com/file/d/0B5nYMTLWCcUqYmZ2QzY5aVR1M00/view?usp=sharing>).

6.5.2. Performance measures and data analysis

Two performance measures were used: Hit rate (true positive) and False Alarm rate (FA, false positive). Figure 22 illustrates the target area, human marking area, and the performance measures using artificial shapes. The circle represents the target to be marked and the rectangle represents the human marking area. The conjunct area between the target and the human marking (colored yellow) is the sum of hit pixels. The target area not marked by the human (colored red) is the sum of miss pixels, and the human marked area that is not part of the target area (colored green) is the sum of FA pixels. The Hit rate [%] was defined as:

$$\frac{HIT}{HIT + MISS} \cdot 100 \quad \text{Equation 2}$$

The FA rate [%] was defined as:

$$\frac{FA}{\text{horizontal resolution} \cdot \text{vertical resolution}} \cdot 100 \quad \text{Equation 3}$$

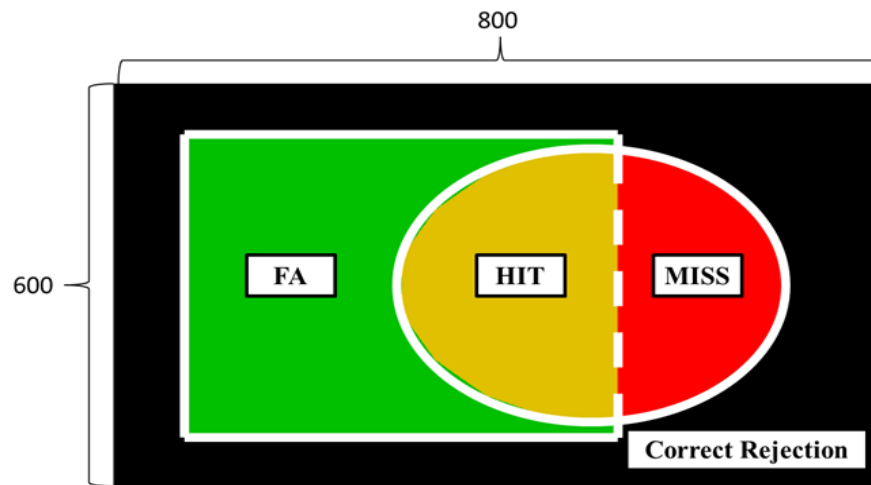


Figure 22 – Performance measures illustration, the circle represents the target, the rectangle represents the human marking.

The F1 score (Sokolova and Lapalme 2009) was on purpose not used as the performance measure so as to be able to control independently the FA and Hit rate depending on the task objective required by the farmer.

A paired t-test design was used for the analysis. Since for each experiment all the users marked the same database images, the statistical paired t-test was used. T-test was used since we had a large population (>30) and assumed normal distribution of their performance. The tests considered statistical significance at or below $\alpha=0.05$.

6.6. Preliminary experiment – evaluating interface learning time

Learning is defined as the time required for a group of people without experience and without interface acquaintance to reach satisfactory use of the interface (Norman 1988). Bringing the users to the same level of expertise is crucial to neutralize the interface learning effect. The goal of this experiment was to find the learning time needed for the users to get to 90% hit rate detection with the interface. Users who reached the target 90% marking hit rate were considered experts. Since the switching time between the images is constant, the learning time can be referred to as the number of images needed for a user to become familiar with the interface.

6.6.1. Experimental setup

Prior to the experiment the participants were instructed on how to use the interface using an explanation slideshow identical for all participants. Using the interface, the participants were instructed to mark the grape clusters in the image as accurately as possible while considering the image switching time. Two switching times were evaluated, 9 and 12 seconds. When the switch time passed, a binary image containing the marked areas (e.g., Figure 17b) was saved for later analysis. After the experiment was finished, each participant completed a NASA TLX workload questionnaire to evaluate the workload experienced by the participant during the target marking. Since the goal of the learning process was to reach 90% hit rate detection, the only performance measure used was the HIT rate value.

6.6.2. Experimental design

A group of 20 students, aged 20 to 30, were randomly divided to 2 groups of 10 students each, and were used as the experiment participants. The experiment was conducted according to the experimental plan described in Table 11. The human-robot collaboration level was set to fully

manual marking and the target marking type was set to constant circle diameter. Each participant group practiced a single image switching time.

Table 11 – Experimental design - learning time.

Group	Image switching time [sec]		Collaboration level	Marking method	Number of images	Total experiments time [sec]
	9	12	level 1 (Manual)	Constant circle diameter		
1	X		X	X	80	720
2		X	X	X	60	720

6.6.3. Results

Learning experiments results indicate that performance increases with a positive trend along time as expected (Figure 23). The interface learning goal was to reach 90% hit detection rate. The cross-sections of the linear trend line with 90% hit were 522 and 366 seconds for the 9 and 12 second image switching times, respectively. Based on this experiment, a set of 30 images was used for the learning stage in all following experiments.

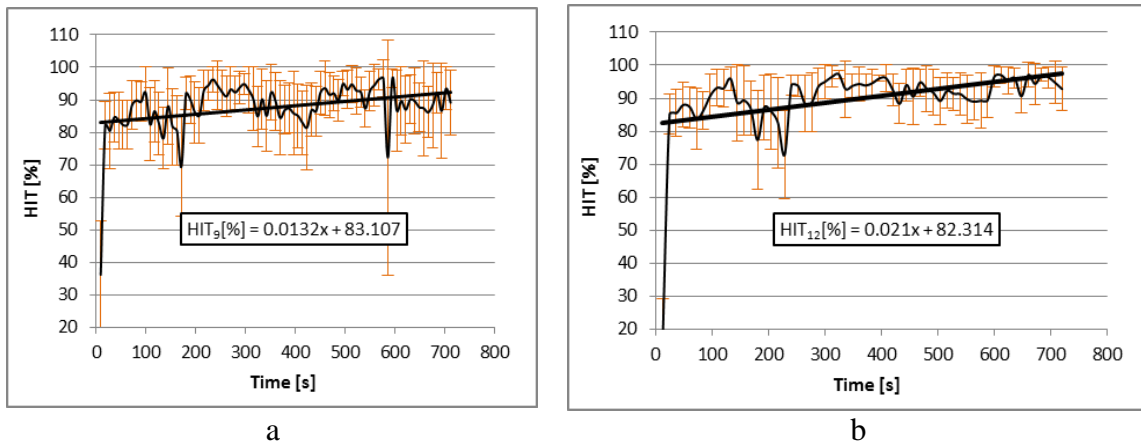


Figure 23 – Learning experiment results.
(a) 9-Second switching time. (b) 12-Second switching time.

6.7. Evaluating human marking methods experiment

The aim of this experiment was to compare the three suggested marking methods. The three marking methods were compared to the fully manual human-robot collaboration method (collaboration level 1), which is the most demanding of the user. Two image switching times, high and low corresponding to the robot's slow and fast movement speeds along the row, were evaluated.

6.7.1. Experimental setup

Prior to the experiment the participants were instructed on how to use the interface using an explanation slideshow. In addition, the performance measures used to analyze the marked images (hit, FA) were explained and the participants were instructed to mark the target accordingly (they were instructed to maximize hit rate and minimize false alarms). The number of images for the prior training was set to 30 based on findings from the learning time preliminary experiment (described in section 6.6). Using the preset switching time and marking method, each group marked the projected images. In order to neutralize the effect of the marking methods sequence on the results, each participant practiced the three marking methods in a random order. After the experiment the participants completed a NASA TLX workload questionnaire (Appendix B.).

6.7.2. Experimental design

A group of 72 students, aged 23 to 30, randomly divided to 2 groups of 36 students each, were used as the experiment participants. The experiment was conducted according to the experimental plan described in Table 12. Excluding the 30 images used for the interface learning process, each participant marked a total of 150 images, 50 for each marking method. The marking methods sequences were randomly selected to neutralize any user fatigue influence.

Table 12 – Experimental design - manual collaboration, three marking methods.

Group	Image switch time [sec]		Marking method		
	12	15	constant circle diameter	ellipse	free hand
1	X		X	X	X
2		X	X	X	X

6.7.3. Results

The results (Figure 24 and Table 15) show that Hit rates are maximized when the users have more time to mark the image. For the two image switching times, the method with the highest hit rate and the minimum miss rate was the constant circle diameter (94.3%, 89.6% and 84.4%, for the constant circle diameter, ellipse, and free hand at 15sec compare to 91.4%, 87.0%, and 82.5% at 12sec

respectively). Minimum FA rate is achieved when the marking method used is free hand marking (13.0% and 10.1% for the ellipse and free hand at 15sec compare to 16.8% and 13.2% at 12sec respectively).

The difference in the number of clicks between the 15[sec] and 12[sec] image switching times (Table 13) indicates that the number of clicks per image is higher when the image switching time is longer with an average difference of 3.47 clicks. There is a strong correlation between the number of clicks to the target size (0.95 and 0.97 for 12[sec] and 15[sec] image switching times, respectively).

Results (

Table 14) indicate that the most comfortable marking method was the constant circle diameter (when the average score was 3.63, 3.25, and 2.84 for the constant circle diameter, ellipse, and free hand respectively).

The preferred marking method depends on the task objective. If the farmer aims to maximize the hit rate the constant circle diameter marking method with the long image switching time should be chosen; if the farmer wants to minimize false alarms the free hand marking method with a short image switching time should be chosen. The ellipse marking method did not indicate any advantage over the other two marking methods and hence was omitted from the analyses.

Table 13 – Number of clicks difference between 15 and 12 seconds (15-12) image switching time.

	constant circle	ellipse	free hand
Average	3.47	3.18	1.29
Standard deviation	1.96	1.01	0.72

Table 14 – Results of ease of use questionnaire.

	constant circle	ellipse	free hand
Average	3.63	3.25	2.84
Standard deviation	1.28	1.18	1.15

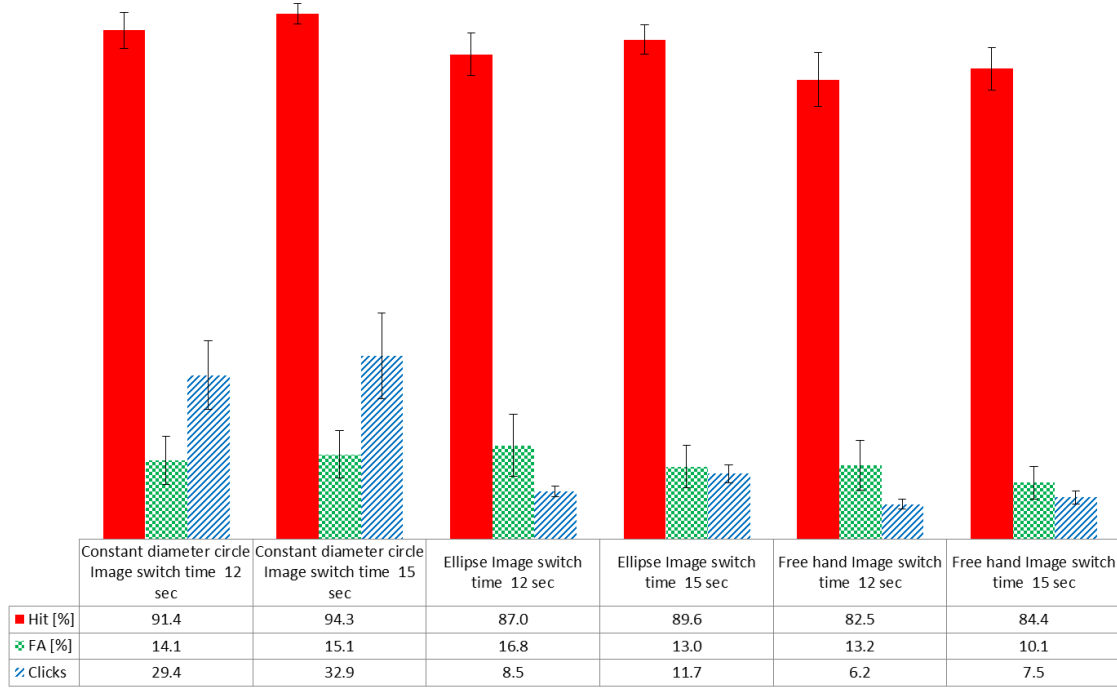


Figure 24 – Results of marking methods comparison experiment for two different switching times.

Table 15 – Marking method results summary. paired t-test, df=49, t-critical=2.0095. a,b are the compared groups, and x is constant.

Image switch time [sec]		Marking method			t-test	t-test
12	15	constant circle diameter	ellipse	free hand	HIT	FA
a	b	x			-11.69	-12.30
a	b		x		-9.49	24.29
a	b			x	-4.91	19.99
x		a	b		11.39	-12.37
x		a		b	15.25	3.61
x			a	b	11.96	16.52
	x	a	b		17.35	13.39
	x	a		b	20.74	24.16
	x		a	b	16.69	21.07

6.8. Evaluating collaboration level and marking method experiment

This experiment aimed to evaluate performance for the different collaboration levels and two target marking methods, the constant circle diameter and the free hand marking method. The ellipse with changeable diameter was not evaluated in this experiment since the previous experiment indicated it has no advantage over the constant circle diameter and the free hand marking method.

6.8.1. Experimental setup

Prior to the experiment the participants were instructed on how to use the interface using an explanation slideshow (included in the thesis DVD \Explanation slideshow\). In addition, the performance measures used to analyze the marked images (hit, FA) were explained and the participants were instructed to mark the target accordingly (they were instructed to maximize hit rate and minimize false alarms). The number of images for the prior training was set to 30 based on findings from the learning time preliminary experiment (described in section 6.6). Using the preset switching time and marking method, each group marked the projected images. In order to neutralize the learning and fatigue effect on the results, each participant practiced one experiment, which consisted of a single switching time, collaboration level, and marking method.

6.8.2. Experimental design

A group of 130 students aged 23 to 30, randomly divided to 8 groups were used as the participants. The experiment was conducted according to the experimental plan described in Table 16. Each participant marked a total of 100 images.

Table 16 – Experimental design.

Group	Image switch time [sec]		Collaboration method		Marking method	
	12	15	level 2	level 3	Constant circle diameter	Free hand
1	X		X		X	
2	X		X			X
3	X			X	X	
4	X			X		X
5		X	X		X	
6		X	X			X
7		X		X	X	
8		X		X		X

6.8.3. Results

The main aim of this experiment was to compare the collaboration levels for the two marking methods. The robot's "task", in the suggested scenario, is to mark the grape clusters using Berenstein, Shahar, Shapiro and Edan (2010) grape detection algorithms. In the second collaboration method (robot suggests, human approves), the robot-detected grape areas were used as recommendations for the human operator. In the third collaboration method (robot marks, human supervises), the robot-detected areas were considered as decisions that the human can later change if necessary. Table 17 summarizes the robot grape detection algorithm hit and false alarm rates.

The results (Figure 25 and

Table 18) indicate that the highest hit rate 92.66%, is achieved with collaboration level 3, constant circle diameter and 15[sec] image switching time and these results are statistically significant. The lowest FA, 2.71%, was achieved with collaboration level 2, free hand and 15 [sec] image switching time. While using collaboration level 2, for the two marking methods, the hit rate was higher when the user had more time for the marking process. While using collaboration level 3 with the constant circle diameter, the hit rate was higher, when the user more time. However, for the free hand marking method, the user showed no improvement he/she had more time. Collaboration level 3 was proven to be better than collaboration level all marking methods and image switching times (

Table 18). Collaboration level 3 showed high FA compared to the corresponding collaboration level 2. The number of clicks using collaboration level 3 is greater than collaboration level 2 for the corresponding marking method and image switching time.

Results from the ease of use questionnaire did not show any statistically significant difference between the different collaboration methods.

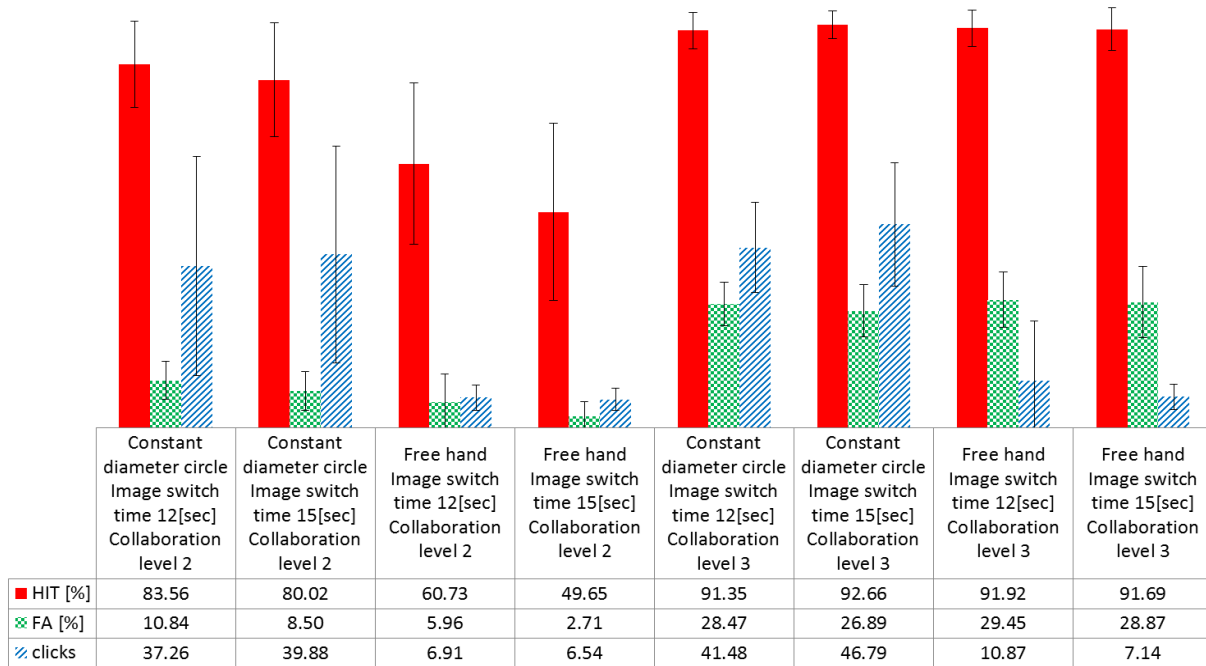


Figure 25 – Results of collaboration level comparison for two marking methods and switching speeds.

Table 17 – Robot automatic image analysis grape detection performance.

	HIT	FA
[%]	83.80	28.44

Standard deviation	12.05	5.64
--------------------	-------	------

Table 18 – Human-robot collaboration level results summary. paired t-test, df=99, t-critical=1.9842. a,b are the compared groups, and x is constant.

Image switching time [sec]		Marking method		Collaboration method		t-test (HIT)	t-test (FA)
12	15	constant circle diameter	free hand	level 2	level 3		
a	b	x		x		9.50	24.67
a	b		x	x		25.42	25.14
a	b	x			x	-6.33	9.61
a	b		x		x	1.40	3.46
x		a	b	x		40.86	31.65
	x	a	b	x		46.88	33.79
x		a	b		x	-2.44	-4.99
	x	a	b		x	3.23	-8.96
x		x		a	b	-17.07	-35.54
	x	x		a	b	-23.31	-38.30
x			x	a	b	-45.18	-50.36
	x		x	a	b	-55.39	-58.26

Collaboration level 2 – robot suggests, human approves

Collaboration level 3 – robot marks, human supervises

7. SITE SPECIFIC TARGET SPRAYING DEVICE

7.1. Overview

The traditional pesticide spraying methods (detailed in section 1) are not suitable for a robotic sprayer since they lack the precision needed for accurately hitting the target while maximizing the hit rate and minimizing the FA rate. Although several agricultural spraying robots have been developed, mostly for weed control and plant protection applications (Mandow, Gomez-de-Gabriel, Martinez, Munoz, Ollero and Garcia-Cerezo 1996; Steward, Tian and Tang 2002; Singh, Burks and Lee 2005; Pergher and Petris 2008; Slaughter, Giles and Downey 2008), they are not suitable for the task of spraying amorphous shapes (such as grape clusters).

To design a spraying device, several different spraying deposition methods were evaluated in simulation. Based on the simulation analyses the best performing device was selected for implementation. A novel site specific spraying device was developed, built, and tested specifically for the task of spraying objects with varying size and amorphous shape while providing maximum hit rate and minimum FA rate.

7.2. Spraying deposition methods

To develop an efficient spraying deposition method it is important to quantify data regarding the target coverage quality in terms of false alarm rate and overlapping of sprays. The assumption is that the targets are accurately detected and that the sprayer aims accurately at the target. The spraying deposition methods are designed to cover the entire target (i.e., 100% target Hit Rate). We do not take into account the effect of spray material. Analytical evaluation of the spraying methods was not possible due to the amorphous shape of the targets and high variability. Therefore, a simulation analysis was developed (described in thesis DVD \Spraying Simulations\). Three types of spraying deposition methods were evaluated. This was published in the ASABE Annual International Meeting (Berenstein and Edan 2012). The simulation results were used to design the spraying device for amorphous shape target such as the grape clusters (section 7.3).

7.2.1. First spraying deposition method – fixed nozzle spacing

The first spraying deposition method, Fixed Nozzle Spacing, is based on existing spraying techniques in which a set of nozzles are organized vertically on a spraying column with predetermined spacing (Figure 26a).

In this method, the nozzles position and spray diameter (nozzle aperture) are set before the spraying process regardless of the targets shape and size. The vertical length between the nozzles is derived from the spray diameter and is set to minimize the sprays circles overlapping (Figure 26b). To enable spraying dispersing like Figure 26b, an electric valve is set for each of the spraying nozzles. The electric valve allows accurate control over the spraying timing.

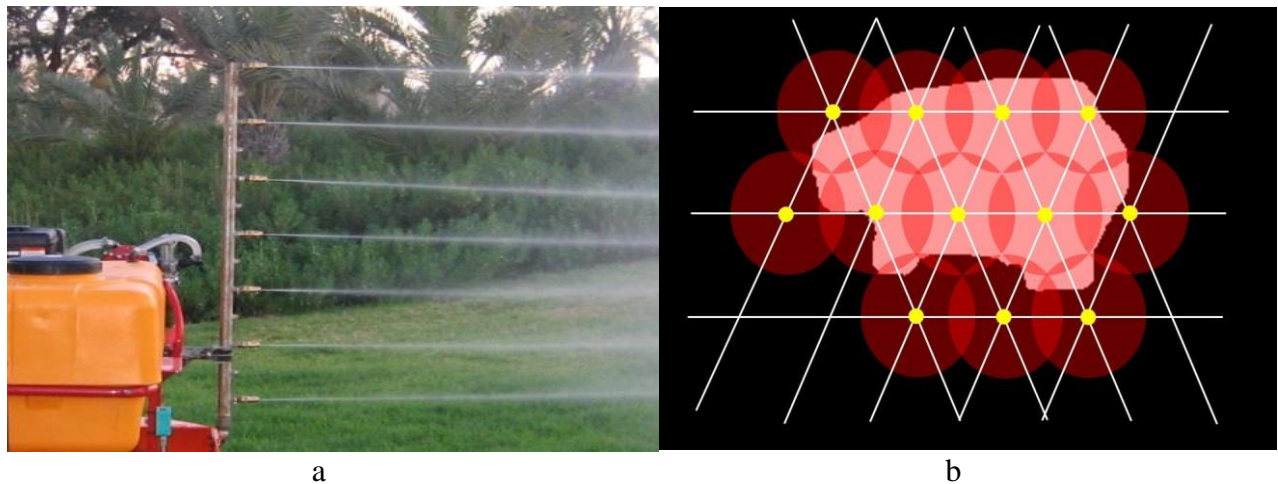


Figure 26 – Fixed nozzle spraying method.
(a) Spraying boom with fixed position nozzles. (b) Nozzle spacing.

7.2.2. Second spraying deposition method – optimal spray coverage

The second spraying method, optimal spray coverage, aims to cover the target area optimally while using a single nozzle, with a preset spray diameter, attached to a pan\tilt head (Figure 27).

The pan\tilt head provides flexible control over the spray position. The target coverage will be similar to the first spraying method with an exception that the area coverage will be optimal.



Figure 27 – Pan\tilt head with spraying nozzle attached.

7.2.3. Third spraying deposition method – one target-one shoot

The third spraying method, One Target-One Shoot (OTOS), is based on the assumption that the spraying circle diameter can be controlled in real-time. With this method, each target will be sprayed once for complete coverage. This type of spraying can be achieved by connecting a single nozzle with a controlled nozzle aperture to a controlled pan\tilt head (Figure 28). The pan\tilt head will direct the nozzle toward the center of the target and by adjusting the spray diameter the entire target will be sprayed (Figure 28).



Figure 28 – Varying spray diameter.

7.2.4. Spraying methods evaluation

The three spraying methods were evaluated using a dataset of 129 images sampled in a commercial vineyard along the season of 2009. The images contained grape clusters images with ground truth marking of the grapes area (Figure 29). Each image was evaluated using computer simulation of the

three spraying methods (described in thesis DVD \Spraying Simulations\) and the results were compared to the corresponding ground truth image. The spraying methods were designed to obtain 100% hit rate so the performance measures were defined as the False Alarm rate (non-target area that was sprayed) and the number of sprays required for the entire image (to cover 100% of the target). To derive the optimal spray diameter the fixed nozzle spacing method and the optimal spray coverage method were evaluated with a range of spray diameters (3-100 [Pixel]).



Figure 29 – (a) Grape clusters. (b) Ground truth of grape clusters.

7.2.5. *Spraying deposition methods – results*

Results of the spraying methods evaluation (Figure 30) are the average outcome of the 129 images used for the simulation. The results shows that for the fixed nozzle spacing and optimal spray coverage spraying methods there is a direct relation between the spray diameter and the pesticide waste given in Equation 4 and Equation 5 respectively (linear interpolation):

$$\text{Pesticide Waste} \left[\text{mm}^2 \cdot 10^3 \right] = 13820 \cdot \text{Spray Diameter} + 54282 \quad \text{Equation 4}$$

$$\text{Pesticide Waste} \left[\text{mm}^2 \cdot 10^3 \right] = 18034 \cdot \text{Spray Diameter} + 30255 \quad \text{Equation 5}$$

Since the OTOS spraying deposition method does not depend on the spray diameter the pesticide waste value is constant (Equation 6):

$$\text{Pesticide Waste} \left[\text{mm}^2 \cdot 10^3 \right] = 125518 \quad \text{Equation 6}$$

The number of sprays per image (Figure 31) shows that for the Fixed Nozzle Spacing and Optimal spray coverage spraying deposition methods there is a power shape function given in Equation 7 and Equation 8 respectively:

$$\text{Number of sprays} = 588.45 \cdot (\text{Spray Diameter})^{-1.208} \quad \text{Equation 7}$$

$$\text{Number of sprays} = 481 \cdot (\text{Spray Diameter})^{-1.08} \quad \text{Equation 8}$$

Since the OTOS spraying deposition method does not depend on the spray diameter, the number of sprays per image is a constant number (Equation 9) representing the average number of targets in one image.

Number of sprays = 7.89

Equation 9

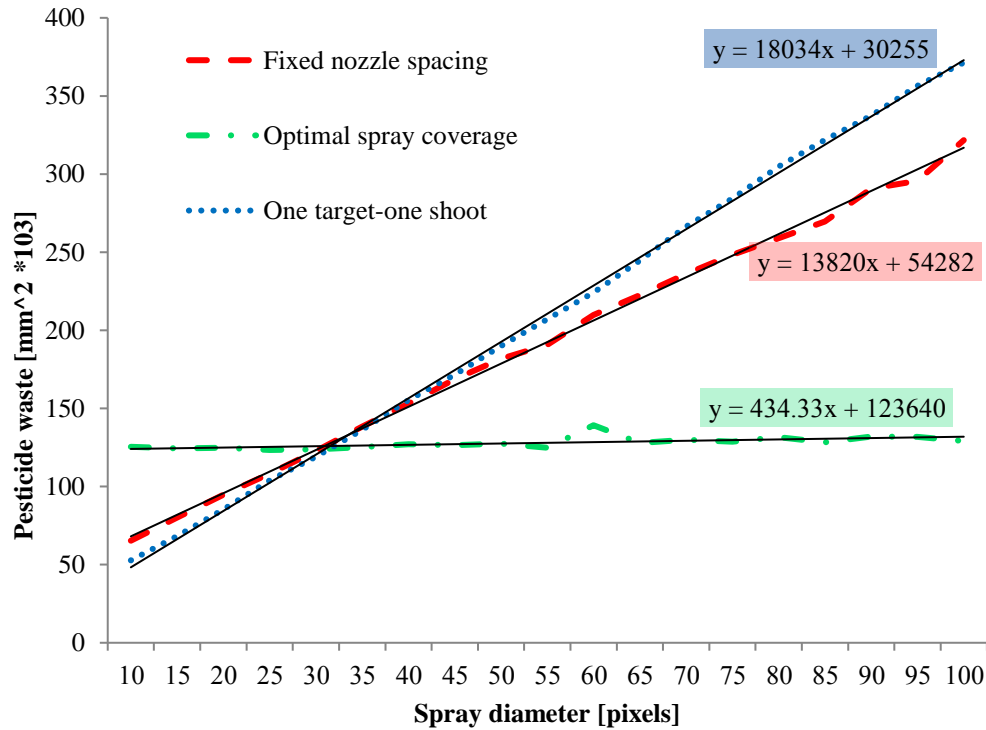


Figure 30 – Pesticide waste (False Alarm + overlapping).

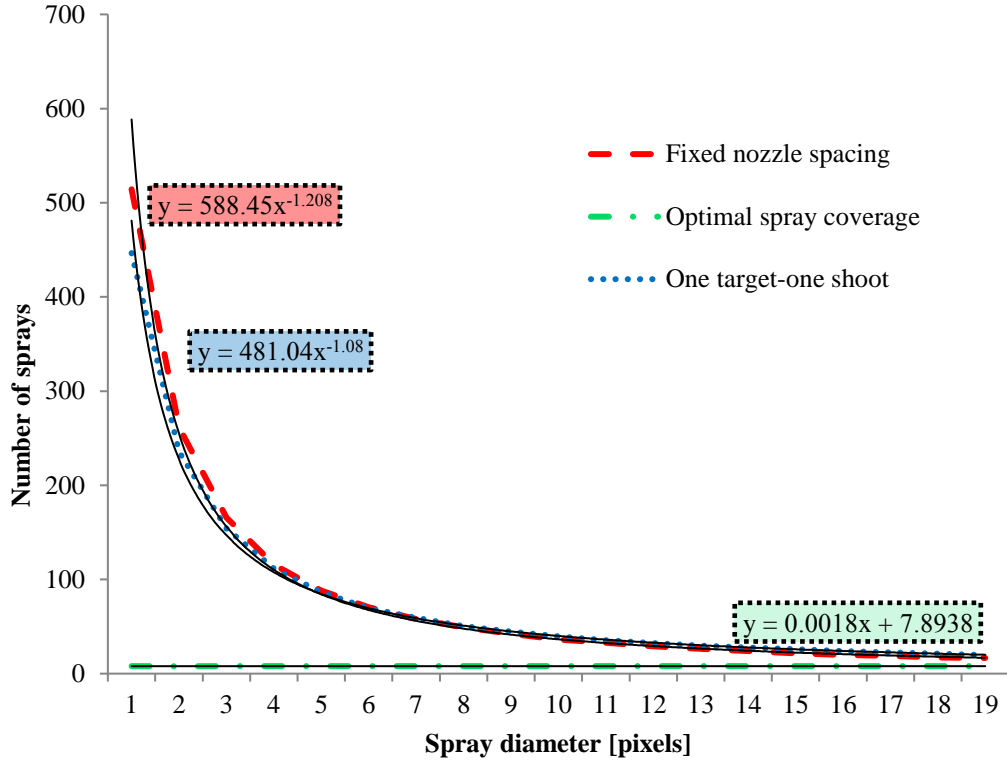


Figure 31 – Number of sprays.

Determining the preferred spraying deposition method best suited for the application is achieved by constructing an economic function for each of the spraying methods (Equation 10, Equation 11, Equation 12). The economic functions include assessment of the related costs due to pesticide waste and the number of sprays. The outcome value of these functions is the farmer expense which must be minimized.

$$V_{\text{Fix NozzleSpacing}}[\$] = (13820 \cdot SD + 54282) \cdot (WV) + (588.45 \cdot SD^{-1.208}) \cdot (ST \cdot TC) \quad \text{Equation 10}$$

$$V_{\text{OptimalSprayCoverage}}[\$] = (18034 \cdot SD + 30255) \cdot (WV) + (481 \cdot SD^{-1.08}) \cdot (ST \cdot TC) \quad \text{Equation 11}$$

$$V_{\text{OTOS}}[\$] = (125518) \cdot (WV) + (7.89) \cdot (ST \cdot TC) \quad \text{Equation 12}$$

where, $V_{\text{SprayMethodType}}[\$]$ is the function result value which represents the cost of spraying one image (one image equal 1.5m of vineyard length), SD is the Spray Diameter used in the spraying process, WV is the pesticide Waste Value [$\$/\text{mm}^2$], ST [Sec] is the Switch Time between targets and TC [$\$/\text{Sec}$] is the Time Cost.

Operational parameters values, updated for nowadays, were calculated to evaluate and compare the economic functions:

- $WV = 10^{-6} [\$]$ (1 liter of pesticide covers 10m² and costs 10\$)
- $TC \cong 0.00695 [$/s]$ (human working hour worth 15\$/h, robot operation worth 10\$/h)
- $ST = 0.2 [s]$ (estimation)

Applying the operational parameters to the economic functions reveals that for the values analyzed the **OTOS spraying method is the least expensive method**, regardless of the spraying diameter (Figure 32).

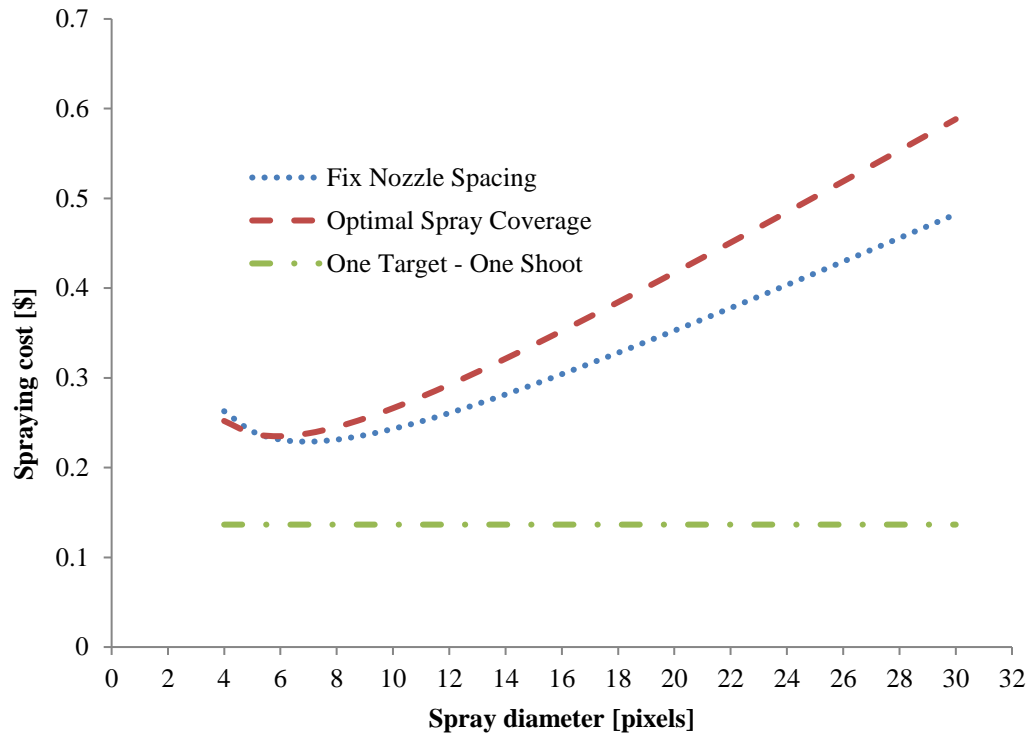


Figure 32 – Economic function results.

Different selection of the operational parameters values can lead to choosing another method rather than One Target-One Shoot spraying method. An equilibrium point between the One Target-One Shoot and the optimal spray coverage method is obtained when $WV = 6 \cdot 10^{-6} [\$]$, implying that the spraying process will be equally costly to the farmer (Figure 33).

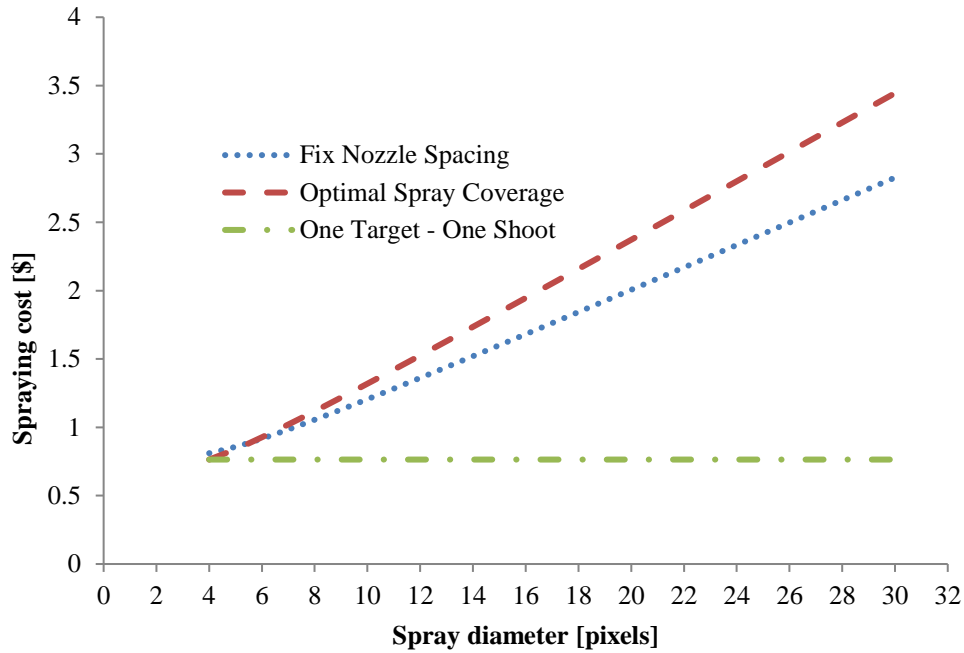


Figure 33 – Economic function results ($WV = 6 \cdot 10^{-6}$ [\$/mm²]).

Additional equilibrium points are described in Table 19.

Table 19 – Equilibrium points.

Method 1	Method 2	WV [\$/mm ²]	TC [\$/s]	ST [s]
One Target-One Shoot	Optimal spray coverage	$6 \cdot 10^{-6}$	0.00695	0.2
One Target-One Shoot	Optimal spray coverage	10^{-6}	0.00695	0.03
One Target-One Shoot	Optimal spray coverage	10^{-6}	0.0012	0.2

7.3. The adjustable spraying device

An adjustable spraying device, ASD, was designed and built as an experimental tool to implement the OTOS spraying method (Berenstein and Edan 2012). The device is mounted to a robotic sprayer able to navigate along vineyard rows and supply pressurized pesticide. The operational concept of the ASD is as follows:

1. Direct the nozzle to face the crop (perpendicular to the crop),
2. Capture an image using the ASD camera,
3. Find the target's position and diameter,
4. For each target perform the following routine:
5. Direct the ASD toward the target center,
6. Adjust the nozzle diameter according to the target diameter, and
7. Open the sprayer electric valve for a specific predefined time.

The ASD is presented in Figure 34. The ASD base is constructed from three aluminum parts, two pressure plates that mount the spraying nozzle and the two line beam lasers, and a shoulder. The shoulder is connected to the pressure plate with 4 screws and can be height adjusted.

A spraying nozzle (AYHSS 16) is constructed from two parts, the nozzle base and the nozzle cup. The nozzle base is mounted to the pressure plates. The pressurized (20 BAR) pesticide hose is connected to the nozzle base and the flow is controlled using an electric valve (on/off). The spraying diameter can be controlled by rotating the nozzle cap over the nozzle base.

A stepper motor, mounted to the shoulder, is used to control the spraying diameter. The stepper motor is connected to the nozzle cap using 2 tangent gears (Figure 34b), one connected to the stepper motor (black, 28T), and the other connected to the spraying nozzle cap (white, 42T). The stepper motor is controlled using a digital stepper motor driver (LEADSHINE DM556). Rotational feedback of the stepper motor is acquired using a rotational potentiometer (10 rounds, 1K Ω) connected to the stepper motor gear. An Arduino (UNO) board closes the stepper motor position loop using feedback from the potentiometer and the desired circular position.

Other peripheral sensors are mounted to the ASD; a laser distance sensor (SICK DX35) for measuring the distance between the device and the target, a color camera (Microsoft studio cam) for capturing images from the field and later used for automatic target detection, and a 2-line beam marking lasers (532 nm, 50m W, 60°) positioned horizontally and vertically for marking a cross (+) over the target. The entire device is mounted on a Pan-Tilt Unit (PTU) (FLIR D46-17) able to rotate horizontally $\pm 180^\circ$ and vertically $+31^\circ - 80^\circ$.

A PC computer is connected to an Arduino board, laser distance sensor, color camera, PTU, and the electric valve controlling the pesticide flow. The main software for managing the ASD was based on Microsoft Visual Studio (c#) (included in the thesis DVD \Robot control software\).

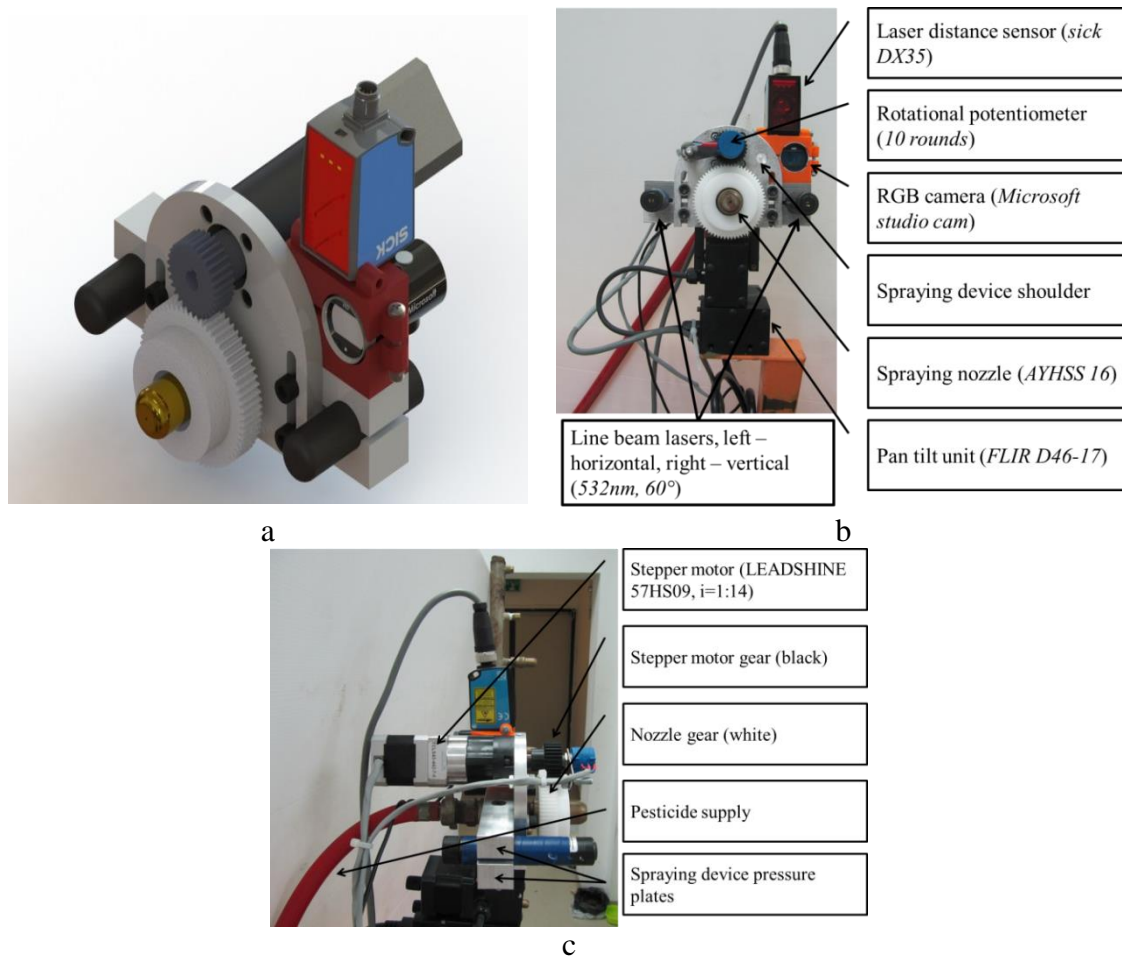


Figure 34 – Spraying device. (a) Isometric view – CAD. (b) Front view. (c) Side view.

7.4. Preliminary experiments

Two preliminary experiments were conducted to evaluate the pesticide flow rate and the spray deposition with different nozzle apertures.

7.4.1. Flow rate evaluation

A flow rate experiment was performed to evaluate the pesticide flow rate for varying spraying nozzle apertures. The experimental setup included setting up a spraying pressure of 20 [BAR] (the recommended pressure for this type of spraying nozzle). The spraying duration was computer controlled using the electric valve.

Twenty-one nozzle apertures that cover all the rotation scale of the nozzle were measured. For each aperture, three sprays were measured with a delay of 4 s between the measurements (the delay was needed to allow the remaining drops to leave the nozzle orifice). The duration of each spray was 1 s. The sprayed material was tap water.

The flow rate evaluation results (Figure 35) show the relation between the flow rate and the corresponding aperture.

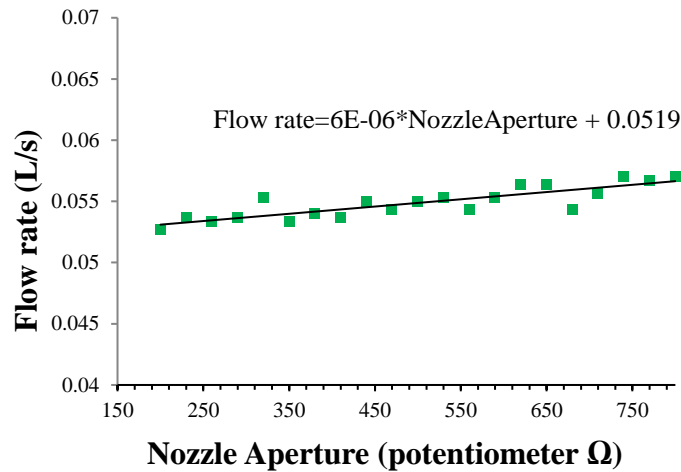


Figure 35 – Flow rate evaluation results.

7.4.2. *Spray diameter evaluation*

Spray diameter was evaluated to find the spray diameter (spray cone) for varying nozzle apertures. Using this relation between the nozzle aperture and the spray diameter, the spray diameter can be adjusted according to the target size.

The experimental setup (Figure 36a,b) included the ASD facing the target base with a target attached. The target base was constructed from steel net and was mounted vertically on a manually controlled conveyor in front of the ASD (Figure 36b).

The target used was a white paper sheet, 0.5 m wide, which was stretched top to bottom and fixed to the target base (Figure 36b shows the target fixed to the target base after spraying). In order to view the spray deposition and post-analyze the position of the spray, a red water-soluble food dye (Florma red 696) was used as pesticide replacement. Each spray repetition included the following steps: (i) attaching a new target to the target base, (ii) setting the nozzle aperture to the desired value, (iii) opening the spray flow, (iv) starting the conveyor movement towards the spray jet, and (v) after the entire target base has crossed the spraying jet, the spray flow is closed and the conveyor stops.

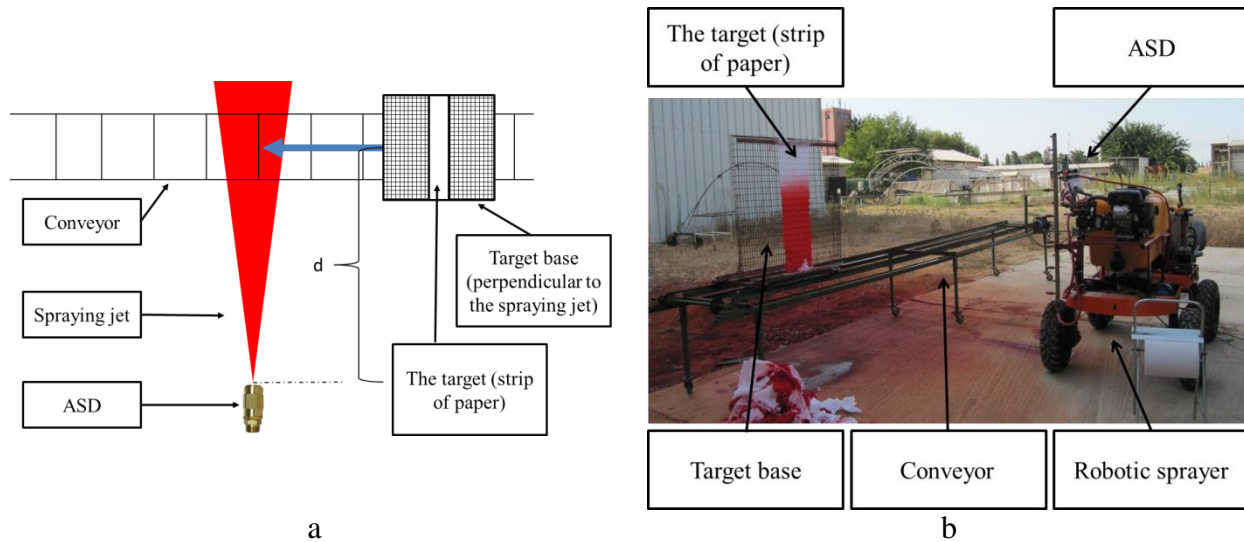


Figure 36 – Experiment configuration.
(a) Experiment scheme. (b) Field view of the experiment.

The ASD software is designed to start capturing a movie from opening to closing of the spray jet using the ASD camera. After each spray repetition, the captured movie is saved for post-analysis. Each movie was manually scanned by a human expert to extract a single image containing the target in mid-frame. The extracted frame is analyzed manually for the spray boundaries (Figure 37). Since the spray is cone-base shaped, the spray diameter can be evaluated by measuring the upper and lower boundaries.

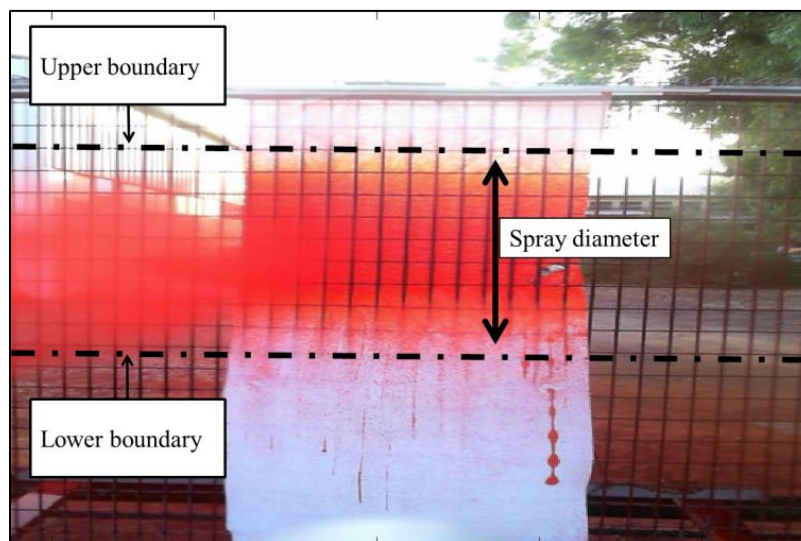


Figure 37 – Sprayed target.

The experimental design included 3 distances between the ASD and the target. For each distance the nozzle aperture measures were between 175 and 210 with increments of 5 (units in potentiometer Ω). Three measurements were conducted for each distance-aperture combination.

The experiment started at dawn ensuring no wind (wind was measured as 0 using Skywatch Xplorer 1).

The experimental results shown in Figure 38 reveal the relation between the nozzle aperture and the spray diameter for three measured distances.

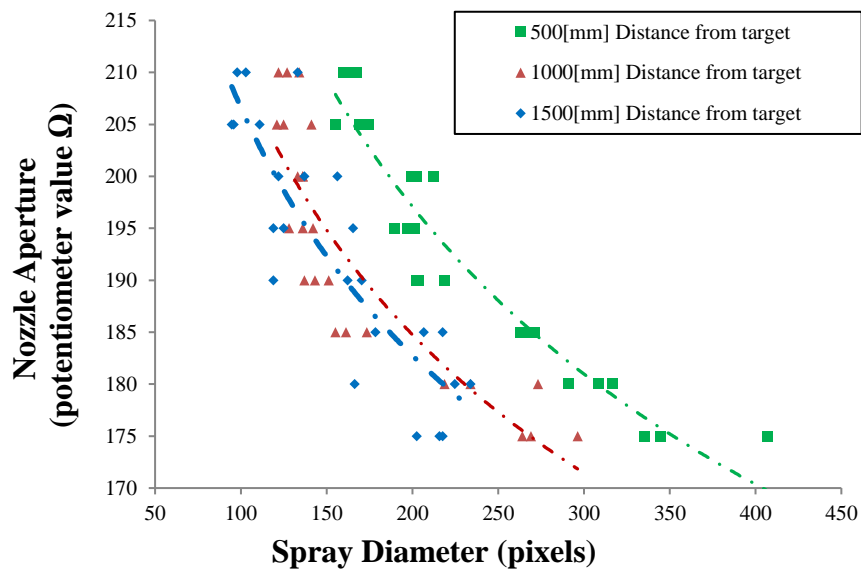


Figure 38 – Experimental results.

Table 20 – Experimental results summary.

Distance	Trend line	R^2	Trend line type
500	$NA=600.22 \cdot SD^{-0.210}$	0.911	Power
1000	$NA=490.97 \cdot SD^{-0.184}$	0.782	Power
1500	$NA=467.12 \cdot SD^{-0.177}$	0.761	Power

Table 20 presents the curve fitting for Figure 38, where NA is the nozzle aperture and SD is the spray diameter. In theory, the three curves are supposed to unite since both the camera field of view and the spraying cone have a linear trajectory. We assume that the spray jet turbulence and air drag affect the spray dispersion. By using the resulting curves for the different distances, the nozzle aperture can be calculated after extracting the target diameter.

The spraying distance in most commercial vineyards is between 500 and 1500 mm. In order to correlate between the spraying distance and the nozzle aperture, an interpolation of the distance and the nozzle aperture is applied.

7.5. Evaluating the ASD performance

An experiment was conducted to evaluate the performance of the ASD while implementing the results of the previous experiment (Figure 38 and Table 20). Currently, the robotic sprayer is designed to perform the spraying task in step mode (Figure 39): the robot travels a single step along the vineyard row, stops, captures image from the field, sprays the targets, and moves another step forward. The experiment is based on the same work procedure.

One of the secondary goals of this experiment was to provide insights regarding the overall work procedure of the complete spraying system which will include the robot equipped with an ASD.

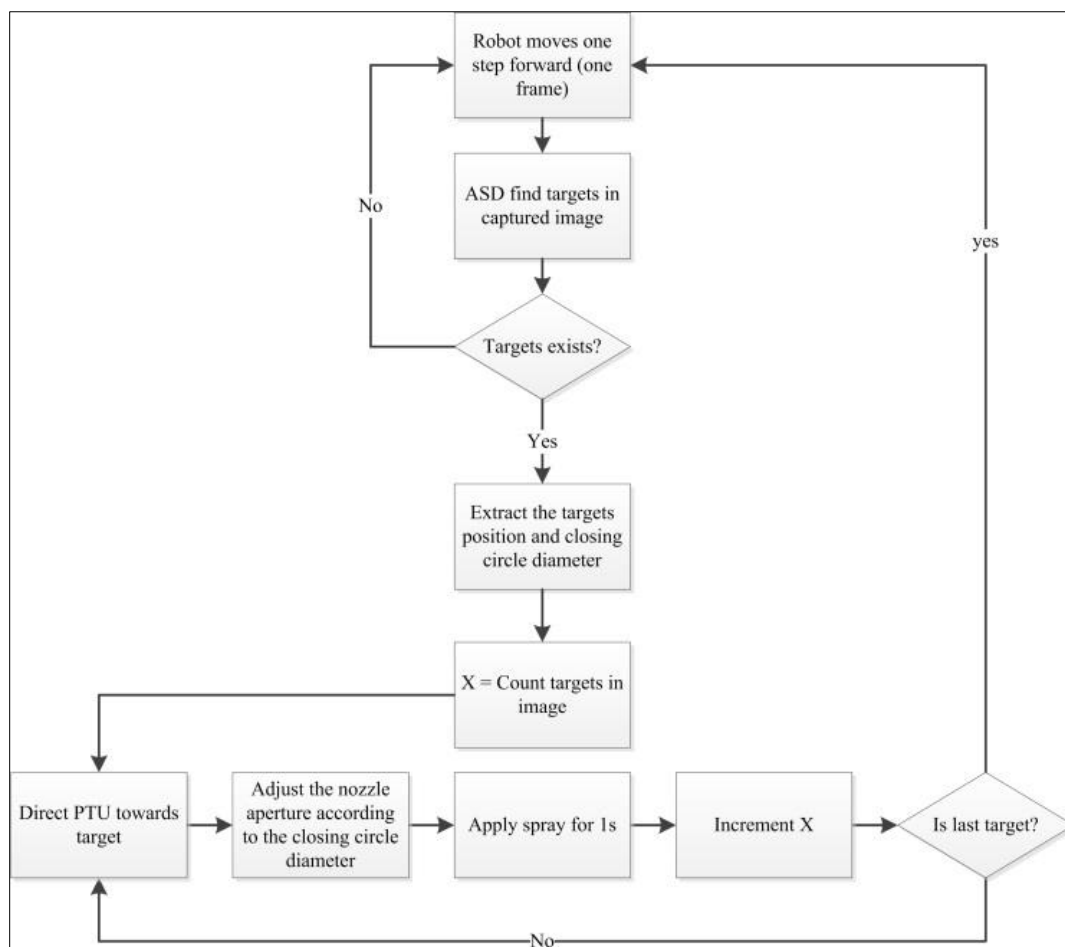


Figure 39 – Robotic sprayer work procedure.

7.5.1. Experimental setup

In the experiment the ASD was attached to the robotic sprayer and was operated similarly to the robotic procedure. According to the robot work procedure (Figure 39), the robotic sprayer should move in step mode along the vineyard row. To avoid path tracking control problems the robotic sprayer was programmed to track a straight base line (red plastic strip 50 mm width) (Figure 41a). The robot is programmed to travel 1.6 m in each step. The ASD is mounted perpendicular to the robot's travel direction and faces the target's base (Figure 41a). The target's base is a polyethylene net (50 mesh), 11 m long, stretched between two anchoring poles, and positioned parallel to the base line. The targets are attached to the target's base and the center of the target is positioned 1.55 m high. In order to ensure a single target per image, the targets were positioned at intervals of 1.6 m, similar to the robot's travel distance.

The targets are blue polyethylene round circles with varying diameters (300, 250, 230, 210, 190, 170, and 150 mm). To simplify the detection and classification of the targets, a red circle was attached to the center of the main target. The diameter of the red circle was one-third of the blue circle diameter.

The target detection algorithm was based on color thresholding and was implemented using Matlab software equipped with the image processing toolbox. The algorithm works as follows:

1. Capture input RGB image (800×600) (Figure 40a),
2. Create three ratio-images, green/red, blue/red, blue/green (Figure 40b,c,d, respectively),
3. Threshold the ratio-images. The threshold value was set as the average image pixel value multiplied by 1.5 (Figure 40e,f,g),
4. Merge (logical AND) the resulting binary images (Figure 40h),
5. Fill holes in the image using morphological operations (using Matlab command *imfill*) and apply the removal of small clusters (<500) that are considered as noise (using Matlab command *bwareaopen*) (Figure 40i).

The next steps were developed to distinguish between true and false targets and were applied to each of the detected targets:

6. Isolate the bounding box of the target (Figure 40j),
7. Convert the RGB image to HSV representation and isolate the hue and saturation channels,
8. Apply thresholds on the hue channel (with a scale of 0~1, $\text{hue} > 0.9$ & $\text{hue} < 0.1$) to extract the red area (Figure 40k),
9. Count the number of red pixels and compare to the number of blue pixels. In theory, the outcome ratio value should be 9; however, since the images are acquired in real world conditions, the ratio allowed is according the following conditional statement:

$7 < \frac{\text{blue} + \text{red}}{\text{red}} < 11$. If the conditional statement is true then the detected target is defined as a

true target, else, the detected target is noted as a false one (Figure 40l).

Following the detection process the program extracts the coordinates of the detected target's center and diameter in pixel units. These measures are used to control the sprayer.

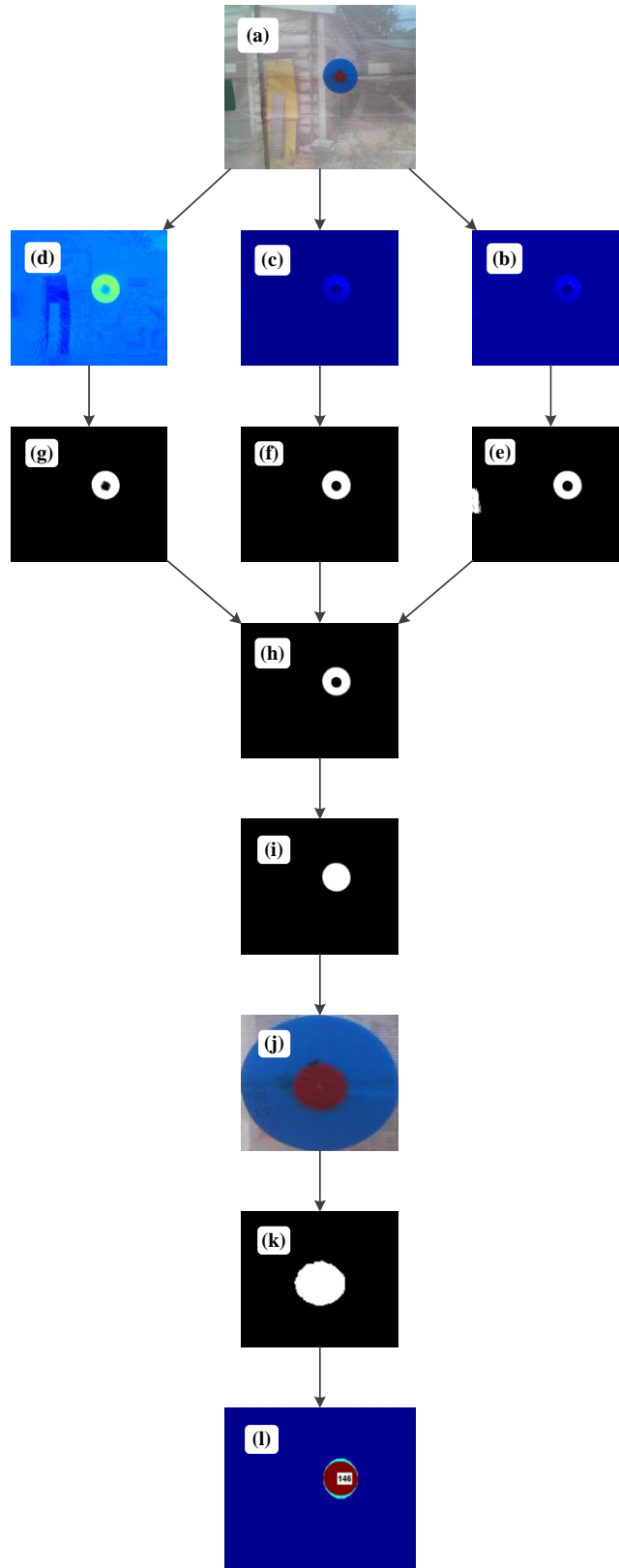


Figure 40 – Target detection procedure. The algorithm output image (I) shows the detected target (red), the surrounding circle (light blue). The number in the circle represents the diameter of the surrounding circle needed to cover the entire target.

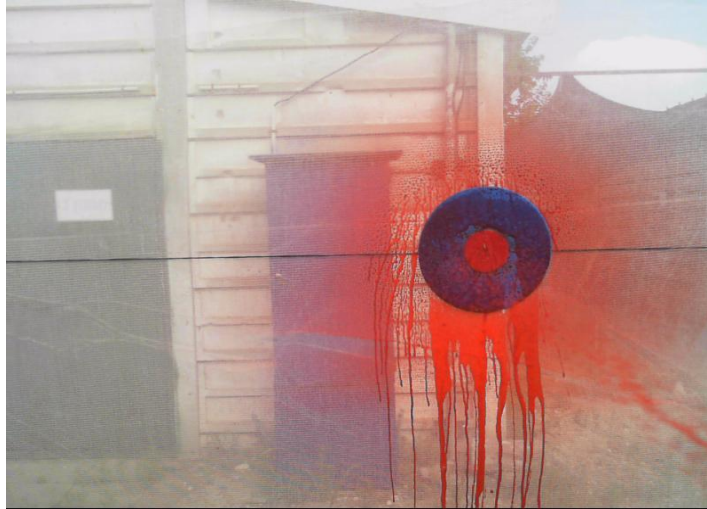


Figure 42 – Image captured immediately after spraying.

7.5.2. Experimental design

The experiment included 12 repetitions of the robot traveling along the base line and spraying the seven targets attached to the target base. Each target was sprayed for 2 s. All experiments were conducted early morning. Measured wind speed was zero in all experiments (measured using Skywatch Xplorer 1).

7.5.3. Experimental results

In addition to the captured images from each spray, a visual inspection was performed immediately after the spray. The visual inspection revealed that each target was fully covered by the spray. The experimental results are summarized in Figure 43. The results show constant increasing of the sprayed diameter with the increment of the target size; however, the ratio between the sprayed diameter and the target size decreases. This ratio can be addressed as the false detection ratio, and according to Figure 43 this ratio decreases with the increase of the target size.

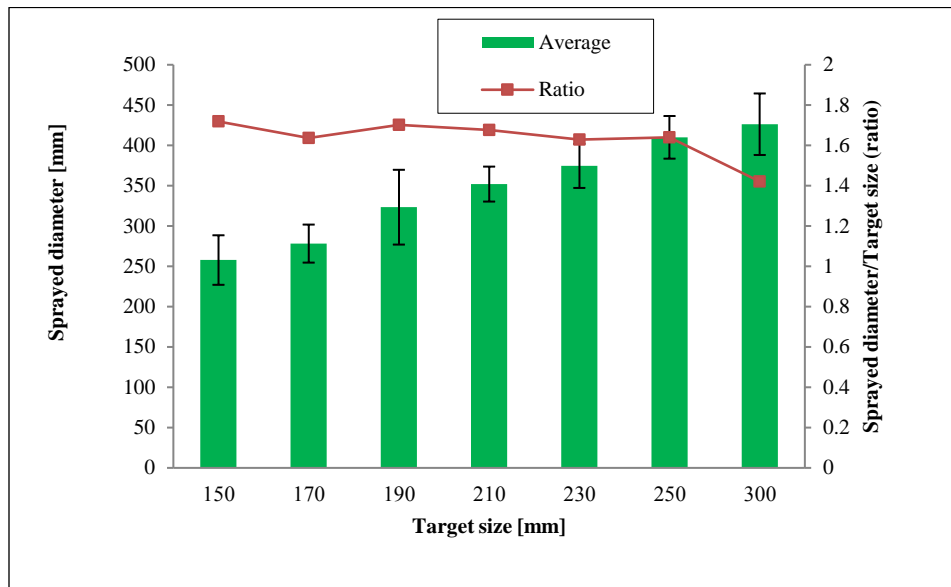


Figure 43 – Experimental results. Each column represents the average sprayed diameters of 12 sprays (robot repetitions). The results standard deviations are shown on each column. Secondary axis (right) measures the ratio between the sprayed diameter and the target size.

8. INTEGRATIVE SITE-SPECIFIC SPRAYER EXPERIMENT

8.1. Overview

The following experiment was designed to demonstrate and evaluate the three main components of the collaboration framework working in sync: human marking methods, levels of human-robot collaboration, and the specific spraying device. For better experimental control, artificial targets were used and robot navigation along the vineyard row was replaced by following red tape fixed to the ground (see video of experiments in the thesis DVD \Integrative site specific sprayer experiment\). By using artificial targets (Figure 47) we were able to ensure 100% detection rate of the robot and control the FA rate. This was important so as to produce optimal and reproducible experimental conditions for the human-robot spraying evaluation. Evaluation in real world vineyards would introduce highly variable scenes with unpredictable detection and false alarm rates which would have disabled systematic evaluation. Furthermore, experiments could not have been repeated in identical conditions.

8.2. Experimental setup

As the human-robot collaboration framework suggests (Figure 16), the human was remotely located at Ben-Gurion University of the Negev located in Beer-Sheva, Israel. The robot was located 100 km from the human operator in Beit Dagan, Israel. The experiment consists of the robotic platform operating in a step mode as described in Figure 44.

8.2.1. Robot side

The robotic platform was programmed to follow a red base line (red plastic strip 50 mm width) (Figure 41a, Figure 45) that was fixed at a 1.6 m distance in parallel to the target's base. During each step, the robot travels 1.6 m to completely change the current frame point of view (POV). The ASD was mounted to the robot, perpendicular to the robot's travel direction, facing the target's base (Figure 45). The target's base was a 50 mesh, polyethylene net, 18 m length, 1.5 m height, mounted 0.5 m from ground level (Figure 45). Fifty targets were randomly spread along the target's base at least 20 cm apart, imitating grape clusters (Figure 45).

The targets were constructed from blue polyethylene plastic and were hand cut according to four shape patterns as shown in Figure 46. The size of each target was measured using machine vision algorithms (geometrical analysis was not possible due to the amorphous shape of the targets). The targets sizes were: 623.7, 648.85, 718.63, 538.88 [cm²] corresponding to the target number in Figure

46 (the program codes for analysis and calculation of the targets' sizes are included in the thesis DVD \Target size calculation\).

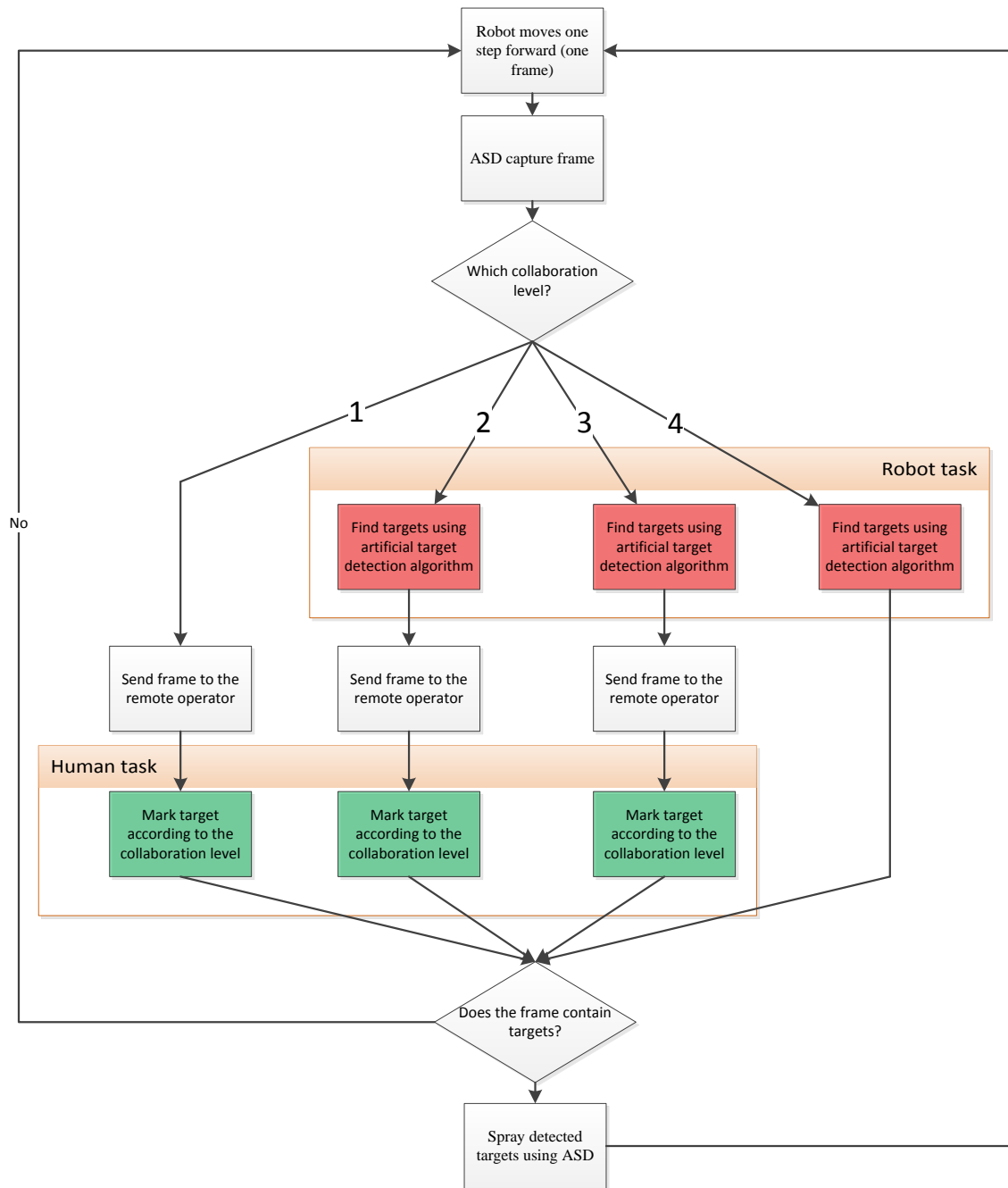


Figure 44 – Robotic sprayer work procedure.

In order to be as close as possible to commercial field conditions the experiment included a pre-defined hit rate (in the shape of targets that the robot cannot detect) and pre-defined false alarm rate. The targets were divided into two groups, 38 targets that can be detected by the robotic sprayer (red

circle in the middle of the target, Figure 47a), and 12 targets that cannot be detected by the robotic sprayer (yellow circle in the middle of the target, Figure 47b).

The developed target detection algorithm is similar to the target detection algorithm described in section 7.5.1 and in Figure 40 with minor adaptation to enable detection of the yellow color. The detection was based on Matlab, using the Matlab Image processing tool (included in the thesis DVD \Artificial targets detection\). The pre-defined FA was added using the Matlab Image processing tool. The mathematical morphology operation *Dilation* was used to expand the computer detected target (Figure 48) (included in the thesis DVD \Adding FA\). Since each of the captured images is unique in the sense of different number of targets, target orientation and position, the added FA is different for each image. The average FA added was 17.3% (with standard deviation of 5.5) of the entire image.



Figure 45 – Robot following red strip and targets spread along plastic net.

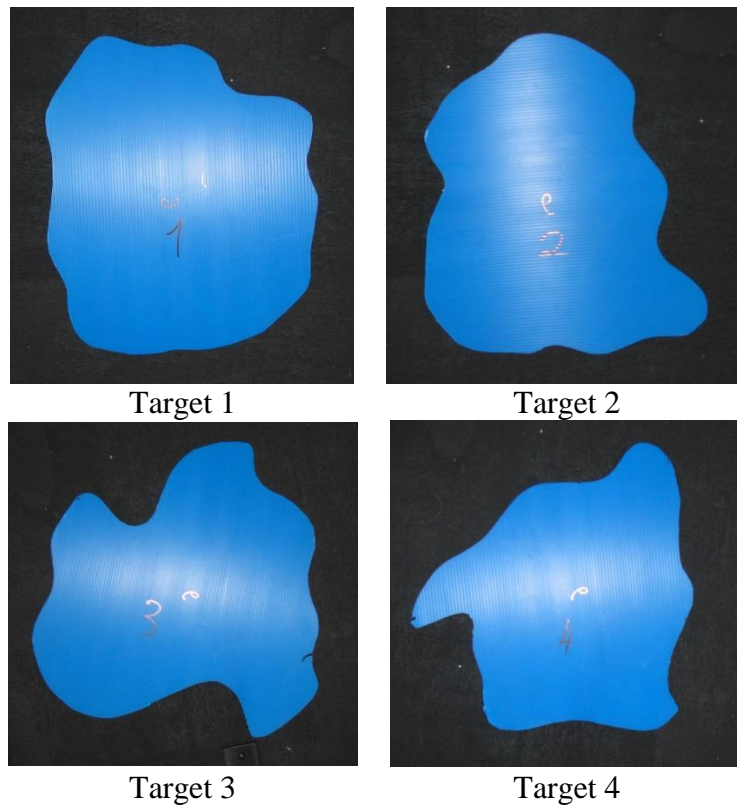


Figure 46 – Target patterns.

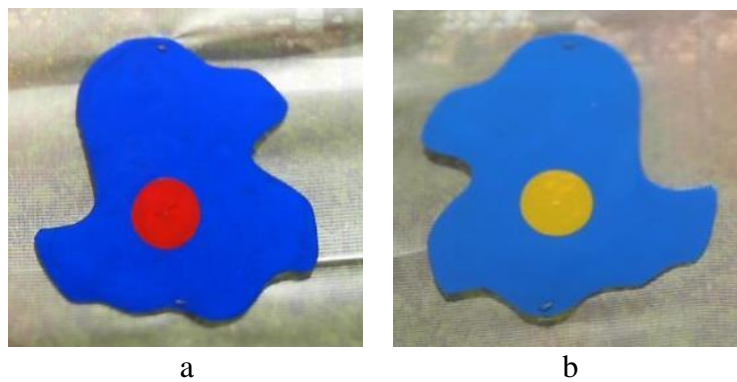


Figure 47 – Target groups. (a) Robot can detect. (b) Robot cannot detect.

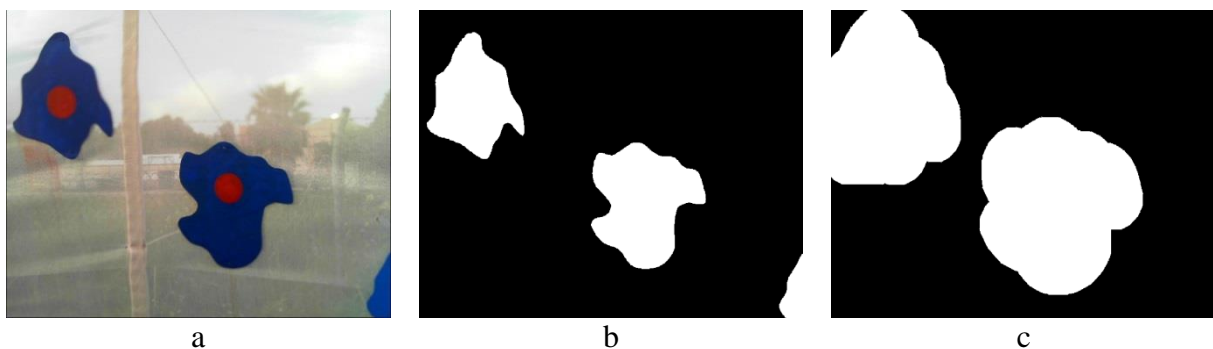


Figure 48 – Adding FA.

(a) Original image. (b) Computer detected. (c) Computer detected with added FA.

Using the ASD, the targets were sprayed with red water-soluble food dye (Florma red 696) (Figure 51). Each target was sprayed for 1 s and immediately after the spraying operation stopped, an image of the spray was captured and saved for post analysis (Figure 51 shows examples of captured targets after the spraying operation).

8.2.2. *Human operations*

The human task is to mark the target area using one of the marking methods described in section 6.3 and according to the collaboration level being evaluated. The human was using a desk computer equipped with a 19” screen (Figure 49). Each user was trained before the experiment with 30 images according to the results described in section 6.6.

According to Figure 44, after each step the robot captured an image using the ASD camera and the target detection process began according to the evaluated collaboration level:

Collaboration level 1: In this fully manual collaboration level, the captured image is sent directly to the remote operator without any detection help from the robot. The remote operator marks the targets and sends the marked frame back to the robot for spraying.

Collaboration level 2: The captured frame is analyzed using the target detection algorithm by the robot and sent to the remote operator as a recommendation about the “whereabouts” of the targets in the frame. The remote operator marks the target while assisting the robotic recommendation and sends the marked frame back to the robot for spraying.

Collaboration level 3: Similar to Collaboration level 2, with the difference that the robot marks the target and the remote operator supervises the detection (can add or remove targets).

Collaboration level 4: Fully autonomous operation, the robot detects the targets using the target detection algorithm and continues directly to the spraying operation without human assistance.

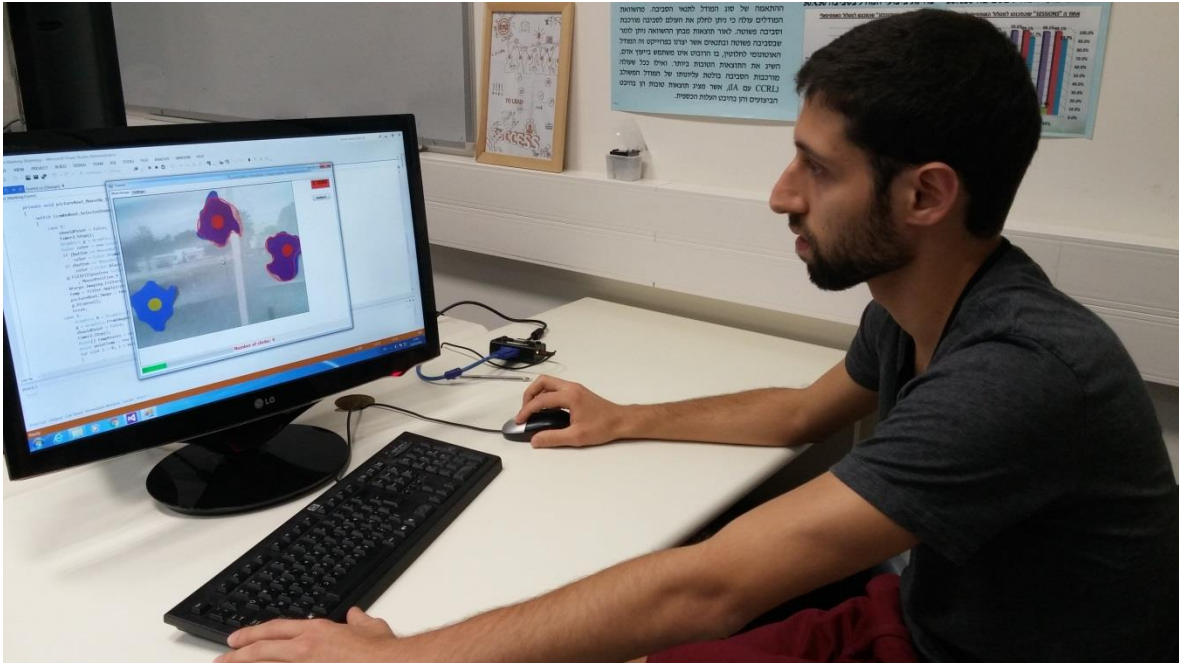


Figure 49 – Human marking targets from a remote computer located 100 km south of the robot in Beer-Sheva, Israel.

8.2.3. *Spray evaluation*

The spray quality was evaluated using three methods:

1. Comparison between the computer-detected targets (Figure 50b) (all the targets – both red and yellow points) and the marked area to spray (Figure 50c) – performance measures: Hit and FA rates,
2. Comparison between the computer-detected targets (Figure 50b) and the area to be sprayed (Figure 50d) (green circles in Figure 50d) – performance measures: Hit and FA rate,
3. Qualitative analysis of the sprayed target (Figure 51). Each sprayed target image was presented to an expert and was marked on a 1 to 5 scale (Figure 51) – performance measure: Hit rate.



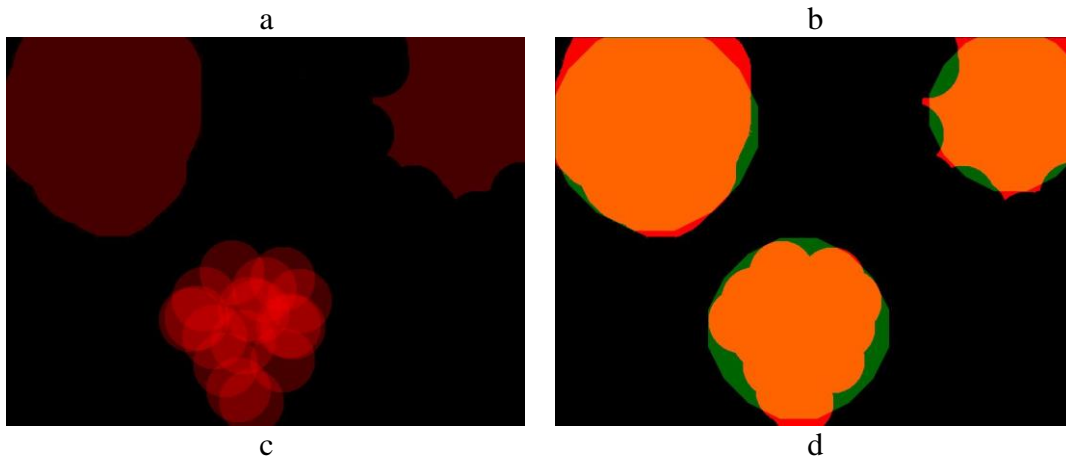


Figure 50 – Evaluation documentation. (a) Captured image. (b) Computer detected. (c) Human and robot combined marking. (d) Green circles represent the area to be sprayed.

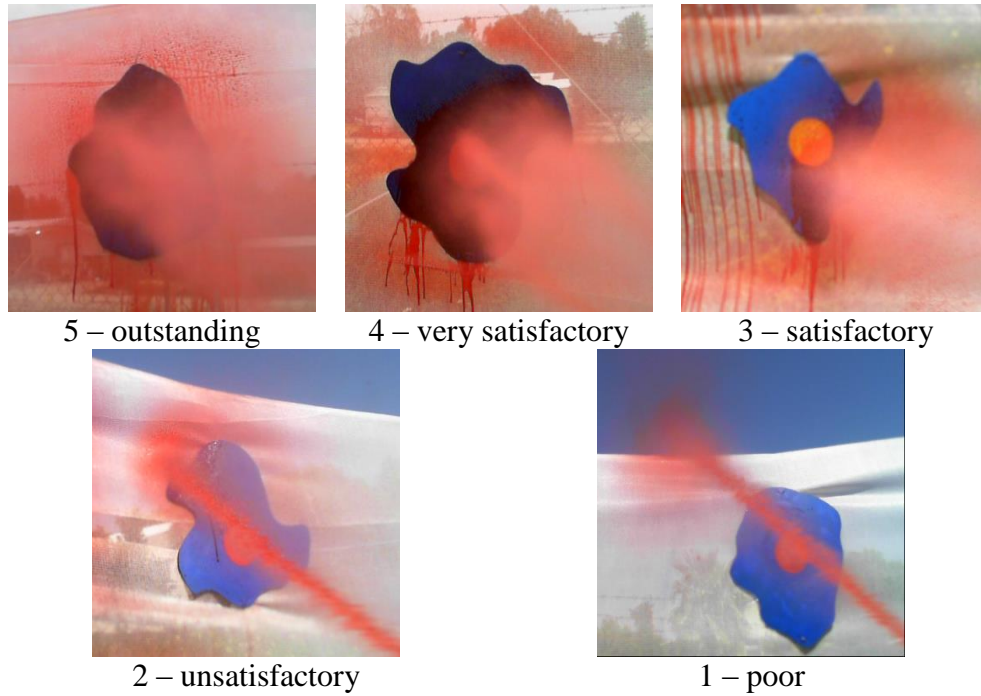


Figure 51 – Target spraying evaluation scale 5 (outstanding) → 1 (poor).

8.3. Experimental design

A group of 20 students, male and female, aged 25 to 40, participated in the experiment. The participants were divided into two groups, one for each marking method (Constant Circle Diameter and Free hand). Each participant practiced the three collaboration levels. For each collaboration level the robot traveled a single time along the target base. The image switching time was set to 12 sec.

For the fourth collaboration level the robot performed 10 repetitions where each included the robot traveling along the target's base with 1.6 [m] intervals, capturing the target's frame, analyzing the captured frame using the artificial target detection algorithm (detailed in section 7.5.1 and Figure 40) (included in the thesis DVD \Artificial targets detection\), and spraying toward each of the detected targets.

8.4. Experimental results

Detailed results are summarized in Appendix C and in the thesis DVD \Final experiment results\. Collaboration level 1 – fully manual. Collaboration level 2 – robot suggests, human approves

Collaboration level 3 – robot marks, human supervises. Collaboration level 4 – fully autonomous

Figure 52 and Collaboration level 1 – fully manual. Collaboration level 2 – robot suggests, human approves

Collaboration level 3 – robot marks, human supervises. Collaboration level 4 – fully autonomous

Figure 53 show the graphic representation of the experimental results, where the columns “marking hit” and “marking FA” represent the hit rate and FA using evaluation method #1 (section 8.2.3), the columns “spray hit” and “spray FA” represent the hit rate and FA using evaluation method #2 (section 8.2.3), and the spray evaluation represents the hit rate using evaluation method #3 (section 8.2.3). Collaboration level 1 – fully manual. Collaboration level 2 – robot

suggests, human approves

Collaboration level 3 – robot marks, human supervises. Collaboration level 4 – fully autonomous

Figure 52 and Collaboration level 1 – fully manual. Collaboration level 2 – robot suggests, human approves

Collaboration level 3 – robot marks, human supervises. Collaboration level 4 – fully autonomous

Figure 53 also present the fully autonomous collaboration level 4 results, which are identical in both figures.

The overall performance of the free hand marking method was better than the circle by 2.8% on average. Hit rate was improved for all cases when using the free hand marking (except for “spray evaluation” in collaboration level 2, robot suggests, human approves). along with the improvement of the Hit rate, the FA measures increased by 4.5% on average, implying more wasted spraying material. In both marking methods (Collaboration level 1 – fully manual. Collaboration level 2 – robot suggests, human approves

Collaboration level 3 – robot marks, human supervises. Collaboration level 4 – fully autonomous

Figure 52, Collaboration level 1 – fully manual. Collaboration level 2 – robot suggests, human approves

Collaboration level 3 – robot marks, human supervises. Collaboration level 4 – fully autonomous

Figure 53) the Hit and FA rates increase with the collaboration level. The best Hit rate results (91.3%) were achieved when using the free hand marking method with collaboration level 3 (robot marks, human supervises).

Another parameter that should be considered is the number of sprays (Table 21). The number of sprays also represents the number of detected targets sprayed where each target is sprayed once. Since the number of targets in each repetition was 50 we can see that some false spraying occurs in all the repetitions. One of the reasons that the number of sprays is higher while using the Free hand

marking method is also due to the marking procedure. For future commercial use, we recommend to filter out small objects in the marked image that due to their small size should not be considered as targets to be sprayed.

Unlike the results reported in section 6.8.3 and presented in Figure 25 where the constant circle diameter shows better performances compared to the free hand marking method, in this experiment the free hand marking method showed a better hit rate for all of the collaboration levels. We assume that the target's shape had some influence on the different marking methods.

The artificial target detection algorithm was designed to detect 76% of the targets (38 targets red circle in the middle among 50 targets in total). Collaboration level 4 (fully autonomous) marking and spraying hit of ~69.5% (Collaboration level 1 – fully manual. Collaboration level 2 – robot suggests, human approves

Collaboration level 3 – robot marks, human supervises. Collaboration level 4 – fully autonomous

Figure 52, Collaboration level 1 – fully manual. Collaboration level 2 – robot suggests, human approves

Collaboration level 3 – robot marks, human supervises. Collaboration level 4 – fully autonomous

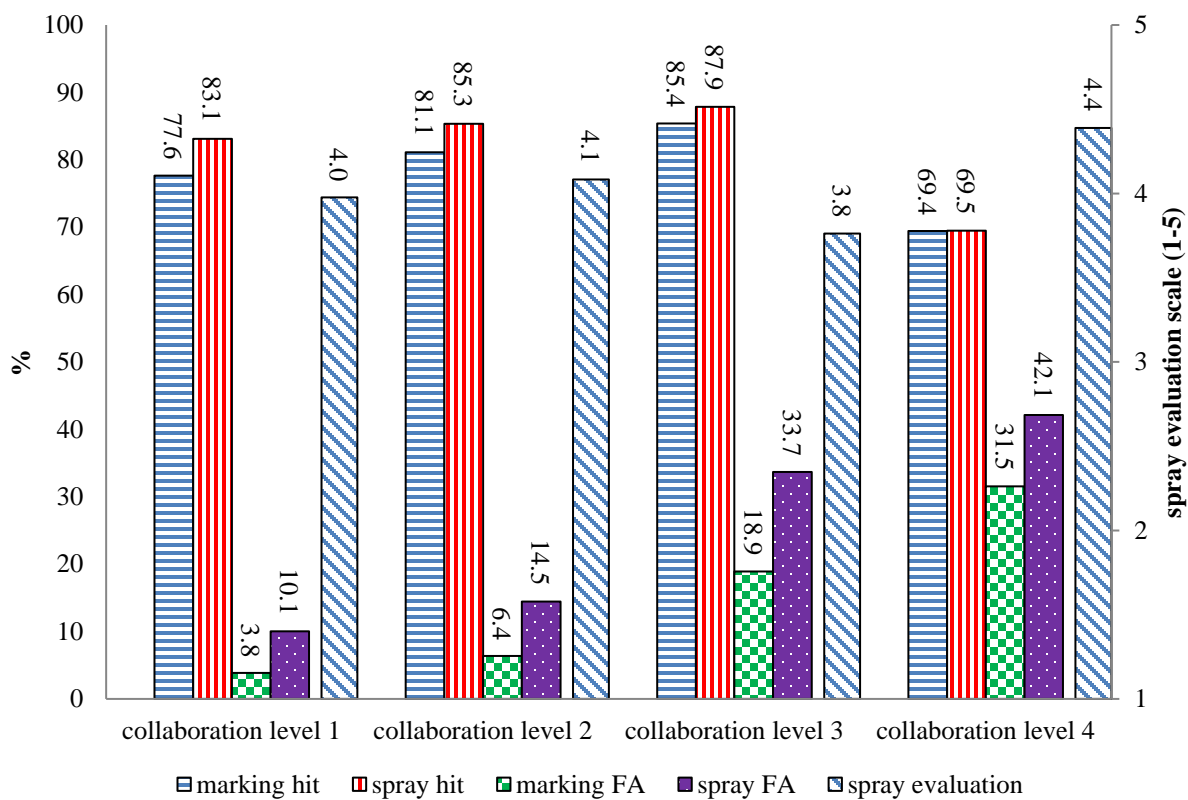
Figure 53).

When there is high importance of low FA we recommend using the circles marking method with collaboration level 1, i.e. fully manual human target marking.

Table 21 – Number of sprays.

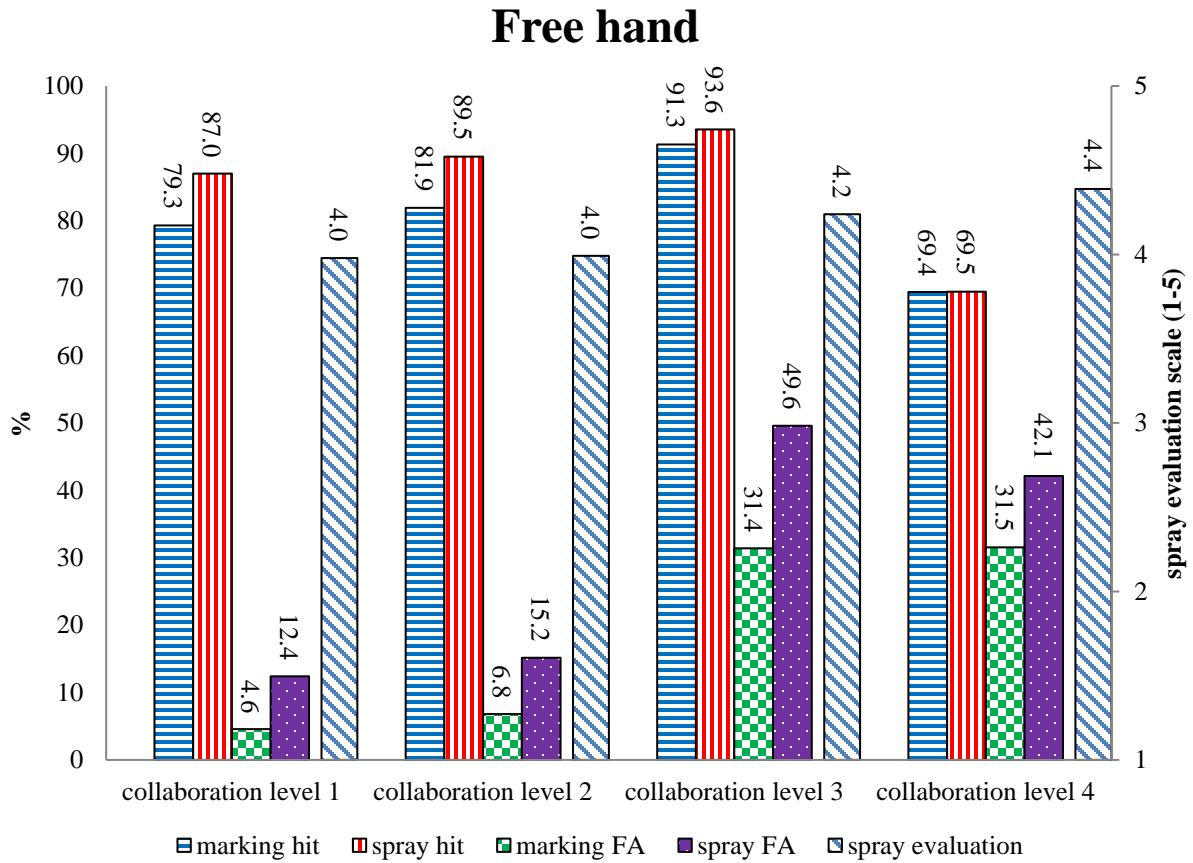
Marking method	Number of sprays			Collaboration 4
	Collaboration 1	Collaboration 2	Collaboration 3	
Circles	57.5	55.0	67.0	41.3
Free hand	64.4	66.4	60.4	

Circles



Collaboration level 1 – fully manual. Collaboration level 2 – robot suggests, human approves
 Collaboration level 3 – robot marks, human supervises. Collaboration level 4 – fully autonomous

Figure 52 – Experimental results for the circles marking method.



Collaboration level 1 – fully manual. Collaboration level 2 – robot suggests, human approves
 Collaboration level 3 – robot marks, human supervises. Collaboration level 4 – fully autonomous

Figure 53 – Experimental results for the free hand marking method.

9. SUMMARY, CONCLUSIONS, AND FUTURE WORK

9.1. Summary and conclusions

A full scale robot was developed for the task of pesticide spraying in vineyards. The robot development included most of the mechanical, hardware, and software needed for the robot to perform the spraying task including grape cluster detection algorithms, human-robot collaboration framework, target marking interface for the remote human, sensors registration algorithm dedicated for the agricultural domain, and a spraying device for accurate target spraying. All modules were evaluated with real field data and were integrated into an operational system which was evaluated in field conditions.

A full scale robotic platform was designed and built to serve as a research tool. The hybrid power sources (two batteries 12v-100Ah combined with a 2500W power generator) enable the robotic platform to work (and experiment) in the field for long time periods without the need for an external power source. The robot kinematic design was proven to travel and maneuver well along commercial vineyard terrain. For future robotic platforms designed to work in the field and based on electrical motors, we recommend to install electrical motors with a planetary gear transmission instead of worm gear transmission like the one installed in this work. One of the characteristics of worm gear is a “self-lock”, when the input shaft (motor) is static, the output shaft behaves like a break (i.e., the input-output of the worm gear is not bidirectional). In some applications the self-lock can be used instead of braking, but when used in an experimental platform in the field (and even in commercial use), in case of a failure, the platform cannot be dragged out of the field and a complicated operation is then required to move the platform.

Although the focus of this thesis was not on the robot's control it must be noted that significant errors in tracking along the robot's path can affect the precision of line-following and hence the spray cone and target coverage. In this work this has been avoided by ensuring accurate path tracking using the well detected red line.

With some adjustments, the robotic platform can be used for other tasks in vineyards such as weed control, pruning, and harvesting. The robotic platform can also be used for tasks in other grove and open field crops and orchards.

A spraying device capable of adjusting the spray diameter was designed, built, and attached to the robotic platform. Much like the robotic platform, the spraying device was designed and built as an

experimental tool with a strong commercial orientation. The suggested device and spraying method show the ability to perform the spraying task efficiently and economically.

The overall spraying duration for a single artificial target was 11 s. This duration included general software commands, communication between main software and peripherals (Matlab, Arduino), machine vision, PTU repositioning, spraying nozzle aperture adjustment, spraying, and capture of image post-spraying. The duration also included some software pauses located in critical points of the software. These pauses were used to control the experiments and to verify that the ASD was functioning as designed. The accumulated time of the pauses was 8 s and spray time was 2 s. By eliminating the software pauses, *the spraying time for a single target can be reduced to 3 s including the 2 s spraying time*. Further time reduction can be achieved by optimizing the machine vision algorithms and the overall ASD managing software.

The system was remotely operated from a distance of 100km. Time delay was not an issue in the experiments (0.05 sec to upload image from the robot to the remote user). As communication hardware is expected to increase speed in future systems, performance will probably not be affected even with increasing distances since we are dealing with single image transfer.

From the mechanical design aspect, we would suggest a more powerful (i.e., higher allowed payload) PTU (e.g., FLIR D48E) than the one used (FLIR D46-17).

Grape cluster and foliage detection algorithms were developed to provide the robotic sprayer with spraying positions. The algorithms were developed under a new concept that considered pesticide reduction as the main optimization parameter. Furthermore, the farmer could select the task objective (maximize hit rate or minimize false alarms). Three algorithms were developed, each based on a different machine vision concept. The algorithms were designed to work autonomously without human help or supervision. The algorithms' detection results show approximately 91% hit rate while minimizing the FA rate to 30%. The optimal algorithm (based on maximum hit rate and minimum FA) was later used as the robot decision regarding the positions of the grape clusters while applying the human-robot collaboration framework.

One of the options to improve the target detection results is by using multiple sensors and applying a sensor fusion algorithm. When using several imagery sensors, each mounted at a different position (location and orientation), it is essential to perform image registration. *A distance-dependent image registration method was developed specifically for the agricultural domain.* Our approach was based on pre-calibrating a distance-dependent TM between the sensors, and representing it in a compact way by regressing the distance-dependent coefficients as distance-dependent functions. In our case

these dependencies ended up linear, but more elaborate DDTM may be obtained in more complicated situations. While the presented approach was developed for an agricultural environment application, it can be applied to other applications that require registration of objects at varying distances. The method can be used to register images from all imaging sensors providing the sensors can detect common control points.

Another option to improve the target detection results is by introducing a human operator in the target detection loop. *A human-robot collaboration framework was developed specifically for the remote target detection task.* The framework included the development of four levels of human-robot collaboration, human target marking interface, and three methods for the human to mark targets remotely. The results from the learning experiment confirmed assumptions made prior to the experiment. Hit rate is maximized and FA is minimized when the human has more time to mark the targets in the image. Additionally, it takes time for the user to learn the system and training is necessary. In our proposed system, learning occurred after presenting 30 images to the user.

The highest hit rate was measured while using the fully manual collaboration method with no robot assistance (collaboration level 1). The users achieved an average of 94.3% hit rate with 15.1 false alarms. However, this was achieved only for a long switching time of 15 sec (corresponding to a robot velocity of 1 m/s). This collaboration level also yielded high FA. When using the faster switching time, the best collaboration level is level 3 (robot marks, human supervises). The lowest FA was measured while using collaboration level 2 (robot suggests, human approves) with the free hand marking method for both image switching times.

The best marking method according to the ease of use questionnaire was the constant circle diameter. An integrative experiment was conducted to demonstrate and evaluate the human marking methods, levels of human-robot collaboration, and the specific spraying device, working in sync. During the experiment, the robot traveled a total distance of 1044 [m] ($16 \text{ users} \times 3 \text{ repetitions per user} \times 18 \text{ [m]}$ for each repetition + $10 \text{ repetitions} \times 18 \text{ [m]}$ for each repetition), captured 1108 frames and sprayed 3378 targets. The experiment shows that despite the high complexity of such a robotic system and framework, collaboration of a human in the spraying process is feasible. The collaboration between the remote robot and the human showed that the hit and the false alarm rate was improved (hit rate increased by 13.4% and false alarm rate decreased by 19.5%) compared to a fully autonomous operation (collaboration level 4).

The results obtained can be used to develop a human-robot operational system by using the best values obtained for the selected criterion (e.g., for highest hit rate use constant circle diameter, image

switching time of 15 [sec], and fully manual collaboration level; for lowest false alarm rate use free hand, image switching time of 15 [sec], and collaboration level 2).

Human-robot collaboration for real world spraying implies that humans will be asked to mark thousands of images (km of vine rows). This is a repetitive task that will most likely cause fatigue and boredom to the remote human collaborator resulting in decrease hit rate and decreased FA. The maximum number of images presented to a user in this study were 150. Human performance limitations over time should be investigated in future work as part of the human-robot collaborative framework as detailed below.

9.2. Future work

Future work can be applied to most of the presented topics.

9.2.1. Robotic platform

The current robotic platform was based on electric motors. The choice of electric motors derived from the ease of control and mechanical design simplicity that was mandatory for such an experimental robotic platform. However, we believe that for such a robot to be accepted by the agriculture industry, the robot should be based on hydraulics instead of an electrical power source. The hydraulic power will provide the robot with the robustness and high wheel torque so needed in agricultural vehicles especially in tough traction grounds.

Another aspect of the robotic platform that should take into consideration for future work is continuous advance of the robotic platform along the row instead of the step mode.

9.2.2. Navigation algorithm and path tracking

A very basic navigation algorithm was designed and implemented allowing the robot to travel along the vineyard row (included in the thesis DVD \vineyard navigation\). The navigation did not include the ability to turn at the end of the row and this was done manually. A robust navigation system should be developed specifically for the vineyard environment. It should probably be based on a multi-sensory system (color camera, laser scanner, GPS, etc.). Another feature missing in the navigation is the end of row turning that is mandatory for such an autonomous system.

Future work should also investigate the effect of path tracking errors on the spray cones and target coverage.

9.2.3. Grape detection

We assumed that a minor percentage of the grape clusters in the images were totally occluded by leaves, branches, and other grape clusters. Future work may treat this subject by adding a wind blower towards the foliage in order to expose the occluded clusters. However, it should be noticed that such a wind blower may diverse the accurate spraying.

Alternatively, a different sensor can be employed to overcome the occluding elements (e.g., thermal camera that is based on based on the temperature difference between the fruit and background. Since the fruit absorbs more heat and radiates more heat in comparison with leaves and other parts of the plant canopy, which allows for distinction between those plant materials with thermal imaging (Gongal, Amatya, Karkee, Zhang and Lewis 2015). The human-robot collaboration framework would not be affected since the sensory output would still be presented as images to the user. Therefore, it could improve detection results due to better performance for detecting occluded fruit (Gongal, Amatya, Karkee, Zhang and Lewis 2015). But, it must be noted that employing a thermal sensor limits the operation to limited time slots along the day and is highly dependent on fruit size (Gongal, Amatya, Karkee, Zhang and Lewis 2015).

9.2.4. Spraying device

While we were able to evaluate the possible pesticide reduction in an experiment that included artificial targets, extensive field experimentation is needed to evaluate the pesticide reduction along with the evaluation of the pesticide application effectiveness. The field experiments are crucial to introduce the spraying device to the agricultural industry.

9.2.5. Image registration

A possible following work can apply the registration method using two-dimensional distance sensors (e.g., Kinect sensor, Time of Flight camera, 3D laser scanner) instead of the one-dimensional distance sensor used in this work. The use of a two-dimensional distance sensor is expected to yield higher accuracy.

9.2.6. Human-robot collaboration

Future work in the field of human-robot collaboration can focus on several human interaction topics such as:

1. Investigate the influence of expertise during the robot operation,
2. Investigate the user's perception of the field environment during remote supervision,
3. Compare different marking aids such as: computer touch screen, tablet, smart-phone,

4. Evaluating the human detection skills without time limitations.

Additionally, studies on human performance and related issues such as fatigue, monitoring, workload and attention should be investigated. This is especially important if the human operator will perform over extended periods of time which might limit performance.

References

- [1] Cho, S. I. and N. H. Ki (1999). "Autonomous speed sprayer guidance using machine vision and fuzzy logic." *Transactions of the ASAE* **42**(4): 1137-1144.
- [2] Singh, S., T. F. Burks and W. S. Lee (2005). "Autonomous robotic vehicle development for greenhouse spraying." *Transactions of the ASAE* **48**(6): 2355-2361.
- [3] Rogan, W. J. and A. Chen (2005). "Health risks and benefits of bis (4-chlorophenyl)-1, 1, 1-trichloroethane (DDT)." *The Lancet* **366**(9487): 763-773.
- [4] Dasgupta, S., C. Meisner, D. Wheeler, K. Xuyen and N. Thi Lam (2007). "Pesticide poisoning of farm workers—implications of blood test results from Vietnam." *International Journal of Hygiene and Environmental Health* **210**(2): 121-132.
- [5] Pimentel, D. and H. Lehman (1993). *The pesticide question: environment, economics, and ethics*. London, Chapman & Hall.
- [6] Reus, J., P. Leendertse, C. Bockstaller, I. Fomsgaard, V. Gutsche, K. Lewis, C. Nilsson, L. Pussemier, M. Trevisan and H. Van der Werf (2002). "Comparison and evaluation of eight pesticide environmental risk indicators developed in Europe and recommendations for future use." *Agriculture, Ecosystems and Environment* **90**(2): 177-187.
- [7] Swan, S. H., R. L. Kruse, F. Liu, D. B. Barr, E. Z. Drobnis, J. B. Redmon, C. Wang, C. Brazil, J. W. Overstreet and S. f. F. F. R. Group (2003). "Semen quality in relation to biomarkers of pesticide exposure." *Environmental Health Perspectives* **111**(12): 1478.
- [8] Slaughter, D., D. Giles and D. Downey (2008). "Autonomous robotic weed control systems: A review." *Computers and Electronics in Agriculture* **61**(1): 63-78.
- [9] Lee, W. S., D. Slaughter and D. Giles (1999). "Robotic weed control system for tomatoes." *Precision Agriculture* **1**(1): 95-113.
- [10] Elkabetz, P., Y. Edan, A. Grinstein and H. Pasternak (1998). Simulation model for evaluation of site-specific sprayer design. *ASAE Annual International Meeting*.
- [11] Goudy, H. J., K. A. Bennett, R. B. Brown and F. J. Tardif (2001). "Evaluation of site-specific weed management using a direct-injection sprayer." *Weed Science* **49**(3): 359-366.
- [12] Gil, E., A. Escol, J. R. Rosell, S. Planas and L. Val (2007). "Variable rate application of plant protection products in vineyard using ultrasonic sensors." *Crop Protection* **26**(8): 1287-1297.
- [13] Lu, J., O. Lamikanra and S. Leong (1995). Effects of Gibberellic Acid on Muscadine Grape Production. *Proceedings-Florida State Horticultural Society, Florida State Horticultural Society*.
- [14] Fidelibus, M. and S. Vasquez (2012). "Using Gibberellic Acid to Reduce Cluster Compactness in Grapes." *USDA, NIFA*.

- [15] Kapach, K., E. Barnea, R. Mairon, Y. Edan and O. Ben-Shahar (2012). "Computer vision for fruit harvesting robots—state of the art and challenges ahead." *International Journal of Computational Vision and Robotics* **3**(1): 4-34.
- [16] Jimenez, A., R. Ceres and J. Pons (2000). "A survey of computer vision methods for locating fruit on trees." *Transactions of the ASAE* **43**(6): 1911-1920.
- [17] Correa, C., C. Valero, P. Barreiro, M. P. Diago and J. Tardáguila (2012). Feature extraction on vineyard by gustafson kessel fcm and k-means. 16th IEEE Mediterranean Electrotechnical Conference (MELECON), IEEE.
- [18] Blackmore, S., H. Have and S. Fountas (2001). A specification of behavioural requirements for an autonomous tractor. 6th International Symposium on Fruit, Potsdam, Germany.
- [19] Berenstein, R. and Y. Edan (2012). Evaluation of marking techniques for a Human-Robot Selective Vineyard Sprayer. International Conference of Agricultural Engineering (CIGR-AgEng), Valencia, Spain, Unpublished.
- [20] Fong, T. and C. Thorpe (2001). "Vehicle teleoperation interfaces." *Autonomous Robots* **11**(1): 9-18.
- [21] Goodrich, M. A. and A. C. Schultz (2007). "Human-robot interaction: a survey." *Foundations and Trends in Human-Computer Interaction* **1**(3): 203-275.
- [22] Jaimes, A. and N. Sebe (2007). "Multimodal human–computer interaction: A survey." *Computer Vision and Image Understanding* **108**(1): 116-134.
- [23] Sim, D. Y. Y. and C. K. Loo (2015). "Extensive assessment and evaluation methodologies on assistive social robots for modelling human–robot interaction—A review." *Information Sciences* **301**: 305-344.
- [24] Bechar, A. and Y. Edan (2003). "Human-robot collaboration for improved target recognition of agricultural robots." *Industrial Robot* **30**(5): 432-436.
- [25] Chen, J. Y., M. J. Barnes and M. Harper-Sciarini (2011). "Supervisory control of multiple robots: Human-performance issues and user-interface design." *IEEE Transactions on Systems, Man, and Cybernetics* **41**(4): 435-454.
- [26] Cherubini, A., R. Passama, P. Fraisse and A. Crosnier (2015). "A unified multimodal control framework for human–robot interaction." *Robotics and Autonomous Systems* **70**: 106-115.
- [27] Adamides, G., C. Katsanos, G. Christou, M. Xenos, N. Kostaras and T. Hadzilacos (2013). Human-Robot Interaction in Agriculture: Usability Evaluation of three Input Devices for Spraying Grape Clusters. EFITA-WCCA-CIGR Conference. Turin, Italy.

- [28] Adamides, G., G. Christou, C. Katsanos, M. Xenos and T. Hadzilacos (2015). "Usability Guidelines for the Design of Robot Teleoperation: A Taxonomy." *IEEE Transactions on Human-Machine Systems* **45**(2): 256-262.
- [29] Berenstein, R., O. B. Shahar, A. Shapiro and Y. Edan (2010). "Grape clusters and foliage detection algorithms for autonomous selective vineyard sprayer." *Intelligent Service Robotics* **3**(4): 233–243.
- [30] Gongal, A., S. Amatya, M. Karkee, Q. Zhang and K. Lewis (2015). "Sensors and systems for fruit detection and localization: A review." *Computers and Electronics in Agriculture* **116**: 8-19.
- [31] Sheridan, T. B. (1992). *Telerobotics, automation, and human supervisory control*. Massachusetts, The MIT Press.
- [32] Berenstein, R., M. Hočevár, T. Godeša, Y. Edan and O. Ben-Shahar (2015). "Distance-Dependent Multimodal Image Registration for Agriculture Tasks." *Sensors* **15**(8): 20845-20862.
- [33] Kent, J. (1992). Pesticides in agriculture. Conference paper to Riverina Outlook Conference.
- [34] Cooper, J. and H. Dobson (2007). "The benefits of pesticides to mankind and the environment." *Crop Protection* **26**(9): 1337-1348.
- [35] Betarbet, R., T. B. Sherer, G. MacKenzie, M. Garcia-Osuna, A. V. Panov and J. T. Greenamyre (2000). "Chronic systemic pesticide exposure reproduces features of Parkinson's disease." *Nature Neuroscience* **3**(12): 1301-1306.
- [36] Eddleston, M., L. Karalliedde, N. Buckley, R. Fernando, G. Hutchinson, G. Isbister, F. Konradsen, D. Murray, J. C. Piola and N. Senanayake (2002). "Pesticide poisoning in the developing world—a minimum pesticides list." *The Lancet* **360**(9340): 1163-1167.
- [37] Dawson, A. H., M. Eddleston, L. Senarathna, F. Mohamed, I. Gawarammana, S. J. Bowe, G. Manuweera and N. A. Buckley (2010). "Acute human lethal toxicity of agricultural pesticides: a prospective cohort study." *PLoS Med* **7**(10): e1000357.
- [38] Remoundou, K., M. Brennan, A. Hart and L. J. Frewer (2014). "Pesticide risk perceptions, knowledge, and attitudes of operators, workers, and residents: a review of the literature." *Human and Ecological Risk Assessment: An International Journal* **20**(4): 1113-1138.
- [39] Tardiff, R. G. (1992). *Methods to assess adverse effects of pesticides on non-target organisms*. London, John Wiley & Sons Ltd.
- [40] Bozdogan, A., N. Yarpuz-Bozdogan and I. Tobi (2015). "Relationship Between Environmental Risk and Pesticide Application in Cereal Farming." *International Journal of Environmental Research* **9**(3): 1047-1054.

- [41] Lambropoulou, D., D. Hela, A. Koltsakidou and I. Konstantinou (2015). Overview of the Pesticide Residues in Greek Rivers: Occurrence and Environmental Risk Assessment. *The Handbook of Environmental Chemistry*: 1-36.
- [42] MOH. (2006). "Pesticide residues in food ", from <http://www.health.gov.il/pages/default.asp?maincat=51&catid=330&pageid=2502>.
- [43] Song, Y., H. Sun, M. Li and Q. Zhang (2015). "Technology Application of Smart Spray in Agriculture: A Review." *Intelligent Automation & Soft Computing* **21**(3): 319-333.
- [44] Edan, Y., N. Kondo and H. Shufeng (2009). *Automation in Agriculture. Handbook of Automation*. S. Y. Nof. Berlin, Springer Verlag: 1092-1128.
- [45] Kondo, N. (1991). Study on grape harvesting robot. IFAC/ISHS workshop, Matsuyama, Japan.
- [46] Edan, Y. and G. E. Miles (1993). "Design of an agricultural robot for harvesting melons." *Transactions of the ASAE* **36**(3): 593-603.
- [47] Monta, M., N. Kondo and K. C. Ting (1998). End-effectors for tomato harvesting robot. *Artificial Intelligence Review*. **12**: 11-25.
- [48] Bulanon, D. M., T. Kataoka, Y. Ota and T. Hiroma (2001). "A machine vision system for the apple harvesting robot." *Journal of Scientific Research and Development (CIGR)* **3**(1): 1-11.
- [49] Van Henten, E. J., J. Hemming, B. A. J. Van Tuijl, J. G. Kornet, J. Meuleman, J. Bontsema and E. A. Van Os (2002). "An autonomous robot for harvesting cucumbers in greenhouses." *Autonomous Robots* **13**(3): 241-258.
- [50] Hannan, M. W. and T. F. Burks (2004). Current developments in automated citrus harvesting. ASAE Annual International Meeting. Ontario, Canada.
- [51] Bac, C. W., E. J. Henten, J. Hemming and Y. Edan (2014). "Harvesting Robots for High-value Crops: State-of-the-art Review and Challenges Ahead." *Journal of Field Robotics* **31**(6): 888-911.
- [52] Zhang, C. and J. M. Kovacs (2012). "The application of small unmanned aerial systems for precision agriculture: a review." *Precision Agriculture* **13**(6): 693-712.
- [53] Xue, X., Y. Lan, Z. Sun, C. Chang and W. C. Hoffmann (2016). "Develop an unmanned aerial vehicle based automatic aerial spraying system." *Computers and Electronics in Agriculture* **128**: 58-66.
- [54] Faiçal, B. S., G. Pessin, G. P. R. Filho, A. C. P. L. F. Carvalho, G. Furquim and J. Ueyama (2014). Fine-Tuning of UAV Control Rules for Spraying Pesticides on Crop Fields. 2014 IEEE 26th International Conference on Tools with Artificial Intelligence.
- [55] Gerrish, J. B., B. W. Fehr, G. R. Van Ee and D. P. Welch (1997). "Self-steering tractor guided by computer-vision." *Applied Engineering in Agriculture* **13**(5): 559-564.

- [56] Toda, M., O. Kitani, T. Okamoto and T. Torii (1999). "Navigation method for a mobile robot via sonar-based crop row mapping and fuzzy logic control." *Journal of Agricultural Engineering Research* **72**(4): 299-309.
- [57] Belforte, G., R. Deboli, P. Gay, P. Piccarolo and D. R. Aimonino (2006). "Robot design and testing for greenhouse applications." *Biosystems Engineering* **95**(3): 309-321.
- [58] Hayashi, S., K. Ganno, Y. Ishii and I. Tanaka (2002). "Robotic harvesting system for eggplants." *Japan Agricultural Research Quarterly* **36**(3): 163-168.
- [59] Stentz, A., C. Dima, C. Wellington, H. Herman and D. Stager (2002). "A system for semi-autonomous tractor operations." *Autonomous Robots* **13**(1): 87-104.
- [60] Blasco, J., N. Aleixos, J. M. Roger, G. Rabatel and E. Molto (2002). "AE—Automation and emerging technologies robotic weed control using machine vision." *Biosystems Engineering* **83**(2): 149-157.
- [61] Strand, B. and A. J. Baerveldt (2002). "An agricultural mobile robot with vision-based perception for mechanical weed control." *Autonomous Robots* **13**(1): 21-35.
- [62] Van Henten, E. J., B. A. J. Van Tuijl, G. J. Hoogakker, M. J. Van Der Weerd, J. Hemming, J. G. Kornet and J. Bontsema (2006). "An autonomous robot for de-leafing cucumber plants grown in a high-wire cultivation system." *Biosystems Engineering* **94**(3): 317-323.
- [63] Khot, L. R., L. Tang and K. Hayashi (2006). Modeling and simulation of a four-wheel-steered agricultural robotic vehicle. ASAE Annual International Meeting. Portland, Oregon.
- [64] Cui, Y., M. Nagata, F. Guo, K. Hiyoshi, O. Kinoshita and M. Mitarai (2007). "study on strawberry harvesting robot using machine vision for strawberry grown on annual hill top (part 2)-ripeness judgment and recognition of peduncle using picking camera, and fabrication of the picking hand." *Journal of The Japanese Society of Agricultural Machinery* **69**(2): 60-68.
- [65] Mittal, R., V. R. Varada, S. Dave, A. Khanna, R. Korpu and S. Tilak (2014). Semi-autonomous arecanut tree-climbing robot. 2014 9th International Conference on Industrial and Information Systems (ICIIS).
- [66] Pérez-Ruiz, M., P. Gonzalez-de-Santos, A. Ribeiro, C. Fernandez-Quintanilla, A. Peruzzi, M. Vieri, S. Tomic and J. Agüera (2015). "Highlights and preliminary results for autonomous crop protection." *Computers and Electronics in Agriculture* **110**: 150-161.
- [67] Durmuş, H., E. O. Güneş, M. Kircı and B. B. Üstündağ (2015). The design of general purpose autonomous agricultural mobile-robot: "AGROBOT". 2015 Fourth International Conference on Agro-Geoinformatics (Agro-geoinformatics).
- [68] Haibo, L., D. Shuliang, L. Zunmin and Y. Chuijie (2015). "Study and experiment on a wheat precision seeding robot." *J. Robot.* **2015**: 12-12.

- [69] Chen, H., T. Fuhlbrigge and X. Li (2008). Automated industrial robot path planning for spray painting process: a review. IEEE International Conference on Automation Science and Engineering (CASE).
- [70] Arikan, S. and T. Balkan (2000). "Process modeling, simulation, and paint thickness measurement for robotic spray painting." Journal of Robotic Systems **17**(9): 479-494.
- [71] Zaki, A. and M. Eskander (2000). Spray painting of a general three-dimensional surface. Proceedings. 2000 IEEE/RSJ International Conference on Intelligent Robots and Systems (IROS 2000) (Cat. No.00CH37113).
- [72] Conner, D. C., A. Greenfield, P. N. Atkar, A. A. Rizzi and H. Choset (2005). "Paint deposition modeling for trajectory planning on automotive surfaces." IEEE Transactions on Automation Science and Engineering **2**(4): 381-392.
- [73] Diao, X. D., S. X. Zeng and V. W. Y. Tam (2009). "Development of an optimal trajectory model for spray painting on a free surface." Computers & Industrial Engineering **57**(1): 209-216.
- [74] Wei, C. and Z. Dean (2009). Tool Trajectory Optimization of Robotic Spray Painting. 2009 Second International Conference on Intelligent Computation Technology and Automation.
- [75] From, P. J., J. Gunnar and J. T. Gravdahl (2011). "Optimal Paint Gun Orientation in Spray Paint Applications-Experimental Results." IEEE Transactions on Automation Science and Engineering **8**(2): 438-442.
- [76] Rodriguez, G. and C. R. Weisbin (2003). "A new method to evaluate human-robot system performance." Autonomous Robots **14**(2): 165-178.
- [77] Chang, Y. C., G. S. Song and S. K. Hsu (1998). "Automatic extraction of ridge and valley axes using the profile recognition and polygon-breaking algorithm." Computers and Geosciences **24**(1): 83-93.
- [78] Ferrell, W. R. and T. B. Sheridan (1967). "Supervisory control of remote manipulation." IEEE Spectrum **4**(10): 81-88.
- [79] Mandow, A., J. M. Gomez-de-Gabriel, J. L. Martinez, V. F. Munoz, A. Ollero and A. Garcia-Cerezo (1996). "The autonomous mobile robot AURORA for greenhouse operation." IEEE Robotics & Automation Magazine **3**(4): 18-28.
- [80] Lee, W. S., D. C. Slaughter and D. K. Giles (1999). "Robotic weed control system for tomatoes." Precision Agriculture **1**(1): 95-113.
- [81] Shin, B. S., S. H. Kim and J. U. Park (2002). Autonomous agricultural vehicle using overhead guide. Automation Technology for Off-Road Equipment, Chicago.

- [82] Lamm, R. D., D. C. Slaughter and D. K. Giles (2002). "Precision weed control system for cotton." *Transactions of the ASAE* **45**(1): 231-238.
- [83] Steward, B. L., L. F. Tian and L. Tang (2002). "Distance-based control system for machine vision-based selective spraying." *Transactions of the ASAE* **45**(5): 1255-1262.
- [84] Nishiwaki, K., K. Amaha and R. Otani (2004). development of nozzle positioning system for precision sprayer. *Automation Technology for Off-Road Equipment*, Kyoto.
- [85] Jeon, H. Y., L. F. Tian and T. Grift (2005). Development of an individual weed treatment system using a robotic arm. *ASABE Annual International Meeting*.
- [86] Younse, P. and T. Burks (2005). Intersection Detection and Navigation for an Autonomous Greenhouse Sprayer using Machine Vision. M.Sc, University of Florida.
- [87] Ogawa, Y., N. Kondo, M. Monta and S. Shibusawa (2006). Spraying robot for grape production. *Springer Tracts in Advanced Robotics*. Berlin, Springer. **24**: 539-548.
- [88] Slaughter, D. C., D. K. Giles and D. Downey (2008). "Autonomous robotic weed control systems: A review." *Computers and Electronics in Agriculture* **61**(1): 63-78.
- [89] Shapiro, A., E. Korkidi, A. Demri, O. Ben-Shahar, R. Riemer and Y. Edan (2009). "Toward elevated agrobotics: Development of a scaled-down prototype for visually guided date palm tree sprayer." *Journal of Field Robotics* **26**(6): 572-590.
- [90] Esau, T. J., Q. U. Zaman, Y. K. Chang, A. W. Schumann, D. C. Percival and A. A. Farooque (2014). "Spot-application of fungicide for wild blueberry using an automated prototype variable rate sprayer." *Precision Agriculture* **15**(2): 147-161.
- [91] Oberti, R., M. Marchi, P. Tirelli, A. Calcante, M. Iriti, E. Tona, M. Hočevár, J. Baur, J. Pfaff, C. Schütz and H. Ulbrich (2016). "Selective spraying of grapevines for disease control using a modular agricultural robot." *Biosystems Engineering* **146**: 203-215.
- [92] Esau, T., Q. Zaman, D. Groulx, K. Corscadden, Y. Chang, A. Schumann and P. Havard (2016). "Economic analysis for smart sprayer application in wild blueberry fields." *Precision Agriculture*: 1-13.
- [93] Cheein, F. A., D. Herrera, J. Gimenez, R. Carelli, M. Torres-Torriti, J. R. Rosell-Polo, A. Escolà and J. Arnó (2015). Human-robot interaction in precision agriculture: Sharing the workspace with service units. *2015 IEEE International Conference on Industrial Technology (ICIT)*.
- [94] Bechar, A., J. Meyer and Y. Edan (2007). An objective function to evaluate performance of human-robot systems for target recognition tasks. *2007 IEEE International Conference on Systems, Man and Cybernetics*.

- [95] Tkach, I., Y. Edan and A. Bechar (2009). Algorithms for dynamic switching of collaborative human-robot system in target recognition tasks. Proceedings IFAC Symposium on Information Control Problems in Manufacturing (INCOM), Moscow, Russia
- [96] Tkach, I. (2009). Switching between collaboration levels in target recognition tasks. M.Sc, Ben-Gurion University of the Negev.
- [97] Yashpe, D. (2009). Influence of human reaction time in human robot collaborative target recognition systems. M.Sc., Ben-Gurion University of the Negev.
- [98] Yashpe, D., A. Bechar and Y. Edan (2009). Influence of human reaction time on performance of human-robot target recognition systems. International Conference on Production Research, Shanghai, China.
- [99] Murakami, N., A. Ito, J. D. Will, M. Steffen, K. Inoue, K. Kita and S. Miyaura (2008). "Development of a teleoperation system for agricultural vehicles." *Computers and Electronics in Agriculture* **63**(1): 81-88.
- [100] Everett, S. E. and R. V. Dubey (1998). Human-machine cooperative telerobotics using uncertain sensor or model data. Proceedings. 1998 IEEE International Conference on Robotics and Automation (Cat. No.98CH36146).
- [101] Ivanisevic, I. and V. Lumelsky (1998). A human-machine interface for teleoperation of arm manipulators in it complex environment. Proceedings. 1998 IEEE/RSJ International Conference on Intelligent Robots and Systems. Innovations in Theory, Practice and Applications (Cat. No.98CH36190).
- [102] Parasuraman, R., T. B. Sheridan and C. D. Wickens (2000). "A model for types and levels of human interaction with automation." *IEEE Transactions on Systems, Man, and Cybernetics* **30**(3): 286-297.
- [103] Aracil, R., M. Ferre, M. Hernando, E. Pinto and J. M. Sebastian (2002). "Telerobotic system for live-power line maintenance: ROBTET." *Control Engineering Practice* **10**(11): 1271-1281.
- [104] Scholtz, J. (2003). Theory and evaluation of human robot interactions. 36th Annual Hawaii International Conference on System Sciences, 2003. Proceedings of the.
- [105] Sierhuis, M., J. M. Bradshaw, A. Acquisti, R. Van Hoof, R. Jeffers and A. Uszok (2003). Human-agent teamwork and adjustable autonomy in practice.
- [106] Fletcher, L., G. Loy, N. Barnes and A. Zelinsky (2005). "Correlating driver gaze with the road scene for driver assistance systems." *Robotics and Autonomous Systems* **52**(1): 71-84.
- [107] Howard, A. M. (2006). Role allocation in human-robot interaction schemes for mission scenario execution. Proceedings 2006 IEEE International Conference on Robotics and Automation, 2006. ICRA 2006.

- [108] Salter, T., K. Dautenhahn and R. Boekhorst (2006). "Learning about natural human–robot interaction styles." *Robotics and Autonomous Systems* **54**(2): 127-134.
- [109] Steinfeld, A., T. Fong, D. Kaber, M. Lewis, J. Scholtz, A. Schultz and M. Goodrich (2006). Common metrics for human-robot interaction. Proceedings of the 1st ACM SIGCHI/SIGART conference on Human-robot interaction. Salt Lake City, Utah, USA, ACM: 33-40.
- [110] Thomaz, A. L. and C. Breazeal (2006). Reinforcement learning with human teachers: evidence of feedback and guidance with implications for learning performance. Proceedings of the 21st national conference on Artificial intelligence - Volume 1. Boston, Massachusetts, AAAI Press: 1000-1005.
- [111] Hancock, P. A., D. R. Billings, K. E. Schaefer, J. Y. C. Chen, E. J. de Visser and R. Parasuraman (2011). "A Meta-Analysis of Factors Affecting Trust in Human-Robot Interaction." *Human Factors* **53**(5): 517-527.
- [112] Pérez-Ruíz, M., D. C. Slaughter, F. A. Fathallah, C. J. Gliever and B. J. Miller (2014). "Co-robotic intra-row weed control system." *Biosystems Engineering* **126**: 45-55.
- [113] Dragan, A. D., S. Bauman, J. Forlizzi and S. S. Srinivasa (2015). Effects of Robot Motion on Human-Robot Collaboration. Proceedings of the Tenth Annual ACM/IEEE International Conference on Human-Robot Interaction. Portland, Oregon, USA, ACM: 51-58.
- [114] Gazquez, J. A., N. N. Castellano and F. Manzano-Agugliaro (2016). "Intelligent low cost telecontrol system for agricultural vehicles in harmful environments." *Journal of Cleaner Production* **113**: 204-215.
- [115] Jacob, M. G. and J. P. Wachs (2016). "Optimal Modality Selection for Cooperative Human–Robot Task Completion." *IEEE Transactions on Cybernetics* **46**(12): 3388-3400.
- [116] Hart, S. G. and L. E. Staveland (1988). Development of NASA-TLX (Task Load Index): Results of Empirical and Theoretical Research. *Advances in Psychology*. A. H. Peter and M. Najmedin, North-Holland. **Volume 52**: 139-183.
- [117] Goodrich, M. A., E. R. Boer, J. W. Crandall, R. W. Ricks and M. L. Quigley (2004). Behavioral entropy in human-robot interaction, DTIC Document.
- [118] Endsley, M. R. (2016). Designing for situation awareness: An approach to user-centered design, CRC press.
- [119] Johnson-Laird, P. N. (1988). The computer and the mind: An introduction to cognitive science, Harvard University Press.
- [120] Vicente, K. (1997). "Should an interface always match the operator's mental model?" *Cseriac Gateway* **8**(1): 1-5.

- [121] Hoffman, R. R., M. Johnson, J. M. Bradshaw and A. Underbrink (2013). "Trust in Automation." *IEEE Intelligent Systems* **28**(1): 84-88.
- [122] Endsley, M. R. (1988). Situation awareness global assessment technique (SAGAT). Proceedings of the IEEE 1988 National Aerospace and Electronics Conference.
- [123] Kaber, D. B., E. Onal and M. R. Endsley (2000). "Design of automation for telerobots and the effect on performance, operator situation awareness, and subjective workload." *Human Factors and Ergonomics in Manufacturing* **10**(4): 409-430.
- [124] Scholtz, J., B. Antonishek and J. Young (2003). Evaluation of operator interventions in autonomous off-road driving, DTIC Document.
- [125] Drury, J. L., J. Scholtz and H. A. Yanco (2003). Awareness in human-robot interactions. Systems, Man and Cybernetics, 2003. IEEE International Conference on.
- [126] Riley, J. M. and M. R. Endsley (2005). Situation awareness in HRI with collaborating remotely piloted vehicles. proceedings of the Human Factors and Ergonomics Society Annual Meeting, SAGE Publications.
- [127] Parasuraman, R., M. Barnes, K. Cosenzo and S. Mulgund (2007). Adaptive automation for human-robot teaming in future command and control systems, DTIC Document.
- [128] Draper, J. V. and L. M. Blair (1996). Workload, flow, and telepresence during teleoperation. Proceedings of IEEE International Conference on Robotics and Automation.
- [129] Adams, J. A. and H. Kaymaz-Keskinpala (2004). Analysis of perceived workload when using a PDA for mobile robot teleoperation. Robotics and Automation, 2004. Proceedings. ICRA '04. 2004 IEEE International Conference on.
- [130] Hill, S. G. and B. Bodt (2007). A field experiment of autonomous mobility: Operator workload for one and two robots. 2007 2nd ACM/IEEE International Conference on Human-Robot Interaction (HRI).
- [131] Prewett, M. S., R. C. Johnson, K. N. Saboe, L. R. Elliott and M. D. Covert (2010). "Managing workload in human-robot interaction: A review of empirical studies." *Computers in Human Behavior* **26**(5): 840-856.
- [132] Liu, S. and M. Whitty (2015). "Automatic grape bunch detection in vineyards with an SVM classifier." *Journal of Applied Logic* **13**(4): 643-653.
- [133] Font, D., T. Pallejà, M. Tresanchez, M. Teixidó, D. Martinez, J. Moreno and J. Palacín (2014). "Counting red grapes in vineyards by detecting specular spherical reflection peaks in RGB images obtained at night with artificial illumination." *Computers and Electronics in Agriculture* **108**: 105-111.

- [134] Nuske, S., K. Wilshusen, S. Achar, L. Yoder, S. Narasimhan and S. Singh (2014). "Automated visual yield estimation in vineyards." *Journal of Field Robotics* **31**(5): 837-860.
- [135] Diago, M.-P., C. Correa, B. Millán, P. Barreiro, C. Valero and J. Tardaguila (2012). "Grapevine yield and leaf area estimation using supervised classification methodology on RGB images taken under field conditions." *Sensors* **12**(12): 16988-17006.
- [136] Reis, M. J., R. Morais, E. Peres, C. Pereira, O. Contente, S. Soares, A. Valente, J. Baptista, P. J. S. Ferreira and J. B. Cruz (2012). "Automatic detection of bunches of grapes in natural environment from color images." *Journal of Applied Logic* **10**(4): 285-290.
- [137] Canny, J. (1986). "A computational approach to edge detection." *IEEE Transactions on Pattern Analysis and Machine Intelligence*(6): 679-698.
- [138] Shin, M. C., D. Goldgof and K. W. Bowyer (1998). An objective comparison methodology of edge detection algorithms using a structure from motion task. *Proceedings. 1998 IEEE Computer Society Conference on Computer Vision and Pattern Recognition (Cat. No.98CB36231)*.
- [139] Sharifi, M., M. Fathy and M. T. Mahmoudi (2002). A classified and comparative study of edge detection algorithms. *Proceedings. International Conference on Information Technology: Coding and Computing*.
- [140] Breiman, L., J. Friedman, C. J. Stone and R. A. Olshen (1984). *Classification and regression trees*, CRC press.
- [141] Sokolova, M. and G. Lapalme (2009). "A systematic analysis of performance measures for classification tasks." *Information Processing & Management* **45**(4): 427-437.
- [142] Norman, D. A. (1988). *The psychology of everyday things*. New York., Basic Books (AZ).
- [143] Steward, B. L., L. F. Tian and L. Tang (2002). "Distance-based control system for machine vision-based selective spraying." *Transactions of the ASAE* **45**(5): 1255.
- [144] Pergher, G. and R. Petris (2008). "Pesticide Dose Adjustment in Vineyard Spraying and Potential for Dose Reduction." *Agricultural Engineering International: The CIGR EJournal*.
- [145] Berenstein, R. and Y. Edan (2012). *Robotic precision spraying methods*. ASABE Annual International Meeting. Dallas, Texas.

Appendices

Appendix A. Kinematic model of the robotic platform.

$$q = \begin{bmatrix} x \\ y \\ \theta \\ \varphi \end{bmatrix}; \text{ State variable}$$

$$A_{01} = \begin{bmatrix} \cos(\theta) & -\sin(\theta) & x \\ \sin(\theta) & \cos(\theta) & y \\ 0 & 0 & 1 \end{bmatrix}; \text{ Rotation matrix from 0 to 1}$$

$$A_{12} = \begin{bmatrix} \cos(\varphi) & -\sin(\varphi) & 0 \\ \sin(\varphi) & \cos(\varphi) & L_1 \\ 0 & 0 & 1 \end{bmatrix}; \text{ Rotation matrix from 1 to 2}$$

$$A_{23} = \begin{bmatrix} 1 & 0 & 0 \\ 0 & 1 & L_2 \\ 0 & 0 & 1 \end{bmatrix}; \text{ Rotation matrix from 2 to 3}$$

$$A_{03} = \begin{bmatrix} \cos(\theta + \varphi) & -\sin(\theta + \varphi) & -L_1 \sin(\theta) - L_2 \sin(\theta + \varphi) + x \\ \sin(\theta + \varphi) & \cos(\theta + \varphi) & L_1 \cos(\theta) + L_2 \cos(\theta + \varphi) + y \\ 0 & 0 & 1 \end{bmatrix}; \text{ Rotation matrix from 0 to 3}$$

$$\text{Back Left Wheel} = \begin{bmatrix} x_{BL} \\ y_{BL} \end{bmatrix} = A_{01} \cdot \begin{pmatrix} -w/2 \\ 0 \\ 1 \end{pmatrix} = \begin{bmatrix} -(1/2) w \cos[\theta] + x \\ -(1/2) w \sin[\theta] + y \end{bmatrix}$$

$$\text{Back Right Wheel} = \begin{bmatrix} x_{BR} \\ y_{BR} \end{bmatrix} = A_{01} \cdot \begin{pmatrix} w/2 \\ 0 \\ 1 \end{pmatrix} = \begin{bmatrix} 1/2 w \cos[\theta] + x \\ 1/2 w \sin[\theta] + y \end{bmatrix}$$

$$\text{Front Left Wheel} = \begin{bmatrix} x_{FL} \\ y_{FL} \end{bmatrix} = A_{03} \cdot \begin{pmatrix} -w/2 \\ 0 \\ 1 \end{pmatrix} = \begin{bmatrix} -(1/2) w \cos[\theta + \varphi] - L_1 \sin[\theta] - L_2 \sin[\theta + \varphi] + x \\ -(1/2) w \sin[\theta + \varphi] + L_1 \cos[\theta] + L_2 \cos[\theta + \varphi] + y \end{bmatrix}$$

$$\text{Front Right Wheel} = \begin{bmatrix} x_{FR} \\ y_{FR} \end{bmatrix} = A_{03} \cdot \begin{pmatrix} w/2 \\ 0 \\ 1 \end{pmatrix} = \begin{bmatrix} 1/2 w \cos[\theta + \varphi] - L_1 \sin[\theta] - L_2 \sin[\theta + \varphi] + x \\ 1/2 w \sin[\theta + \varphi] + L_1 \cos[\theta] + L_2 \cos[\theta + \varphi] + y \end{bmatrix}$$

$$\text{Back Left Speed} = \begin{bmatrix} \dot{x}_{BL} \\ \dot{y}_{BL} \end{bmatrix} = \begin{bmatrix} \dot{x} + 1/2 w \sin[\theta] \dot{\theta} \\ \dot{y} - 1/2 w \cos[\theta] \dot{\theta} \end{bmatrix}$$

$$\text{Back Right Speed} = \begin{bmatrix} \dot{x}_{BR} \\ \dot{y}_{BR} \end{bmatrix} = \begin{bmatrix} \dot{x} - 1/2 w \sin[\theta] \dot{\theta} \\ \dot{y} + 1/2 w \cos[\theta] \dot{\theta} \end{bmatrix}$$

$$\text{Front Left Speed} = \begin{bmatrix} \dot{x}_{FL} \\ \dot{y}_{FL} \end{bmatrix} = \begin{bmatrix} 1/2 (2 \dot{x} + (-2L_1 \cos[\theta] - 2L_2 \cos[\theta + \varphi] + w \sin[\theta + \varphi]) \dot{\theta} + (-2L_2 \cos[\theta + \varphi] + w \sin[\theta + \varphi]) \dot{\varphi}) \\ \dot{y} + 1/2 (-w \cos[\theta + \varphi] + 2L_1 \sin[\theta] + 2L_2 \sin[\theta + \varphi]) \dot{\theta} - (w \cos[\theta + \varphi] + 2L_2 \sin[\theta + \varphi]) \dot{\varphi} \end{bmatrix}$$

$$\text{Front Right Speed} = \begin{bmatrix} \dot{x}_{FR} \\ \dot{y}_{FR} \end{bmatrix} = \begin{bmatrix} \dot{x} + 1/2 (-2L_1 \cos[\theta] + 2L_2 \cos[\theta + \varphi] + w \sin[\theta + \varphi]) \dot{\theta} - (2L_2 \cos[\theta + \varphi] + w \sin[\theta + \varphi]) \dot{\varphi} \\ 1/2 (2 \dot{y} + (w \cos[\theta + \varphi] - 2L_1 \sin[\theta] - 2L_2 \sin[\theta + \varphi]) \dot{\theta} + (w \cos[\theta + \varphi] - 2L_2 \sin[\theta + \varphi]) \dot{\varphi}) \end{bmatrix}$$

$$\begin{aligned}
\text{Back Left Speed} &= Rot_1 \begin{bmatrix} \dot{x}_{BL} \\ \dot{y}_{BL} \end{bmatrix} = -\cos[\theta] \dot{x} + \sin[\theta] (\dot{y} - w \cos[\theta] \dot{\theta}) \\
\text{Back Right Speed} &= Rot_1 \begin{bmatrix} \dot{x}_{BR} \\ \dot{y}_{BR} \end{bmatrix} = -\cos[\theta] \dot{x} + \sin[\theta] (\dot{y} + w \cos[\theta] \dot{\theta}) \\
\text{Front Left Speed} &= Rot_2 \begin{bmatrix} \dot{x}_{FL} \\ \dot{y}_{FL} \end{bmatrix} = -\cos[\theta + \varphi] \dot{x} + \sin[\theta + \varphi] \dot{y} + L_2 \cos[2(\theta + \varphi)] \dot{\theta} + L_1 \cos[2\theta + \varphi] \dot{\theta} - \\
&\quad 1/2 w \sin[2(\theta + \varphi)] \dot{\theta} + L_2 \cos[2(\theta + \varphi)] \dot{\varphi} - 1/2 w \sin[2(\theta + \varphi)] \dot{\varphi} \\
\text{Front Right Speed} &= Rot_2 \begin{bmatrix} \dot{x}_{FR} \\ \dot{y}_{FR} \end{bmatrix} = -\cos[\theta + \varphi] \dot{x} + \sin[\theta + \varphi] \dot{y} + L_2 \cos[2(\theta + \varphi)] \dot{\theta} + L_1 \cos[2\theta + \varphi] \dot{\theta} + \\
&\quad 1/2 w \sin[2(\theta + \varphi)] \dot{\theta} + L_2 \cos[2(\theta + \varphi)] \dot{\varphi} + 1/2 w \sin[2(\theta + \varphi)] \dot{\varphi}
\end{aligned}$$

Appendix B. Workload questionnaire

In order to avoid confusion among the experiments' participants, the workload questionnaire was presented in the Hebrew language.

שאלון - שיטות סימון

לפניך מספר שאלות. עבור כל שאלה הקף את התשובה הכי מתאימה כאשר 1- במידה מועטה, 5- במידה רבה מאוד. ענה על השאלות במקום המתאים.

עבור השיטה שבה מסמנים את המטרות עם עיגול בקוטר קבוע-

1. באיזו מידה השיטה היתה נוחה וקלה לשימוש?

מידה מועטה 1	2	3	4	5 מידה רבה מאוד
מה היה נוח/ לא נוח?				
<hr/>				
מה היית משנה וכיצד?				
<hr/>				

2. באיזו מידה את/ה חושב/ת שהצלחת לזהות ולסמן את המטרות?

מידה מועטה 1	2	3	4	5 מידה רבה מאוד
--------------	---	---	---	-----------------

עבור השיטה שבה מסמנים את היקף המטרות ביד חופשית (כמו בצייר)-

3. באיזו מידה השיטה היתה נוחה וקלה לשימוש?

מידה מועטה 1	2	3	4	5 מידה רבה מאוד
מה היה נוח/ לא נוח?				
<hr/>				
מה היית משנה וכיצד?				
<hr/>				

4. באיזו מידה את/ה חושב/ת שהצלחת לזהות ולסמן את המטרות?

מידה מועטה 1	2	3	4	5 מידה רבה מאוד
--------------	---	---	---	-----------------

עבור השיטה שבה מסמנים את המטרות באמצעות אליפסה בקוטר משתנה-

5. באיזו מידה השיטה היתה נוחה וקלה לשימוש?

מידה מועטה 1 2 3 4 5 מידה רבה מאוד

מה היה נוח/ לא נוח? _____

מה היית משנה וכיצד? _____

6. באיזו מידה את/ה חושב/ת שהצלחת לזהות ולסמן את המטרות?

מידה מועטה 1 2 3 4 5 מידה רבה מאוד

7. באיזו מידה מהירות החלפת התמונות היתה מתאימה?

מידה מועטה 1 2 3 4 5 מידה רבה מאוד

האם לדעתך תוספת זמן היתה מסייעת לך? מדוע? _____

Appendix C. Integrative site-specific sprayer experiment – detailed results.

	user name	average															number os sprays			FA added by the compu	FA added by the compu		
		collaboration 1					collaboration 2					collaboration 3										spray evaluation	
		marking hit	spray hit	marking FA	spray FA	num of targets	marking hit	spray hit	marking FA	spray FA	num of targets	marking hit	spray hit	marking FA	spray FA	num of targets	col 1	col 2	col 3				
		roee	87.2	93.5	2.7	10.3	3.4	77.5	83.2	2.5	9.1	2.8	80.3	84.6	8.1	19.4	4.0	4.1	3.6	3.4	62.0	54.0	76.0
asaf	79.3	84.7	3.9	9.8	3.1	89.7	93.2	6.5	15.7	3.2	78.4	84.4	12.3	24.9	4.4	3.7	3.8	3.2	55.0	58.0	79.0	17.9	7.2
ben	64.8	72.1	1.2	5.4	2.7	76.1	80.4	4.1	10.6	2.8	86.8	87.3	31.1	49.1	3.2	4.4	4.4	4.1	51.0	50.0	57.0	18.2	7.7
guy	84.2	87.9	7.2	16.8	3.0	79.1	82.1	5.5	13.4	2.7	84.6	88.7	12.4	23.9	4.2	4.2	4.6	3.8	56.0	49.0	75.0	19.7	6.5
liad	82.1	85.2	3.5	9.7	3.2	81.3	82.6	9.6	18.6	2.8	89.1	89.3	30.6	48.4	3.2	4.1	4.2	4.2	64.0	51.0	58.0	17.6	5.0
oded	74.2	80.9	2.8	7.7	3.3	78.9	82.9	10.2	19.1	3.1	85.8	86.7	21.0	36.3	3.3	4.2	4.3	3.8	60.0	55.0	59.0	17.1	4.9
shay	61.2	66.3	4.4	9.4	2.8	78.6	84.5	5.8	14.7	2.8	84.0	85.3	18.6	35.0	3.5	3.5	3.8	3.4	49.0	51.0	63.0	16.0	7.5
yossi	88.0	94.2	4.9	11.3	3.4	87.8	93.7	6.6	14.4	3.4	94.3	96.6	17.4	32.3	3.6	3.7	4.0	4.3	63.0	72.0	69.0	16.8	4.1
average	77.6	83.1	3.8	10.1	3.1	81.1	85.3	6.4	14.5	3.0	85.4	87.9	18.9	33.7	3.7	4.0	4.1	3.8	57.5	55.0	67.0	17.6	6.1
std	10.1	9.8	1.8	3.3	0.3	5.0	5.1	2.6	3.5	0.2	5.0	4.0	8.4	11.0	0.5	0.3	0.3	0.4	6.2	5.9	7.2	1.9	0.7

		average															number os sprays			FA added by the compu	FA added by the compu			
		collaboration 1					collaboration 2					collaboration 3										spray evaluation		
		user name	marking hit	spray hit	marking FA	spray FA	num of targets	marking hit	spray hit	marking FA	spray FA	num of targets	marking hit	spray hit	marking FA	spray FA	num of targets	col 1	col 2	col 3				
free hand	ben harel	85.7	90.5	5.1	13.1	3.9	91.7	96.1	8.9	18.1	4.0	95.7	97.5	26.5	40.4	3.5	4.1	4.4	4.6	71.0	72.0	67.0	15.0	4.1
	dror	86.7	92.5	3.7	9.2	3.6	84.3	90.1	2.3	6.7	3.3	93.4	94.6	29.2	49.3	3.5	4.3	3.9	4.4	65.0	60.0	63.0	17.1	5.1
	inbar	63.4	77.6	0.9	4.0	3.5	58.8	77.9	0.4	3.2	3.4	75.6	81.7	22.6	31.3	3.7	3.8	3.8	4.3	63.0	65.0	29.0	14.7	4.0
	matan	69.3	79.9	2.9	12.6	2.9	85.3	93.7	10.2	26.6	3.7	94.0	96.7	35.9	52.4	3.5	3.2	3.6	4.1	53.0	63.0	63.0	18.3	5.4
	ofir	85.1	90.2	2.3	8.6	3.3	85.1	89.6	2.8	9.0	3.4	89.9	91.9	31.4	47.6	3.2	4.0	3.8	3.6	62.0	64.0	59.0	17.8	5.9
	roy	82.6	87.2	8.7	15.6	3.8	87.5	93.4	15.5	27.6	4.2	92.9	94.5	34.2	54.8	3.7	4.2	4.1	4.3	69.0	75.0	66.0	16.1	4.7
	sridatta	82.4	90.8	11.2	29.6	3.9	82.8	88.7	11.5	21.8	4.0	94.3	95.7	36.4	70.0	3.9	4.0	4.1	4.4	70.0	72.0	70.0	17.1	4.0
	yarden	79.2	87.5	1.7	6.6	3.3	79.7	86.8	2.8	8.1	3.3	94.5	96.0	34.8	51.1	3.7	4.2	4.3	4.2	62.0	60.0	66.0	19.3	5.4
	average	79.3	87.0	4.6	12.4	3.5	81.9	89.5	6.8	15.2	3.7	91.3	93.6	31.4	49.6	3.6	4.0	4.0	4.2	64.4	66.4	60.4	16.9	4.8
std	8.5	5.4	3.6	7.9	0.4	9.9	5.6	5.4	9.6	0.3	6.6	5.1	4.9	11.2	0.2	0.3	0.3	0.3	6.9	7.1	6.5	1.8	0.5	

Appendix D. Table of contents of thesis DVD

Each bullet represent a library in the thesis DVD:

- Adding FA
- Artificial targets detection
- Explanation slideshow
- Foliage and Grapes Detection Algorithms
- Human-Robot Collaboration
- Image registration files
- Integrative site specific sprayer experiment
- Papers
- Robot control software
- Robotic platform CAD files
- Spraying Simulations
- Target size calculation
- vineyard navigation

תקציר

רקע ומטרות המחקר

עבודה זו מתמקדת בפיתוח תשתית וכלים חדשניים עבור יישום שיתוף פעולה של משתמש אנושי מרוחק ומערכת רובוטית לצורך ביצוע משימת ריסוס חומרי הדברה בחקלאות בכלל ובכרמי ענבים בפרט.

השימוש בחומרי הדברה הינו חלק בלתי נפרד מהחקלאות העולמית. בין 30% ל 35% הפסדי יכול אשר נגרמים כתוצאה ממחלות ומזיקים יכולים להמנע על ידי השימוש בחומרי הדברה. למרות שחומרי הדברה הכרחיים לחקלאות המודרנית, הם רעילים ומסוכנים לאדם ולסביבה. שיטות מודרניות ליישום חומרי הדברה בכרמי ענבים כוללות אדם שהולך לאורך הגידול ומרסס מטרות באופן נקודתי על ידי מרסס גב מוטורי וריסוס ממוכן בו אדם נוהג בטרקטור מרסס אשר מיישם את הריסוס באופן כוללני ללא יכולת התמקדות במטרות ספציפיות. למרות השימוש באמצעי מיגון (מסכת מיגון אישית ומערכת טיהור אוויר לטרקטור) האדם עדיין חשוף לחומרי הדברה מסוכנים אשר מסוכנים לבריאות האדם.

טכנולוגיות רובוטיות עשויות לספק אמצעי להפחתת תלות החקלאות בחומרי הדברה, לשפר קיימות ולהפחית את השפעת חומרי ההדברה על הסביבה. מרסס רובוטי יכול להפחית את כמות השימוש בחומרי הדברה ולצמצם את חשיפת האדם לחומרי הדברה במהלך פעולת ההדברה.

משימת הריסוס של הרובוט מחולקת לשלוש תתי משימות: ניווט הרובוט לאורך הגידול, זיהוי המטרה וריסוס המטרה. עבודה זו התמקדה בשתי תתי המשימות האחרונות, זיהוי המטרה וריסוסה.

מטרת עבודה זו הינה לפתח מערכת שיתוף פעולה אדם-רובוט לצורך ביצוע משימת ריסוס חומרי הדברה בכרמי ענבים. מטרות המחקר הספציפיות הן לפתח מערכת רובוטית לגלילית המתאימה לריסוס כרמים, פיתוח מערכת לזיהוי אשכולות ענבים ועלווה, פיתוח תשתית שבה האדם המרוחק מהמקום והרובוט בשדה יבצעו במשותף את פעולת הריסוס הנקודתי ולפתח אמצעי ריסוס מדויק. שיתוף פעולה בין משתמש אנושי לרובוט לצורך זיהוי אשכולות הענבים עשוי לתרום למערכת זיהוי מדויקת, פשוטה, גמישה ועמידה להפרעות תוך שימוש ביתרונותיו של האדם והרובוט. מערכת מסוג זה תהיה מסוגלת להתמודד עם משימות זיהוי מורכבות ומשתנות. יתרון נוסף של מערכת שיתוף פעולה בין האדם לרובוט הינה היכולת להרחיק את האדם מאזור הריסוס, ולהפחית את הפגיעה בסביבה תודות לחיסכון כמותי של חומרי הדברה זאת על ידי ריסוס נקודתי מדויק של המטרה.

שיטות

מערכת רובוטית מצוידת במתקן ריסוס בעל קוטר משתנה ובעלת היכולת לתקשר עם משתמש מרוחק פותחה ונבנתה. שיטות שיטוף פעולה בין האדם לרובוט פותחו ובנוסף פותחו שיטות לסימון המטרות על ידי המשתמש האנושי.

מערכת רובוטית חקלאית פותחה ככלי מחקר לצורך איפשור ניסויי שדה ובחינה של תנאים חיצוניים המשקפים את התנאי בהם רובוט ריסוס עתידי עשוי להיתקל ולהתמודד. מרכב הרובוט בנוי משתי פלטפורמות זהות אשר מחברות ביניהן בעזרת מחבר קארדן. כושר העמסה של כל פלטפורמה הינו 300 ק"ג. כל פלטפורמה מכילה שני גלגלים, אחד בכל צד, ומנוע חשמלי מחובר ישירות לכל גלגל. המערכת הרובוטית מצוידת בכל אמצעי החומרה

והתוכנה אשר דרושים להפעלתה, כגון, מחשב, מסך, סוללות, גנרטור וחיישנים שונים (מצלמות דיגיטליות, חיישני מרחק). מודל קינמטי פותח באופן ייעודי עבור הרובוט לצורך ניווט המערכת לאורך נתיב מוגדר.

אלגוריתמי זיהוי אשכולות ענבים ועלווה פותחו ונבחנו. האלגוריתמים פותחו תחת תפיסה חדשנית אשר מתייחסת לאחוז ההפחתה בחומרי הדברה כפרמטר ראשוני לביצוע אופטימיזציה להפחתה. שלושה אלגוריתמי זיהוי אשכולות פותחו ובנוסף פותח אלגוריתם בודד לזיהוי עלוות הכרם. האלגוריתמים נבחנו בעזרת סט תמונות שצולמו בכרם מסחרי. אלגוריתם זיהוי העלווה בוסס על ייחודיות הצבע הירוק שמאפיין את העלווה. אלגוריתמי זיהוי אשכולות הענבים התבססו על: הבדל פילוג גבולות (edge detection) בין אשכול ענבים לבין עלוות הכרם, עץ החלטות תוך שימוש במספר רב של פרמטרים והשוואת תבניות גבול בין אשכול ענבים לבין עלווה. האלגוריתמים פותחו תוך ניסיון למקסם את אחוז הזיהוי ולמזער את אחוז הסימון יתר.

שיטות שיתוף פעולה בין משתמש אנושי לבין מערכת רובוטית מרוחקת פותחו לצורך הערכת ההשפעה של שילוב משתמש אנושי במערכת לזיהוי אשכולות הענבים על אחוזי הזיהוי ועל ההשפעה הכללית על המערכת. השיטות שפותחו כללו שלוש שיטות לסימון מטרות על ידי משתמש אנושי אשר ממוקם מרוחק מהמערכת הרובוטית (עיגול בקוטר קבוע, אליפסה בקוטר משתנה ויד חופשית). בנוסף, פותחו ארבע שיטות לאופן שיתוף הפעולה בין האדם המרוחק לבין הרובוט (ידני לחלוטין, רובוט ממליץ-אדם מחליט, רובוט מחליט-אדם מפקח ורובוט אוטונומי לחלוטין). כל אחת משיטות סימון המטרות ושיטות שיוף הפעולה בין האדם לרובוט נבחנו בעזרת נסיינים תוך שימוש בתמונות שצולמו בכרמים מסחריים. ממשק אדם מחשב פותח ויושם לצורך בחינת שיטות סימון המטרות ואפשרויות שיתוף הפעולה בין האדם לרובוט. הממשק שימש לבחינת השיטות במעבדה וכן לבחינת השיטות במהלך ניסוי בתנאי חוץ.

לצורך יישום חומרי ההדברה באופן מדויק כלפי המטרה (אשכול הענבים) פותח מתקן לריסוס מטרה בודדת. כיוון שהמטרות (אשכולות הענבים) הינן מטרות בעלות צורה לא קבועה וגודל משתנה, פיית ריסוס בעלת יכולת שינוי מפתח נחוצה לצורך התאמת מפתח הריסוס למטרה הספציפית וזאת לצורך כיסוי מלא של המטרה תוך צימצום ריסוס יתר. התפקיד הבסיסי של המתקן הינו שינוי קוטר הריסוס לפי קוטר המטרה. פיית ריסוס מסחרית (AYHSS 16) אשר מורכבת משני חלקים, בסיס הפייה וראש הפייה, משנה את קוטר הריסוס על ידי סיבוב ראש הפייה ביחס לבסיסה. בסיס הפייה מעוגן למתקן הריסוס ואילו ראש הפייה מחובר דרך גלגל שיניים למנוע צעד אשר אחראי על מיקומו הרדיאלי. בנוסף, מתקן הריסוס כולל מצלמת דיגיטאלית צבעונית (לצורך צילום המטרות), חיישן מרחק ושני צייני לייזר בעלי מפתח מניפה (צייני הלייזר מייצרים קו על המטרה וכאשר אחד מוצב אופי והשני אנכי מתקבל צלב + על המטרה). המתקן מקובע ליחידת צידוד הגבהה (PTU) שתפקידה לכוון את פיית הריסוס כלפי המטרה. לצורך הערכת ביצועי מתקן הריסוס בוצעו מספר ניסויים שכללו ניסוי לבחינת ספיקת הריסוס כפונקציה למפתח פיית הריסוס, ניסוי להערכת קוטר הריסוס כפונקציה של הזווית הרדיאלית של ראש הפייה וניסוי אשר בוחן את תיפקוד המתקן בריסוס מטרות בעלות קוטר משתנה.

ניסויים

מספר ניסויים בוצעו לצורך הערכת: אלגוריתמי זיהוי אשכולות הענבים והעלווה, שיטות סימון המטרות על יד משתמש אנושי, רמות שיתוף הפעולה בין האדם לרובוט, מתקן הריסוס המדויק וניסוי המערכ הכוללת. מטרתם העיקרית של הניסויים היה להעריך אלמנטים שונים במערכת הרובוטית בתנאים הדומים ככל האפשר לתנאי השדה האמיתי. לצורך כך, צולמו סט תמונות משני כרמים מסחריים אשר שימשו לצורך הערכת אלמנטים שונים של התשתית הרובוטית.

ניסוי ריסוס כולל של המערכת הרובוטית בוצע לצורך הערכה והדגמה של שלוש מרכיבים עיקריים של המערכת הרובוטית עובדים במשולב ובתיאום: סימון המטרות על ידי משתמש אנושי מרוחק, רמות שיתוף פעולה אדם-רובוט ומתקן ריסוס מדויק. לצורך שליטה טובה יותר בניסוי נעשה שימוש במטרות ריסוס מלאכותיות (לעומת אשכולות ענבים אמיתיים) ובמקום לנווט את הרובוט לאורך כרם ענבים, הרובוט עקב אחרי סרט אדום שהוצמד לקרקע. במהלך הניסוי הרובוט עבר דרך כוללת של 1044 מ' (16 משתמשים \times 3 חזרות לכל משתמש \times 18 מ' לכל חזרה + 10 חזרות אוטונומיות \times 18 מ' לכל חזרה), צולמו 1108 תמונות שהכילו וריסוס 3378 מטרות. הניסוי הראה שלמרות המורכבות הגבוהה של המערכת הרובוטית והתשתית, שיתוף האדם בתהליך הינו אפשרי ואף מעלה את ביצועי סימון המטרות וריסוסן. שיתוף הפעולה בין האדם לרובוט הראה כי אחוזי הפגיעה במטרה ואחוזי ריסוס היתר שופרו (אחוזי הפגיעה עלו ב 13.4% ואחוזי ריסוס היתר פחתו ב 19.5%) לעומת ריסוס אוטונומי (ללא התערבות אדם).

תוצאות

אלגוריתמים לזיהוי אשכולות ענבים ועלווה

עיבוד נתוני הביצועים של שלוש האלגוריתמים לזיהוי אשכולות ענבים הראו כי אחוז הזיהוי המקסימאלי יכול להגיע ל 91% תוך הפחתת השימוש בחומרי הדברה ב 30%. זמן ריצה של המינימאלי והמקסימאלי של האלגוריתמים היה 0.65 ו 1.43 שניות בהתאמה. תוצאות אלו מתייחסות ליכולת המחשב לזהות את אשכולות הענבים ללא התערבות אדם בתהליך הזיהוי. לצורך שיפור יכולת זיהוי המטרות שולב האדם בתהליך הזיהוי ובתשתית המערכת.

שיתוף פעולה אדם-רובוט

תהליך הלמידה לשימוש בממשק לסימון מטרות הוערך תחת ההנחה שהמשתמש מנוסה בממשק כאשר אחוזי זיהוי וסימון המטרות עוברות את רף ה 90%. בניסוי להערכת משך זמן הלימוד (כמות תמונות הנדרשת) התגלה כי סימון של 30 תמונות יביא את המשתמש האנושי לרף אחוזי הזיהוי הנדרשים (90%). תהליך הלמידה בשימוש בממשקי סימון המטרות הועבר לכל מתנסה חדש בניסויים שמפורטים בהמשך.

ניסויי שיטות הסימון הראו כי אחוז הזיהוי הגבוה וזיהוי יתר נמוך מתקבל כאשר למשתמשים יש יותר זמן לסמן את המטרות (כפי שנצפה מראש). בשימוש ברמת שיתוף הפעולה אדם-רובוט הראשונה (רמת שיתוף פעולה בה לאדם יש שליטה מוחלטת בסימון המטרות ללא התערבות מחשב), אחוז הזיהוי הגבוה ביותר שנצפה הינו 94.3% (עם אחוז זיהוי יתר של 15.1%) תוך שימוש בשיטת הסימון עיגול בקוטר קבוע עם 15 שניות לסמן כל תמונה. אחוז זיהוי היתר הנמוך ביותר שנצפה הינו 10.1% תוך שימוש בשיטת סימון יד חופשית ו15 שניות לסמן כל תמונה.

כיוון ששיטת הסימון אליפסה לא הראתה כל הצטיינות על שיטות הסימון האחרות, שיטה זו לא נוסתה בניסויי המשך של רמות שיתוף פעולה אדם-רובוט.

תוצאות ניסויי שיתוף הפעולה אדם-רובוט הראו כי אחוזי הזיהוי הגבוהים ביותר, 92.66%, התקבלו תוך שימוש ברמת שיתוף פעולה השלישית (רמה בה הרובוט מסמן מטרות והאדם מפקח ויכול להוסיף ולמחוק מטרות), תוך שימוש בשיטת הסימון עיגול בקוטר קבוע וזמן סימון מטרות של 15 שניות. אחוזי סימון היתר הנמוכים ביותר, 2.71%, התקבלו תוך שימוש ברמת שיתוף פעולה השנייה (רמה בה הרובוט ממליץ על מיקומי המטרות והאדם מחליט מה לסמן), תוך שימוש בשיטת סימון יד חופשית וזמן חילוף תמונה של 15 שניות.

מתקן לריסוס מטרות מדויק

ניסוי ספיקת חומר הריסוס בוצע תחת לחץ משאבה קבוע של 20 [באר]. הניסוי הראה קשר לינארי המתאר את

$$\text{הקשר בין הספיקה לבין מפתח פיית הריסוס: } \left[\frac{L}{sec} \right] = 0.0519 \cdot flow\ rate + 6 \cdot 10^{-6} \cdot nozzle\ aperture$$

ניסוי לבחינת הריסוס המדויק תוך שינוי קוטר המטרות הראה כי בבחינה ויזואלית של המטרות שרוססו, כל המטרות כוסו באופן מוחלט בחומר ההדברה. התוצאות הראו כי מפתח הריסוס גדל עם הגדלת קוטר המטרה אך היחס בין קוטר הריסוס וקוטר המטרה ירד. יחס זה מייצג את יחס ריסוס היתר שיוורד ככל שהמטרה גדלה.

ניסוי ריסוס משולב

באופן כללי, תוצאות הניסוי תוך שימוש בשיטת סימון יד חופשית היו טובות מאשר שיטת הסימון עיגול עם קוטר קבוע. אחוזי הזיהוי היה טוב יותר בכל במקרים כאשר נעשה שימוש בשיטת סימון יד חופשית (למעט בהערכת הריסוס ברמת שיתוף הפעולה השנייה). יחד עם השיפור באחוזי הזיהוי נצפו עלייה באחוזי ריסוס היתר, כלומר, נעשה יותר שימוש מיותר בחומרי הדברה. בשתי שיטות הסימון שנבחנו, עיגול עם קוטר קבוע ויד חופשית, אחוזי הזיהוי עלו ואחוזי סימון היתר פחתו עם העלאת רמת שיתוף הפעולה בין האדם לרובוט. תוצאות אחוזי הזיהוי הטובות ביותר, 93.6%, התקבלו תוך שימוש בשיטת סימון יד חופשית ורמת שיתוף פעולה השלישית.

סיכום

מערכת רובוטית לריסוס משולבת אדם תוכננה, נבנתה ונוסתה. המערכת הרובוטית מציגה יכולת לבצע את המשימות הנחוצות לרובוט ריסוס בכרס מסחרי. עבודה זו מציגה את היכולת של מערכת רובוטית לריסוס לשלב משתמש אנושי מרוחק בפעולת סימון המטרות תחת שיטות שונות של שיתוף פעולה.

התרומה העיקרית של עבודה זו הינה הצגת פונקציונליות מלאה של התשתית לשיתוף פעולה אדם-רובוט במשימה לריסוס אשכולות ענבים בכרם. במהלך העבודה נבחנו רמות שיתוף פעולה שונות וכן שיטות שונות בהם אמור המשתמש האנושי לסמן את המטרות לריסוס. תרומה נוספת של עבודה זו הינה הצגת מתקן לריסוס מדויק וסלקטיבי אשר מאפשר ליישם ריסוס מדויק כלפי המטרות שסומנו. התוצאות והנתונים שהופקו מעבודה זו יכולים לשמש לצורך פיתוח מערכות אדם-רובוט יישומיות תוך יישום התוצאות האפטימליות (לדוגמא, עבור אחוזי זיהוי גבוהים שימוש בשיטת סימון עיגול בקוטר קבוע, זמן חילוף תמונה של 15 שניות ורמת שיתוף פעולה ראשונה, עבור אחוזי סימון יתר נמוכים, שימוש ביד חופשית, זמן חילוף תמונה של 15 שניות ורמת שיתוף פעולה שניה).

אנו מקווים כי כל או חלק מעבודה זו יתרום לפיתוח מערכת רובוטית מסחרית משולבת אדם. דבר זה יגרום לנזק סביבתי מופחת ויתרום לבריאות האדם על מניעת חשיפה לחומרי הדברה רעילים.

מילות מפתח : הנדסה חקלאית, מיכון חקלאי, שיתוף פעולה אדם-רובוט, עיבוד תמונה, ראייה ממוחשבת, זיהוי אובייקטים, חומרי הדברה, חקלאות מדויקת, רובוט לריסוס, ריסוס

הצהרת תלמיד המחקר עם הגשת עבודת הדוקטור לשיפוט

אני החתום מטה מצהיר/ה בזאת : (אנא סמן) :

X חיברתי את חיבורי בעצמי, להוציא עזרת ההדרכה שקיבלתי מאת מנחה/ים.

X החומר המדעי הנכלל בעבודה זו הינו פרי מחקרי מתקופת היותי תלמיד/ת מחקר.

X בעבודה נכלל חומר מחקרי שהוא פרי שיתוף עם אחרים, למעט עזרה טכנית הנהוגה בעבודה ניסיונית. לפי כך מצורפת בזאת הצהרה על תרומתי ותרומת שותפי למחקר, שאושרה על ידם ומוגשת בהסכמתם.

תאריך 20.6.2016 שם התלמיד/ה רון ברנשטיין



חתימה

העבודה נעשתה בהדרכת פרופ' יעל אידן

במחלקה להנדסת תעשייה וניהול

בפקולטה למדעי ההנדסה

Yael Eden


מערכת רובוטית משולבת אדם לריסוס סלקטיבי בכרמים

מחקר לשם מילוי חלקי של הדרישות לקבלת תואר "דוקטור לפילוסופיה"

מאת

רון ברנשטיין

הוגש לסינאט אוניברסיטת בן גוריון בנגב



אישור המנחה

אישור דיקן בית הספר ללימודי מחקר מתקדמים ע"ש קרייטמן

20 ליוני 2016

י"ד בסיוון תשע"ו

באר שבע

מערכת רובוטית משולבת אדם לריסוס סלקטיבי בכרמים

מחקר לשם מילוי חלקי של הדרישות לקבלת תואר "דוקטור לפילוסופיה"

רון ברנשטיין

הוגש לסינאט אוניברסיטת בן גוריון בנגב

20 ליוני 2016

י"ד בסיוון תשע"ו

באר שבע